Chapter 4

X-changing information on X inactivation

This chapter has been published in

Tahsin Stefan Barakat, Iris Jonkers, Kim Monkhorst and Joost Gribnau (2010)
"X-changing information on X inactivation"
Experimental Cell Research 316:679-687

X-changing information on X inactivation

Tahsin Stefan Barakat[1], Iris Jonkers[1,2], Kim Monkhorst[1,3] and Joost Gribnau[1,4]

[1]Department of Reproduction and Development, Erasmus MC, University Medical Center, Rotterdam, the Netherlands, [2]Current address: Department of Molecular Biology and Genetics, Cornell University, Ithaca, USA, [3]Current address: Department of Pathology, Erasmus MC, University Medical Center, Rotterdam, the Netherlands, [4]corresponding author

Contact details:
Joost Gribnau
Department of Reproduction and Development, Room Ee 09-71
Erasmus MC
PO Box 2040, 3000 CA Rotterdam
The Netherlands
Phone +31-10-7043069
Fax +31-10-7044736
Email: j.gribnau@erasmusmc.nl

Abstract

In female somatic cells of mammalian species one X chromosome is inactivated to ensure dosage equality of X-encoded genes between females and males, during development and adulthood. X chromosome inactivation (XCI) involves various epigenetic mechanisms, including RNA mediated gene silencing in *cis*, DNA methylation, and changes in chromatin modifications and composition. XCI therefore provides an attractive paradigm to study epigenetic gene regulation in a more general context. The XCI process starts with counting of the number of X chromosomes present in a nucleus, and initiation of XCI follows if this number exceeds one per diploid genome. Recently, X-encoded RNF12 has been identified as a dose-dependent activator of XCI. In addition, other factors, including the pluripotency factors OCT4, SOX2 and NANOG, have been implicated to play a role in suppression of initiation of XCI. In this review, we highlight and explain these new and old findings in the context of a stochastic model for X chromosome counting and XCI initiation.

Introduction

In mammalian species the dosage of X-linked genes is equalized between XX females and XY males by inactivation of one of the two X chromosomes in every female cell [30]. In mouse, X chromosome inactivation (XCI) is present in two forms. In the extra-embryonic tissues XCI is imprinted, with the paternal X chromosome (Xp) being inactivated in all cells [53]. This process is initiated very early during development, around the two- to eight-cell stage [51-52], and is maintained in the developing extra-embryonic tissues of the embryo, including the fetal placenta. In contrast, the Xp is reactivated in the inner cell mass (ICM), which gives rise to the embryo proper, after which random X inactivation is initiated around day 5.5 of development. After the inactive X chromosome (Xi) is established by random XCI of either Xp or Xm, this inactive state is propagated clonally. Also in the human embryo proper, XCI is random and initiated early during development [368]. Whether the imprinted form of XCI is present in the early human embryo is not clear, and conflicting reports claim either the presence or absence of imprinted XCI in human extra-embryonic tissues [369-370, 373-374, 376].

In mouse, two X-linked genes, *Xist* and *Tsix*, have been identified to play an important role in XCI [84-86, 93-94, 119]. Both genes were mapped to the X inactivation center (Xic, **Figure 1**), that was determined by genetic studies revealing a maximum region of 10 megabases on the X chromosome required for XCI [72, 974]. Although *Xist* is a non-coding gene, the *Xist* transcript is spliced and poly-adenylated. Accumulation of processed *Xist* RNA on the Xi in *cis* is a decisive factor leading to inactivation. *Tsix* is transcribed anti-sense to *Xist* and overlaps completely with *Xist* [118]. *Tsix* transcripts are also spliced and poly-adenylated, and *Tsix* transcription is initiated at different promoters. *Tsix* and *Xite*, the latter acting as an enhancer of *Tsix* [136], are both transcribed from the active X chromosome (Xa) before and at the onset of XCI, and are involved in down-regulation of *Xist*, counteracting X inactivation. The XCI process involves different phases, starting with a counting and choice process which includes determination of the number of X

chromosomes and the choice which X will be inactivated. Subsequently, the Xi is established through recruitment of different chromatin modification complexes, and the silent state is then maintained through an almost unlimited number of cell divisions, throughout development and adult life [33]. In this review, we will focus on the mechanisms directing the XCI counting and choice process. For a detailed description of mechanisms involved in the establishment and maintenance we refer to a complementary recent review [975].

Counting and initiation of X inactivation

XCI is initiated if the number of X chromosomes exceeds one per diploid genome set. In the female embryo proper, and also in differentiating female ES cells in culture, the choice is random with respect to the parental origin of the X to be inactivated. Several genes and chromosomal regions have been attributed to be involved in the counting process. Removal or addition of regions involved in counting can lead to complete or partial loss of initiation of XCI in female cells, or an opposite effect, leading to XCI on both X chromosomes in female cells, or even initiation of XCI in male cells. Transgenic male ES cell lines with autosomal insertions of small transgenes (30-80kb) covering *Xist* and *Tsix*, or *Xist* alone revealed, besides autosomal spreading of transgenic *Xist* in *cis*, ectopic XCI of the single X chromosome in a significant proportion of cells [167, 169]. This indicated that gene(s) or elements(s) involved in determining the number of X chromosomes may be located within the region covered by these transgenes. Different male *Tsix* mutant ES cell lines indeed displayed initiation of XCI on the single X chromosome, which suggested a direct role for *Tsix* in the XCI counting process (**Figure 1**) [123, 127, 178]. Interestingly, the same mutations did not affect counting in heterozygous female cells, which almost exclusively inactivate the mutated *Tsix* allele [119-120].

Studies with female cell lines and mice with deletions of parts of *Xist* showed that *Xist* is required for XCI to occur in *cis* [93-95]. However, *Xist* transcription and the deleted part of the *Xist* gene are not involved in the counting process because initiation of XCI in heterozygous female *Xist* mutant cells still occurred on the wild type X chromosome [104, 176-177]. We recently deleted a region spanning more than 60 kb including *Xist*, *Tsix* and *Xite* (ΔXTX) from one X chromosome in female cells [179]. As for the studies which involved *Xist* sequences alone, female cells with a heterozygous deletion of this region still initiate XCI on the wild type X chromosome. These findings indicate that *Xist*, *Tsix* and *Xite* affect the choice process by playing an important role in 'in *cis*' inactivation, but are not required for 'in *trans*' communication regulating the counting process. This is also supported by our findings that BAC transgenes covering *Xist* or *Tsix* alone or both *Xist* and *Tsix* do not induce XCI on the endogenous X, which contrasts previous reports,and suggest that *Xist* and *Tsix* may only play a marginal role in the counting process. The results obtained with the heterozygous ΔXTX ES cells and studies with BAC and YAC transgenes also indicated that factors involved in the counting process are located outside the region covering *Xist*, *Tsix* and *Xite* [166, 175, 187].

Models for XCI counting and choice

The initial step in the XCI process has always been viewed to be the result of a mutual exclusive choice process leading to inactivation of only one X chromosome in every female

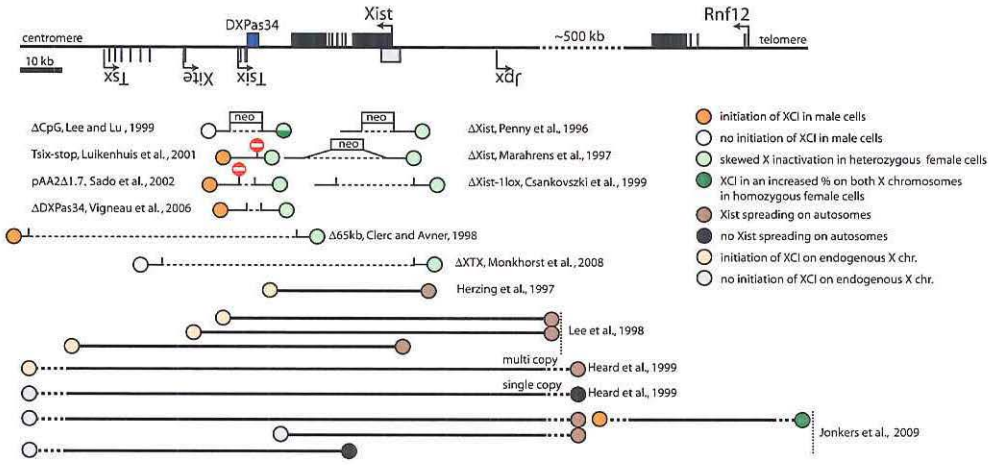

Figure 1: *Xist* and *Tsix* mutations and transgenes
Schematic representation of part of the Xic, including the location and size of the different *Xist* deletions, and *Tsix* deletions and stop cassettes described in this article (thin dashed line represents the sequence removed). The colored circles indicate the results obtained. The relative size and location and experimental findings of the cosmid and BAC sequences covering *Rnf12*, *Xist* or *Tsix* alone, or *Xist* and *Tsix* used in transgenic studies are shown below (thick dashed line represents sequences not shown on the map).

cell. Several models have been postulated that explain the XCI process based on this assumption. The blocking factor (BF) model states that a limiting factor blocks XCI on one X chromosome in a diploid cell; either one of the two X chromosomes in female cells or the single X chromosome in male cells [72]. The cell is able to count, because the BF is encoded by an autosomal gene, and thus the excess of autosomes over X chromosomes determines whether enough BF is present in order to inhibit XCI on one X chromosome in a diploid background. The putative BF binds an element in the Xic that prevents *Xist* to accumulate on that X chromosome in *cis*. However, if this allele is impaired for XCI, because *Xist* is deleted for example, then the cell should not be able to inactivate, which would result in death of half the cell population. In contrast, cells with a heterozygous *Xist* deletion all make the right choice and initiate XCI on the wild type X chromosome, resulting in primary non-random XCI [176-177]. Therefore, a positive XCI factor was hypothesized, named the competence factor (CF). One model comprising the combined action of a BF and CF postulates that the abundantly present CF inactivates all X chromosomes but not the one to which BF is bound [177]. Another hypothesis states that also the X-encoded CF is limiting and is titrated away by one 'copy' of the autosomally-encoded BF, which corresponds to a single X chromosome. When more than one X chromosome is present in a diploid background, the extra copies of CF will not be titrated by the BF, and will inactivate the remaining unprotected X chromosome(s) [119, 976].

The main problem of the BF model is that a single entity, acting as a single 'copy' or molecule, is present in a diploid cell, which binds only one X chromosome. Cell-to-cell variegation is likely to make such a system unstable. A model in which not one entity, but many factors bind only one of two X chromosomes in a female diploid cell would

overcome this problem [164-165]. The so-called symmetry-breaking model that follows from this, states that blocking complex, composed of many autosomally encoded molecules that will bind to the DNA and itself through self-assembly, will form on one X chromosome at the onset of XCI. Computational analysis shows that self-assembly is energetically more favorable on only one X chromosome in a nucleus, rather than on two. Unfortunately, evidence of formation of such a complex, on the active X and at the onset of XCI, has not been presented yet.

Unlike the blocking factor models, the alternate state model postulates that the choice of an X chromosome to be inactivated is intrinsically determined by the chromatin state of the X prior to XCI [181]. The nature of this chromatin state is unknown, but can be determined by allelic cohesion differences present after DNA replication. An X chromosome with sister chromatids in more close proximity is more prone to XCI than an X with sister chromatids farther apart [181]. Differences in sister chromatid cohesion may reflect local *Xist* spreading in *cis*, which could be transient but is locked in at the onset of XCI, thereby ensuring random XCI. However, the reported correlation is not absolute, and also in cells that show primary non-random X inactivation, due to *Xist* or *Tsix* deletions, the ratio between cells with either more separated or more closely associated sister chromatids changes marginally, arguing against a direct involvement of sister chromatid cohesion in XCI choice.

A different model is based on the observation that co-localization, or pairing, of the Xics of the two X chromosomes in XX ES cells precedes XCI. This get-together of the X chromosomes is very transient and can only be observed in a subset of cells, but does occur more frequently than what would be expected from random co-localization of the Xics [182-183]. Several regions within the Xic are involved in pairing. A *Tsix* or *Xite* deletion in female ES cell lines results in loss of pairing and loss of random XCI [182-183, 185]. However, single copy *Xist/Tsix/Xite* transgenes cannot induce X-autosome pairing [182], indicating that another pairing region is crucial for initiation of XCI. Indeed, a BAC sequence located ~400 kb upstream of *Xist* was found to pair with other copies of the same region, and to induce *Xist* transcription in male ES cells when randomly integrated [187]. This region was named the X-pairing, *Xpr*, region, and it was suggested that the *Xpr* region is essential for sensing the presence of more than one X chromosomal allele and subsequent initiation of XCI. In this model, pairing of the *Tsix* and *Xite* region between two X chromosomes provides a feedback loop to prevent inactivation of the second X chromosome [187]. *Trans*-acting factors suggested to be involved in the proposed pairing are CTCF and OCT4. Knock-down of both CTCF and OCT4 was reported to counteract the pairing, but whereas knock-down of CTCF in female cells results in reduced initiation of XCI, knockdown of OCT4 results in inactivation of both X's in an increased number of female cells [185-186]. This indicates that the pairing model might not be the best model to explain random XCI. Interestingly, it was observed that transcriptional activity of *Tsix* and *Xist* is another requirement for pairing [185]. When DNA polymerase II transcription is inhibited, pairing of the *Tsix* and *Xist* regions is lost [977]. This result might indicate that the pairing events observed are not the cause of XCI, but a consequence of transcriptional activation of *Xist* and flanking genes at the onset of XCI, which may result in relocation of the Xic in the nucleus.

A stochastic model for initiation of XCI

All the above mentioned models predict a mutual exclusive and deterministic XCI process, in which a single X is inactivated in every female cell. Interestingly, *in vivo* and *in vitro* studies indicate that this is not the case. *In vivo* studies with diploid and tetraploid XX and XXXX embryos indicated the presence of a substantial population of cells with too many Xa's [162]. *In vitro* studies performed by us and others with diploid and tetraploid ES and ICM cells confirmed this finding, and also revealed a significant percentage of cells with too many Xi's [179, 188]. Cells with too many Xi's have to a lesser extent also been reported in embryos, but selection against these cell types is most likely more stringent than cells with too many Xa's. The fact that XCI is almost never initiated in diploid XY and tetraploid XXYY cells, indicates that initiation of XCI on too many X chromosomes in diploid XX and tetraploid XXXY and XXXX cells cannot be attributed to noise in the counting and initiation mechanism. Based on these findings we have proposed a stochastic mechanism directing the XCI process, in which every X chromosome has an independent probability to initiate XCI, eliminating the requirement for a choice process [179]. Comparison of the relative number of cells that initiated XCI between different diploid, triploid and tetraploid ES cells indicates that the X to autosome ratio determines the probability for an X chromosome to be inactivated [189]. The probability is most likely the resultant of one or more X-encoded XCI-activators and autosomally encoded XCI-inhibitors that promote or repress *Xist* accumulation, respectively. Upon development or differentiation, the concentration of the XCI-activator will rise and/or the concentration of the XCI-inhibitor will drop, and in female cells this will be sufficient to generate a specific probability in time for enough *Xist* to accumulate and start to spread in *cis* (**Figure 2A**). The XCI-inhibitor is involved in setting up a threshold that has to be overcome by *Xist* to accumulate. Because the XCI-activator gene is X-linked, spreading of *Xist* will down regulate the XCI-activator gene(s) in *cis* to a level below the threshold, thereby preventing the second X chromosome from inactivation. In this model, initiation of spreading is a stochastic event, so that the chance for silencing of the XCI-activator gene(s) on either X is equal, if not influenced by differential allelic properties of the individual X chromosomes. In male cells the concentration of the XCI-activator will not be sufficient to break the threshold and initiate XCI. Studies with female cell lines and mice that harbor *Xist* or *Tsix* mutations that affect the expression of one of the genes indicate that *Xist* and *Tsix* are the major players in setting up the probability, and that the XCI-activators and XCI-inhibitors are likely to act through these genes. Recently, we and others have identified several genes encoding one XCI-activator and several XCI-inhibitors.

XCI-activators and -inhibitors

In a stochastic model for XCI, preferential and timely initiation of XCI in female cells is obtained through a sex-dependent dosage difference in one or more X-encoded XCI-activators that promote *Xist* accumulation. An XCI-activator can act directly on transcription initiation of *Xist*, and/or in an indirect manner, by suppression of *Tsix* expression (**Figure 2B**). Several findings supported the presence of one or more XCI activators. Luciferase transgenes linked to an *Xist* promoter are higher expressed in female compared to male cells [89]. Also, female cells with a heterozygous deletion of the region encompassing *Xist*, *Tsix* and *Xite* still initiate XCI, indicating that an additional X-encoded

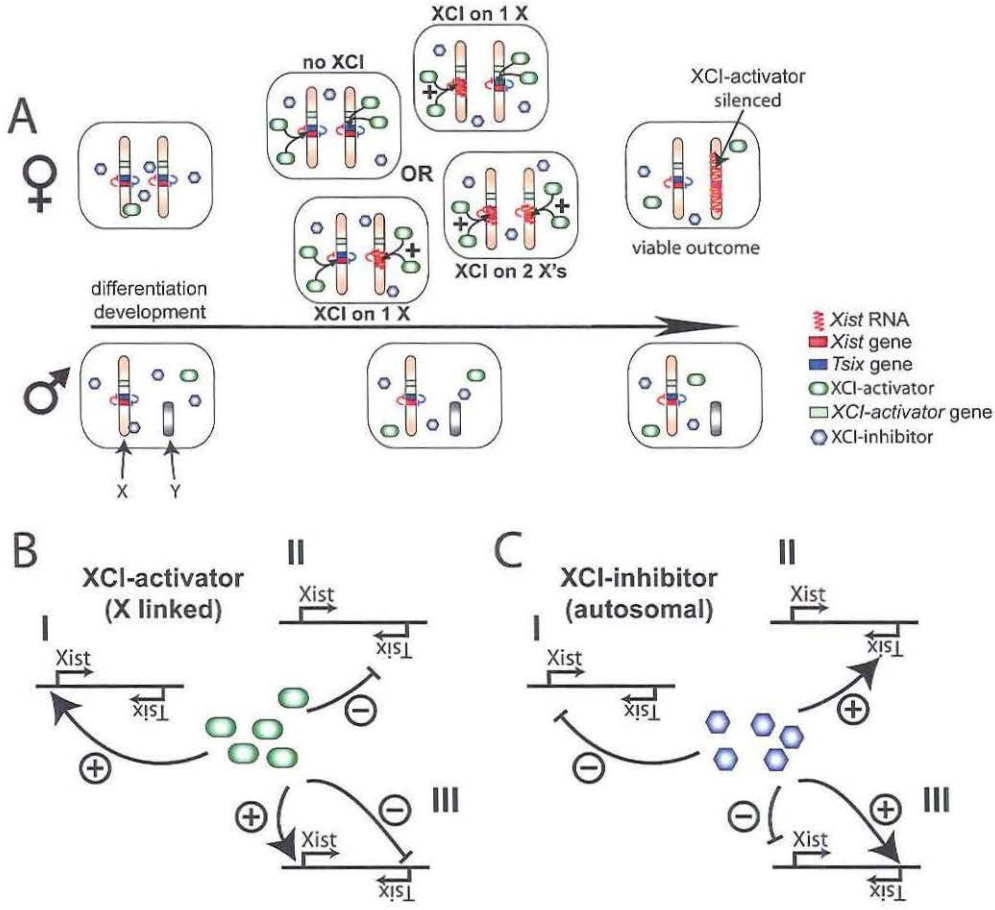

Figure 2: A stochastic model for XCI
A) Upon differentiation or development the concentration of the XCI-activator increases (green), or the concentration of the XCI-inhibitor drops (blue), or a combination of these changes occurs (both options are shown). As a result, in female cells and not in male cells, accumulation of *Xist* in *cis* (+) is initiated with a specific probability (arrows, all four possible outcomes are shown). *Xist* mediated silencing of the XCI-activator gene in *cis* and a subsequent drop in the XCI-activator concentration prevents initiation of XCI on the second X. **B)** XCI-activators can act by activation of *Xist* (I), by suppression of *Tsix* (II), or through both mechanisms (III). **C)** XCI-inhibitors can act by suppression of *Xist* (I), by activation of *Tsix* (II), or through both mechanisms (III).

protein or X-linked element is involved in XCI [179]. Furthermore, XCI initiation in cells with different X-to-autosome ratios displays a correlation between the rate of initiation and the X:A ratio, also supporting the presence of an X-encoded activator of XCI [189].

We recently identified X-encoded RNF12 as a dose-dependent XCI-activator [174]. Transgenic expression of additional copies of the *Rnf12* gene result in ectopic initiation of XCI on the single X in male cells and on both X's in an increased percentage

of female cells. *Rnf12* expression and over-expression correlates with initiation of XCI, and heterozygous *Rnf12*+/- female ES cells displayed reduced initiation of XCI upon differentiation. *Rnf12* encodes the E3 ubiquitin ligase RNF12 (RLIM), involved in the regulation of LIM-homeodomain transcription factors, telomere length homeostasis, and estrogen receptor alpha (ERα signaling; however, none of the known targets or partners of RNF12 have been implicated in XCI. These findings indicate a versatile role for *Rnf12* in embryonic development, and suggest that the regulation of XCI piggybacks onto existing developmental mechanisms. Although our findings indicate that RNF12 is an important XCI-activator, they also indicate that more XCI-activators are involved. X-chromosomal regions potentially harboring XCI-activator genes are the recently identified *Xpr* region, and regions including *Xist* and *Tsix*. However, in the same study we could not detect any effect of transgenes covering the *Xpr* and *Xist/Tsix* regions on initiation of XCI on the endogenous X chromosome(s), and we suggest that additional genes encoding XCI-activators will be located more distal to *Rnf12* or proximal to *Tsix*.

An inhibitor of XCI is most likely autosomally encoded, and will be involved in activation of *Tsix* expression and/or direct repression of *Xist* (**Figure 2C**). Among the proteins involved in *Tsix* regulation are the insulator protein CTCF and the transcription factor yin yang 1 (YY1), for which several tandemly organized binding sites have been identified both in the *DXpas34* region, which is involved in *Tsix* regulation, and the *Xite* promoter. Knockout studies involving *Yy1*, or partial ablation of *Yy1* and *Ctcf* through RNAi mediated repression, revealed down-regulation of *Tsix* expression and concomitant up-regulation of *Xist* expression, supporting a role for YY1 and CTCF in *Tsix* expression [193]. Proteins initially implicated to act directly on *Xist*, bypassing *Tsix* mediated repression, are the pluripotency factors SOX2, NANOG and OCT4. ChIP experiments have identified binding sites for these factors in intron 1 of *Xist*, and *Nanog* deficient ES cells showed up-regulation of *Xist* [191]. Up-regulation of *Xist* precedes down-regulation of *Tsix*, suggesting a *Tsix* independent mechanism for these three pluripotency factors in suppression of *Xist*. Interestingly, a different study indicates that OCT4 also binds the *DXPas34* element and the *Xite* promoter, and interacts with CTCF suggesting that OCT4 also acts in a *Tsix* dependent pathway [186].

Determining the probability to initiate XCI

XCI-inhibitors are expected to set up the threshold that has to be overcome by *Xist* to allow accumulation and silencing in *cis*. *Tsix* knockout studies have indicated that *Tsix* is an important player in setting up the in *cis* threshold for *Xist* accumulation. *Tsix* is involved in accumulation of chromatin modifications at the *Xist* promoter [89, 111], and anti-sense transcription through the *Xist* promoter is required for proper *Xist* suppression [112]. Whether the action of *Tsix* and accumulation of histone modifications at the *Xist* promoter involves a small regulatory RNA pathway, in which factors such as Dicer are involved, remains speculative and is still a matter of debate [132-134]. OCT4, SOX2 and NANOG-mediated silencing of *Xist* appears to act both in *Tsix*-dependent and -independent pathways, indicating that different mechanisms are involved in setting up the threshold. Sex-specific initiation of XCI, however, can never be accomplished only by autosomally encoded factors such as SOX2, OCT4 and NANOG, because the concentration of these factors is most likely the same in male and female cells (unless their concentration would

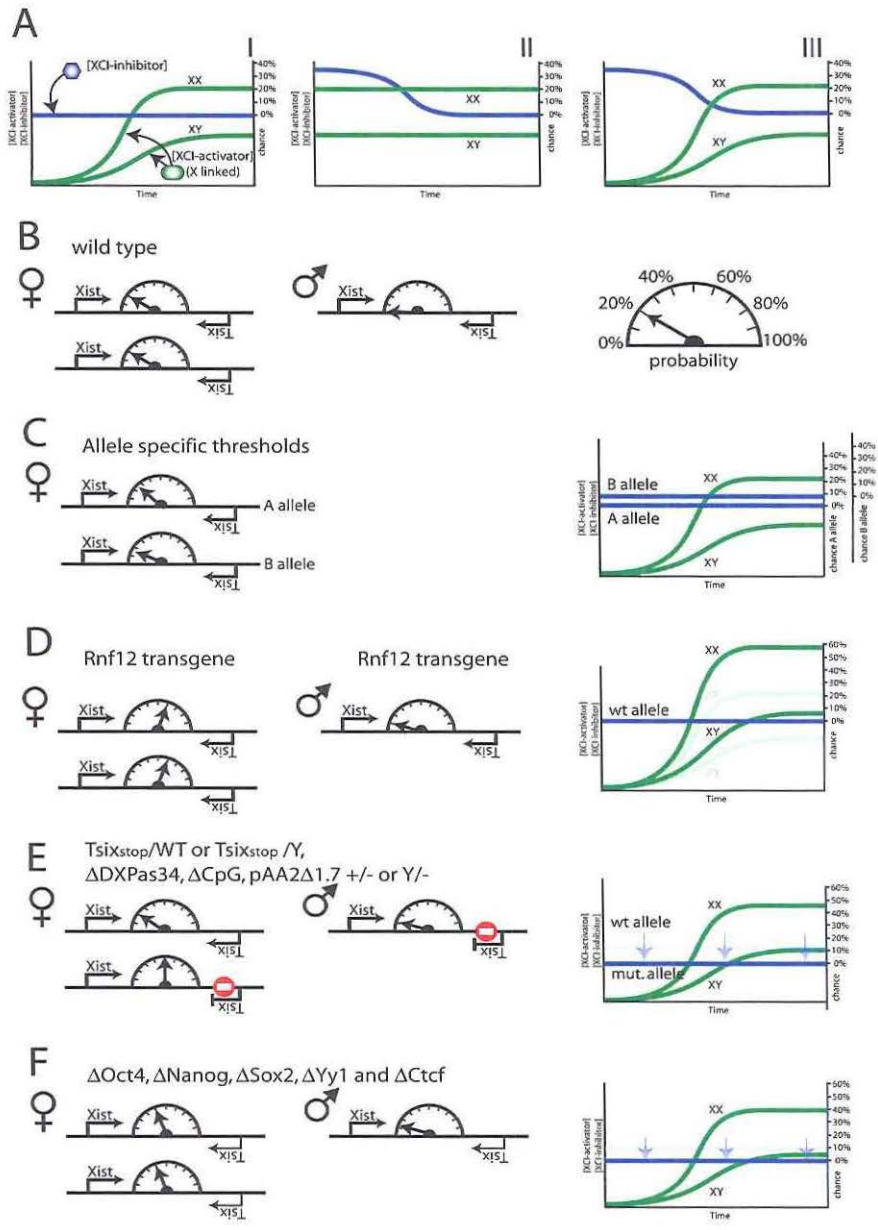

Figure 3: Determining the probability

A) Three possible mechanisms to determine the probability to initiate XCI. I) The concentration of the X-encoded XCI-activator increases in time upon onset of ES cell differentiation or in development (green line), and only in female cells the concentration is sufficient to break a stable threshold (blue line) required to generate a probability to initiate XCI. The probability shown on the Y-axis is an estimated

be regulated by an X-encoded factor). Key to the counting and initiation process is therefore the presence of X-encoded activators such as RNF12 that are differentially expressed between male and female cells. We have found that upon differentiation of ES cells, the concentration of RNF12 increases, and the concentration of other XCI-activators may increase as well. In contrast, the concentration of XCI-inhibitors will decrease during differentiation, as indeed was found for OCT4, SOX2 and NANOG, or might stay the same, as observed for YY1 and CTCF. Most likely, different combinations of changes are involved (**Figure 3A**, [978]). The combined changes will lead to increased *Xist* expression, either because XCI-activators activate *Xist* or suppress *Tsix*, or exert an effect through both mechanisms (**Figure 2B**). Currently, we do not know whether RNF12 acts through *Xist*, *Tsix* or both.

In one model, *Tsix* suppression is *Xist* independent, and stochastic inactivation of *Tsix* through the action of RNF12 and/or other XCI-activators allows accumulation of *Xist* and subsequent silencing in *cis*. Autonomous silencing of *Tsix* in male cells during ES cell differentiation indeed supports a mechanism in which *Tsix* is down-regulated independent of *Xist*. On the contrary, a mechanism by which *Tsix* is silenced though the action of *Xist* is supported by the finding that increased expression of *Xist*, effectuated by insertion of a neo cassette upstream of the *Xist* promoter, increases the probability for the mutated X chromosome to be inactivated [104]. In a model where *Xist* silences *Tsix*, *Xist* gene transcription activation depends on the concentration of RNF12 and other XCI-activators and is stochastic, thus resulting in increased bursts of RNA polymerase II activity initiated in one time frame. On the contrary, transcription initiation of *Tsix* is constant or decreases in time. In the battle between *Xist* and *Tsix*, *Xist* transcripts are more likely to reach the poly-adenylation sequence, resulting in a stabilized transcript, which will aid *Xist* mediated silencing of *Tsix*. Either mechanism or a combination of the two may be applicable to explain the XCI counting and initiation process. So far there is no clear evidence whether *Tsix* silencing at the onset of XCI is mediated by *Xist* or not, and further experimental evidence needs to be obtained to answer this question.

Figure 3: continued
cumulative probability of one day. II) The XCI-inhibitor concentration drops in time, lowering the threshold. The XCI-activator concentration is constant but is twice as high in female compared to male cells, which is sufficient to generate a probability to initiate XCI only in female cells. III) A combination of mechanisms I and II. **B)** In wild type female cells the concentration of the XCI-activator is sufficient to generate a probability to initiate XCI on both X chromosomes (left). In male cells the XCI-activator concentration is too low for XCI to be initiated (middle). The probability scale is shown on the right. **C)** In cells with two different alleles for instance due to SNPs, the alleles show differential *Xist* or *Tsix* expression and allele specific thresholds (blue lines) determine the probability to initiate XCI. **D)** In male (left) and female cells (middle) with a transgene covering *Rnf12* or another XCI-activator gene, the concentration of RNF12 and the other XCI-activator(s) is increased leading to an increased probability to initiate XCI in male and female cells. The graph to the right shows the threshold level and the XCI-activator concentration in transgenic (green line) and wild type (light green line) male and female cells, according to mechanism I from A (graphs for the other mechanisms are not shown). **E)** In heterozygous and hemizygous *Tsix*-stop, ΔDXPas34, ΔCpG and pAA2Δ1.7 cells the allele specific threshold of the mutated allele is lowered (blue line), resulting in an increased probability for this allele to initiate XCI. Note that the probability for the mutated allele to initiate XCI is higher in female compared to male cells. **F)** In cells with a reduced concentration of OCT4, NANOG, SOX2, YY1 and CTCF, the threshold is lowered (blue lines), resulting in an increased probability to initiate XCI for both X chromosomes in female cells, and for the single X in male cells. Also here the probability in female cells is higher compared to male cells.

In female cells, and not in male cells, the concentration of RNF12 and other XCI-activators is expected to be sufficient to generate a probability to initiate XCI on each X chromosome. This probability is expected to be modest, but in the time window where XCI can be initiated, it will be continuously present until XCI is initiated on one or more X chromosomes, resulting in silencing of the XCI-activator genes in *cis* and a drop in the concentration of RNF12 and other XCI-activators and the probability to initiate XCI. This feedback mechanism prevents XCI on the second X in female cells, and the *Xist* promoter on this Xa will be silenced through persistent expression of *Tsix* (similar to *Xist* in male cells). Silencing is most likely consolidated by chromatin modifiers and the action of DNA methyl transferases DNMT1, DNMT3a, and DNMT3b [89, 113-114, 298]. On the Xi, *Tsix* is silenced, and it is expected that a lower concentration of RNF12 and other XCI-activators is sufficient to maintain *Xist* expression on this X chromosome.

Predictions of a stochastic model

A stochastic model for XCI predicts that every X chromosome in a nucleus has a probability to initiate XCI [179]. Using a computer simulation model we have been able to match experimentally obtained data with differentiating female XX ES cells using a probability that plateaus at a ~20% per day probability to initiate XCI for each X chromosome in a female diploid cell [189]. Applying a lower or higher probability results in too many cells with two Xa's or Xi's, respectively. Nevertheless, also with a probability of 20% a significant percentage of cells in our simulations end up with two Xa's or Xi's, resulting in a reduced number of female cells compared to male cells (12% reduction). Studies of early mouse embryos indeed indicate that female embryos are significantly smaller than male embryos between 6.5 and 10.5 dpc [979]. This effect is also present in a comparison between XO and XX female mice, suggesting a role for XCI related cell death in the reported size difference.

Besides the balance between the XCI-activator and -inhibitor concentrations that determine the probability of XCI in *trans*, allele specific thresholds will be involved in setting up the probability for each X chromosome in *cis* (**Figure 3B** and **C**). Promoter SNP's or mutations affecting transcription initiation of *Xist*, *Tsix* or *Xite*, will have an effect on the probability to initiate XCI. Indeed, a SNP in a domain of the human *XIST* promoter implicated in CTCF binding results in complete skewing of XCI in favor or against inactivation of the polymorphic allele depending on the nucleotide change [452]. Similarly, mouse *Xist* and *Xite* promoter SNPs have been reported to co-segregate with skewing of XCI [452, 980].

We recently identified RNF12 as the first transacting factor involved in activation of XCI [174]. Additional copies of *Rnf12* result in an increased probability to initiate XCI in transgenic female cells resulting in a high percentage of cells with two Xi's (**Figure 3D**). Also in *Rnf12* transgenic male cells XCI is initiated in a significant percentage of cells. Over-expression of RNF12 even results in XCI in undifferentiated *Rnf12* transgenic female cells, supporting a dose dependent role for RNF12 in activation of XCI. This also indicates that the other unidentified XCI-activators are expressed in undifferentiated ES cells. The mechanism by which RNF12 activates XCI is unclear, but ectopic induction of XCI in human RNF12 transgenic mouse cells suggests that RNF12 acts through *XIST/Xist*, as evidence for a role of human *TSIX* in XCI is missing.

In recent years, several *cis* and *trans* acting factors have been identified which are good candidates for setting up the threshold required for XCI to be initiated with a specific probability. A stochastic model predicts that a change in the threshold level will have a different effect in male *versus* female cells, because the XCI-activator level is sex dependent (**Figure 3B**, **E** and **F**). Indeed, female cells with mutations that down-regulate or completely abolish *Tsix* expression, thereby lowering the threshold, show a much higher percentage of inactivation of the mutated allele than male cells containing the same mutations (**Figure 3E**) [127, 179]. This effect could explain the reported sex-ratio distortion in hemi/homozygous *Tsix* mutant mice, in favor of male mice, which may not or only occasionally initiate XCI on the single X chromosome while female cells initiate XCI on both X chromosomes much more frequently [180]. In contrast to the ΔCpG mutation used for this study, other reported *Tsix* deletions and *Tsix* stop alleles did result in a substantial percentage of male cells showing ectopic initiation of XCI, indicating that the ΔCpG mutation represents a hypomorphic allele with a threshold that is higher than other reported *Tsix* mutations. Depletion of *Oct4* also has a more profound effect on XCI in female compared to male cells (**Figure 3F**) [186]. These findings support a role for *Tsix* and OCT4 in determining the threshold for XCI to be initiated, and show that XCI counting and initiation is regulated through an intricate balance between these factors and other inhibitors and activators of XCI. So far RNF12 is the only identified XCI-activator, which acts in concert with the XCI-inhibitors, OCT4, SOX2, NANOG, CTCF and YY1, but more XCI-activators and XCI-inhibitors are likely to be involved. Identification of all XCI-activators and -inhibitors and unraveling of the interplay between these factors will be crucial for a further understanding of the XCI process.

Acknowledgements

We would like to thank all members of the laboratory for helpful discussions, and J. Anton Grootegoed and Hikke van Doorninck for critically reading the manuscript.

Chapter 5

RNF12 activates Xist and is essential for X chromosome inactivation

This chapter has been published in

Tahsin Stefan Barakat, Nilhan Gunhanlar, Cristina Gontan Pardo, Eskeatnaf Mulugeta Achame, Mehrnaz Ghazvini, Ruben Boers, Annegien Kenter, Eveline Rentmeester, J.Anton Grootegoed and Joost Gribnau (2011)
"RNF12 activates *Xist* and is essential for X chromosome inactivation"
PLoS Genetics 2011;7(1):e1002001

Addendum:
Tahsin Stefan Barakat, Nilhan Gunhanlar and Joost Gribnau
"Mice deleted for *Xist* intron 1 mice do not show an X chromosome inactivation phenotype"
(Work in progress)

RNF12 activates *Xist* and is essential for X chromosome inactivation

Tahsin Stefan Barakat[1], Nilhan Gunhanlar[1], Cristina Gontan Pardo[1], Eskeatnaf Mulugeta Achame[1], Mehrnaz Ghazvini[1,2], Ruben Boers[1], Annegien Kenter[1], Eveline Rentmeester[1], J. Anton Grootegoed[1] and Joost Gribnau[1,3]

[1]Department of Reproduction and Development, Erasmus MC, University Medical Center, Rotterdam, The Netherlands.
[2]Erasmus Stem Cell Institute, Erasmus MC, University Medical Center, Rotterdam, The Netherlands.
[3]corresponding author

Contact details:
Joost Gribnau
Department of Reproduction and Development
Erasmus MC
Room Ee 09-71
PO Box 2040
3000 CA Rotterdam
The Netherlands
Phone +31-10-7043069
Fax +31-10-7044736
Email: j.gribnau@erasmusmc.nl

Abstract

In somatic cells of female placental mammals, one of the two X chromosomes is transcriptionally silenced to accomplish an equal dose of X-encoded gene products in males and females. Initiation of random X chromosome inactivation (XCI) is thought to be regulated by X-encoded activators and autosomally encoded suppressors, controlling *Xist*. Spreading of *Xist* RNA leads to silencing of the X chromosome in *cis*. Here, we demonstrate that the dose dependent X-encoded XCI activator RNF12/RLIM acts in *trans*, and activates *Xist*. We did not find evidence for RNF12-mediated regulation of XCI through *Tsix* or the *Xist* intron 1 region, which are both known to be involved in inhibition of *Xist*. In addition, we found that *Xist* intron 1, which contains a pluripotency factor binding site, is not required for suppression of *Xist* in undifferentiated ES cells. Analysis of female *Rnf12*$^{-/-}$ knockout ES cells showed that RNF12 is essential for initiation of XCI, and is mainly involved in the regulation of *Xist*. We conclude that RNF12 is an indispensable factor in up-regulation of *Xist* transcription, thereby leading to initiation of random XCI.

Author Summary

In all placental mammals, the males have only one X chromosome per diploid genome, as compared to the females having two copies of this relatively large chromosome, carrying more than 1000 genes. Hence, the evolution of the heterologous XY sex chromosome pair has resulted in an inevitable need for gene dosage compensation between males and females. This is achieved at the whole chromosome level, by transcriptional silencing of one of the two X chromosomes in female somatic cells. Initiation of X chromosome inactivation (XCI) is regulated by X-encoded activators and autosomally encoded suppressors, controlling *Xist* gene transcription. Spreading of *Xist* RNA in *cis* leads to silencing of one of the X chromosomes. Previously, we obtained evidence that the X-encoded E3 ubiquitin ligase RNF12 (RLIM) is a dose-dependent XCI activator. Here, we demonstrate that RNF12 exerts its action in *trans*, and find that RNF12 regulates XCI through activation of transcription from the *Xist* promoter. Furthermore, analysis of female *Rnf12*$^{-/-}$ knockout ES cells shows that RNF12 is essential for initiation of XCI and that loss of RNF12 resulted in pronounced and exclusive down-regulation of *Xist*. It is concluded that RNF12 is an indispensable factor in *Xist* transcription and activation of XCI.

Introduction

X chromosome inactivation (XCI) in placental mammals is random with respect to the parental origin of the X chromosome that undergoes inactivation, during early embryonic development [30]. In contrast, in marsupials and mouse extra-embryonic tissues XCI is imprinted. Imprinted XCI always targets the paternally inherited X chromosome (Xp), and is initiated during the early cleavage divisions [51-53]. In the inner cell mass (ICM) of the mouse blastocyst, the paternally inherited inactive X chromosome is reactivated, after which random XCI is initiated around 5.5 days of embryonic development.

In mouse, two non-coding X-linked genes, *Xist* and *Tsix*, play a central role in the random XCI mechanism. Upon initiation of XCI, *Xist* is up-regulated on the future inactive X chromosome (Xi), and the transcribed RNA spreads along the X in *cis*, directly and indirectly recruiting chromatin modifying enzymes acting to establish the Xi [74, 85-86]. *Tsix* is a negative regulator of *Xist*; the *Tsix* gene overlaps with *Xist* but is transcribed in the anti-sense direction [118-119].

Random XCI is a stochastic process in which each X chromosome has an independent probability to become inactivated [179, 189]. Initiation of XCI is thought to be regulated by X-encoded activators and autosomally encoded inhibitors [179, 910]. With two active X chromosomes, female cells will have a concentration of XCI activators two-fold higher than male cells, sufficiently different to drive XCI in female cells only. Rapid down-regulation of XCI activator genes in *cis*, after initiation of XCI on either one of the X chromosomes, prevents initiation of XCI on the second X chromosome.

XCI inhibitors are involved in maintaining a threshold for XCI to occur. So far, several XCI inhibitors have been identified, acting through different mechanisms, in mouse. YY1 and CTCF act as positive regulators of *Tsix*, by binding the DXpas34 *Tsix* regulatory element [193]. The pluripotency factors OCT4, SOX2 and NANOG were proposed to regulate XCI by binding to intron 1 of *Xist* and suppressing *Xist* expression directly [191]. OCT4 and SOX2 have also been implicated in the positive regulation of *Tsix* and *Xite*, the latter being an enhancer of *Tsix* [186]. These findings indicate that several proteins and pathways act in concert to suppress *Xist* transcription and to block *Xist* RNA spreading in *cis*.

XCI activators could act by activation of *Xist*, but also by suppression of negative regulators of *Xist* such as *Tsix* and the *Xist* intron 1 region. Recently, we identified RNF12 (RLIM) as the first X-linked activator of XCI [174]. This E3 ubiquitin ligase is involved in regulation of LIM-homeodomain transcription factors and telomere length homeostasis, through degradation of LDB1 and TRF1, respectively [893-894]. Previously, we found that additional transgenic copies of the *Rnf12* gene encoding this protein resulted in induction of XCI on the single X in transgenic male cells, and on both X chromosomes in a high percentage of female cells. XCI was also affected in *Rnf12*$^{-/-}$ ES cells supporting a dose-dependent role for RNF12 in activation of XCI. In the present study, we aimed to dissect the role of RNF12 in XCI, and we obtained evidence that RNF12 regulates XCI in *trans*, by activation of the *Xist* promoter. In addition, the generation and analysis of *Rnf12*$^{-/-}$ ES cells indicated that RNF12 is required for the XCI process and appears to be involved in XCI mainly by activation of *Xist*. The results reinforce that RNF12 is a key player in regulation of the XCI process.

Results

RNF12 acts in trans to activate XCI

XCI is regulated by several *cis* elements, and *Rnf12* is located in close proximity to *Xist* (~500kb). Therefore, we aimed to test whether all the activity of RNF12 is mediated in *trans*. Our previous studies showed that *Rnf12*$^{+/-}$ female ES cells induce XCI in a reduced number of ES cells. Here, we rescued 129/Sv / Cast/Ei (129/Cas) polymorphic *Rnf12*$^{+/-}$ female ES cells by introducing a 129 BAC (RP24-240J16) construct covering *Rnf12*. RT-PCR analysis followed by RFLP detection confirmed expression of the transgenic copies of *Rnf12* (**Figure 1A**). *Xist* RNA-FISH analysis, to detect the *Xist* coated inactive X chromosome (Xi) in day 3 differentiated transgenic ES cell lines with one additional copy of *Rnf12*, shows that XCI was restored to wild type level (**Figure 1B**). In line 20, with 5 transgenic copies of *Rnf12* the percentage of cells with one or two Xi's is even more pronounced, supporting a dose dependent role of RNF12 in XCI (**Figure 1B, 1C**). XCI is skewed in wild type 129/Cas female ES cells towards inactivation of the 129 X. This is due to the presence of different X-linked *cis* elements (Xce) that affect random choice [446]. RT-PCR detecting a length polymorphism was used to distinguish *Xist* emanating from either the 129 or the Cas alleles. We observed that skewed XCI is more pronounced in the *Rnf12*$^{+/-}$ cells, as compared to XCI in wild type cells at day 3 of differentiation (**Figure 1D**). This could be caused by selection against cells inactivating the wild type X chromosome, which would result in complete loss of RNF12 from these cells. However, RNF12 possibly is not essential for cell survival, also of differentiated cells, so that selection against cells inactivating the wild type X chromosome might point to a role for RNF12 in maintaining *Xist* expression. In the rescued cell lines, *Xist* was up-regulated from both alleles at day 3 of differentiation (**Figure 1D**). This result demonstrates that RNF12 activates XCI in *trans*.

Counteracting roles for RNF12 and NANOG

One possible mechanism for regulation of XCI by RNF12 might be a direct interaction with *Xist* RNA to target chromatin components. However, examination of day 3 differentiated female cells by immunocytochemistry detecting RNF12, together with the Polycomb protein SUZ12 which accumulates on the Xi [97-98], excludes this possibility (**Figure 2A**). Interestingly, we noticed that the RNF12 staining intensity was much more dynamic in female compared to male cells (**Figure 2B**, **Figure S1**). Also, in female cells, a SUZ12 coated Xi appeared mainly in cells with low RNF12 staining (**Figure 2A**, **Figure S2**, and data not shown). Immunostaining of differentiating female ES cells indicated a negative correlation between expression of RNF12 and NANOG, although expression was not completely mutually exclusive (**Figure 2C**). To analyze this in more detail, we targeted an *Rnf12* promoter-mCherry construct into ES cells, also harboring a knock-in GFP transgene in the *Nanog* and *Oct4* loci. We analyzed expanded individual clones and pooled clones and obtained similar results. FACS analysis, prior to differentiation and at different time points after differentiation of these double transgenic ES cell lines, showed a negative correlation between RNF12-mCherry and NANOG-GFP expression, but not for RNF12-mCherry and OCT4-GFP (**Figure 2D**, **E**, **Figure S3**). Our findings therefore suggest specific counteracting regulatory roles for RNF12 and NANOG in XCI, which might include an inhibitory effect of NANOG on *Rnf12* transcription. Interestingly, NANOG has been

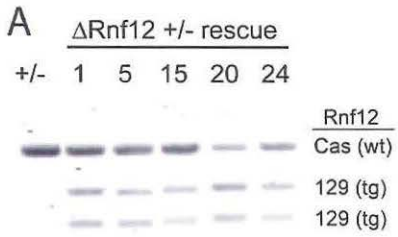

B

line	qPCR copy nr	RNA FISH day 3 1xXist	RNA FISH day 3 2xXist
ΔRnf12+/-	1	33%	0%
wild type	2	51%	1%
1	2	42%	0%
5	2	65%	5%
15	2	58%	2%
20	6	78%	17%
24	2	64%	4%

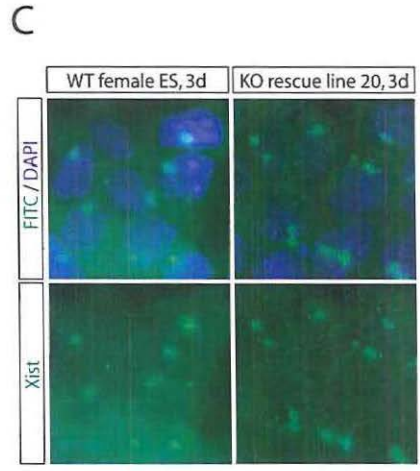

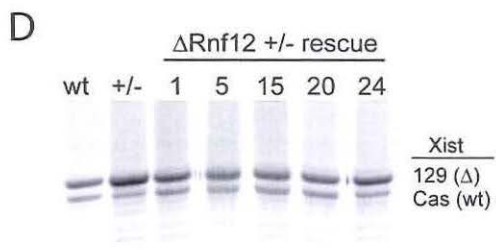

Figure 1: RNF12 activates X chromosome inactivation in *trans*
A) Allele specific RT-PCR analysis of *Rnf12* expression with RNA isolated from day 3 differentiated female *Rnf12*$^{+/-}$ ES cells (Cas/129, 129 *Rnf12* targeted), and rescued cell lines obtained after stable integration of an 129 *Rnf12* transgene. NheI digested 129 products were separated from undigested Cas products. **B)** Overview of RNA-FISH experiments detecting *Xist* expression in female wild type, *Rnf12*$^{+/-}$ and *Rnf12*$^{+/-}$ rescued cell lines. qPCR copynumber analysis was performed on genomic DNA. RNA-FISH analysis was performed on day 3 differentiated ES cells, and the percentage of cells harboring one *Xist* coated X chromosome (*Xist* cloud (=Xi), 1x *Xist*) or two *Xist* coated X chromosomes (2x *Xist*) was determined. **C)** Representative pictures of RNA-FISH analysis, detecting *Xist* (FITC) in day 3 differentiated female wild type and *Rnf12*$^{+/-}$ rescued ES cells (line 20, *Rnf12* over-expression). DNA is counterstained with DAPI in all RNA-FISH slides. **D)** Allele specific RT-PCR analysis of day 3 differentiated wild type, *Rnf12*$^{+/-}$ and *Rnf12*$^{+/-}$ rescued cell lines, detecting an *Xist* length polymorphism that discriminates 129 and Cas *Xist*.

implicated in the regulation XCI by direct suppression of *Xist* in ES cells, and *Xist* suppression in the ICM of the developing blastocyst corresponds with up-regulation of NANOG expression [367]. Therefore, mutual exclusive expression of RNF12 and NANOG may be required for initiation of XCI.

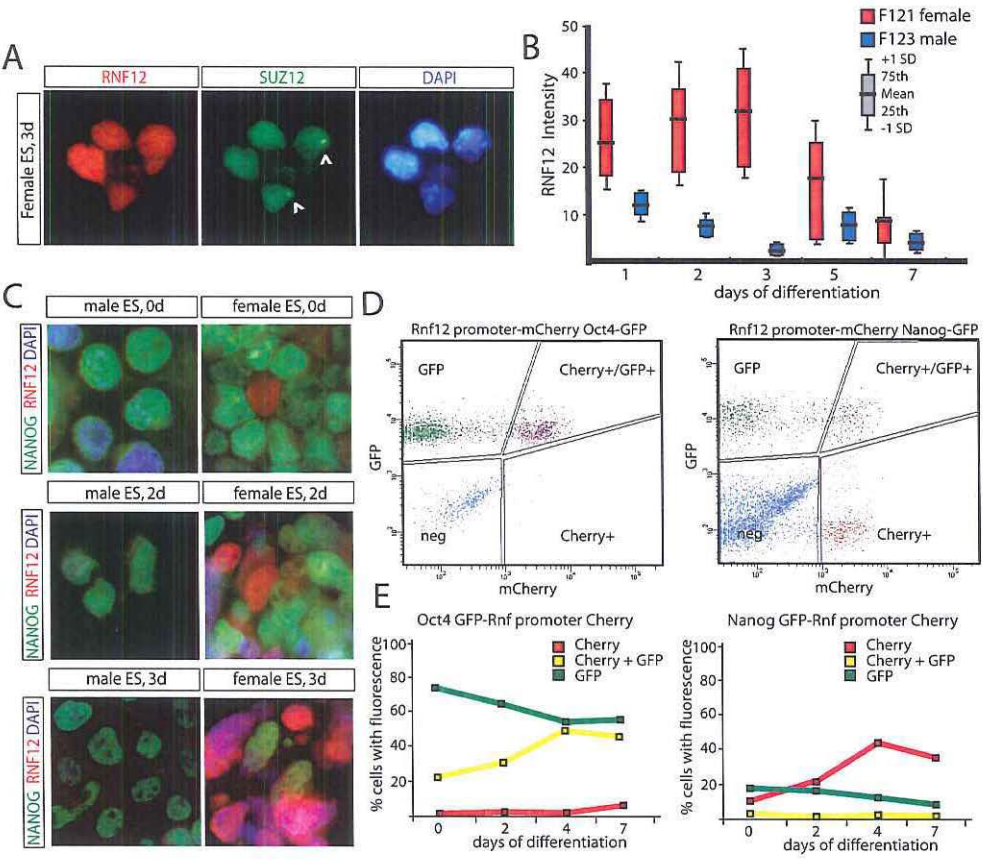

Figure 2: Counteracting roles for RNF12 and NANOG in XCI

A) Immunocytochemistry detecting RNF12 (Alexa 546) and SUZ12 (Alexa 488) in day 3 differentiated female ES cells. Cells showing accumulation of SUZ12 on the X chromosome (Xi) show low levels of nuclear RNF12, suggesting that RNF12 is downregulated upon XCI. RNF12 does not accumulate on the SUZ12 coated Xi. **B)** Quantification of RNF12 staining intensities in female and male ES cells at different timepoints of differentiation. Red and blue box plots show results for female and male cells, respectively. Mean, interquartil range and standard deviation are indicated. N > 100 cells per timepoint. Female cells show higher staining intensities and more fluctuation of RNF12 expression compared to male cells. **C)** Immunocytochemistry detecting RNF12 (rhodamine) and NANOG (FITC) in undifferentiated and day 2 and 3 differentiated male and female ES cells. **D)** FACS analysis of NANOG-GFP (right panel) and OCT4-GFP (left panel) ES cells transgenic for an *Rnf12*-mCherry promoter construct. FACS plots show results of undifferentiated ES cells. Cells are gated for GFP+, Cherry+, GFP+Cherry+ or negative. Results of a representative experiment are shown. **E)** Quantification of FACS analysis of NANOG-GFP (right panel) and OCT4-GFP (left panel) ES cells transgenic for an *Rnf12* mCherry promoter construct. Cells were differentiated for up to 7 days, and the percentage of positive cells was determined (Cherry+, red line; GFP+, green line; Cherry+GFP+, yellow line).

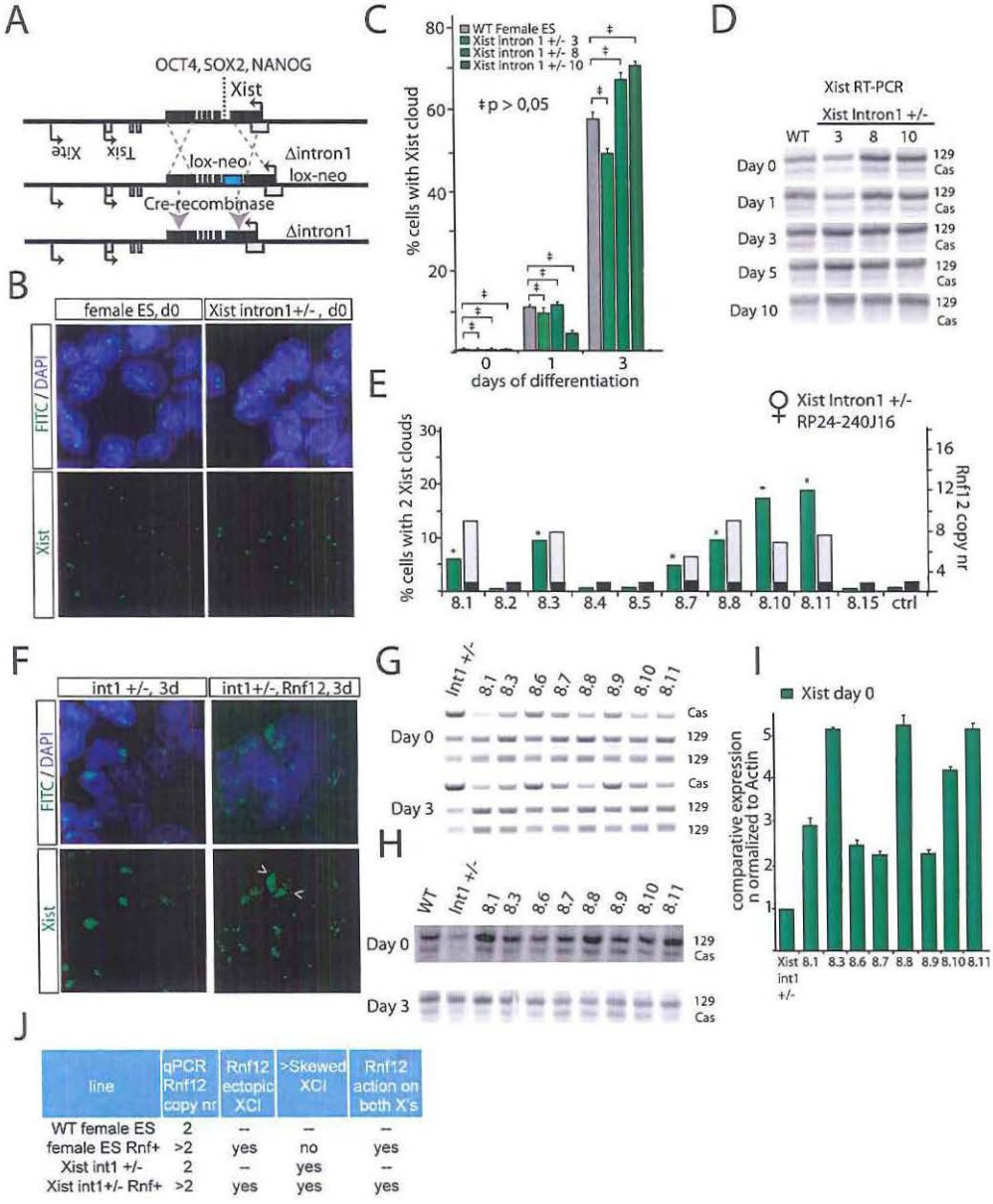

J

line	qPCR Rnf12 copy nr	Rnf12 ectopic XCI	>Skewed XCI	Rnf12 action on both X's
WT female ES	2	–	–	–
female ES Rnf+	>2	yes	no	yes
Xist int1 +/-	2	–	yes	–
Xist int1+/- Rnf+	>2	yes	yes	yes

Figure 3: RNF12 initiates XCI independent of pluripotency factor binding to *Xist* intron 1
A) Schematic representation of part of the X chromosome and the strategy to target the *Xist* intron 1 pluripotency factor binding sites. A BAC targeting construct replacing *Xist* intron 1 by a floxed neomycin resistance cassette (Neo) was used to target specifically the 129 allele in Cas/129 female ES cells. The Neo cassette was looped out after transient expression of Cre recombinase. **B)** RNA-FISH analysis detecting *Xist* (FITC) in undifferentiated female wild type and *Xist* $^{\text{intron 1+/-}}$ ES cells. In both wild type and *Xist* intron 1 deleted cells, only pinpoint signals are visible, representing basal *Xist* and *Tsix* expression.

RNF12 does not regulate XCI through Xist intron 1

Recently, the first intron of *Xist* has been identified as a region involved in recruitment of three pluripotency factors, OCT4, NANOG and SOX2 [191]. It was shown that down-regulation of *Nanog* and *Oct4*, through gene ablation, resulted in an increase in *Xist* expression, and initiation of XCI in male cells. Interestingly, the intron 1-mediated suppression of XCI was suggested to directly act on *Xist*, without involvement of *Tsix*. To study if RNF12 might regulate XCI by interfering with binding of pluripotency factors to the intron 1 region of mouse *Xist*, we removed 1.2 kb of *Xist* intron 1 including all reported NANOG, OCT4 and SOX2 binding sites by homologous recombination with a BAC targeting construct, without disturbing the integrity of the *Xist* transcript. Targeted clones were screened by PCR amplification of a targeted RFLP (BsrgI) in female F1 2-1, 129/Cas polymorphic ES cells, which was confirmed by Southern blotting, followed by Cre mediated loop-out of the kanamycin/neomycin resistance cassette (**Figure 3A**, **Figure S4**). *Xist* RNA-FISH at different time points of differentiation of several *Xist*$^{\text{intron 1}-/-}$ ES cell lines indicated that XCI is initiated with the same kinetics as in wild type cells, and showed that the intron 1 region is not required for repression of *Xist* in undifferentiated ES cells or early during initiation of XCI (**Figure 3B**, **3C**, and **Figure S4G**). Nevertheless, *Xist* specific RT-PCR, detecting a length polymorphism distinguishing 129 and Cas *Xist*, showed enhanced skewing at day 3 of differentiation towards 129 *Xist* expression, suggesting a role for the intron 1 region in suppressing *Xist* at later stages of differentiation, when NANOG, OCT4 and SOX2 are expressed at a lower level (**Figure 3D**). To test an involvement of the intron 1 region in RNF12-mediated activation of XCI, we introduced an *Rnf12* BAC transgene into the *Xist*$^{\text{intron 1}+/-}$ ES cell lines. Additional copies of *Rnf12* resulted in induction of *Xist*, even in undifferentiated ES cells (**Figure 3E**, **3F**, **3I**), confirming our previous findings [174]. However, allele specific RT-PCR did not point to an increased preference for expression of the mutated or wild type allele, in undifferentiated ES cells (**Figure 3G**, **3H**), indicating that RNF12-mediated action on XCI does not require the *Xist* intron 1 region (**Figure 3J**). At day 3 of differentiation, in several cell lines, we found higher expression of Cas *Xist* in *Rnf12* transgenic *Xist*$^{\text{intron 1}+/-}$ cells compared to *Xist*$^{\text{intron 1}+/-}$ only cells. We attribute this finding to an increase in the percentage of cells with two *Xist* clouds.

Figure 3: continued
C) Bar graph showing the percentage of wild type and *Xist* $^{\text{intron 1}+/-}$ ES cells that initiated XCI, detected by *Xist* RNA-FISH, at different time points of EB differentiation. No statistical significant differences were noticed between the wild type control and the cell lines harboring a deletion of *Xist* intron 1 (95% confidence interval, N>100 cells per time point ‡ p>0.05). **D)** Allele specific RT-PCR analysis detecting *Xist* expression in female wild type and *Xist* $^{\text{intron 1}+/-}$ cell lines (clone 3, 8 and 10) during differentiation. **E)** qPCR analysis to determine the *Rnf12* copy number in *Xist* $^{\text{intron 1}+/-}$ ES cells transgenic ES cell lines (transgenic, grey, and endogenous, black, copy number), and percentage of cells with two *Xist* clouds at day 3 of differentiation. **F)** RNA-FISH analysis detecting *Xist* (FITC) in day 3 differentiated *Xist* $^{\text{intron 1}+/-}$ ES cells, without (left panels) and with (right panels) an *Rnf12* transgene. The *Xist* clusters in one cell with two *Xist* clusters are indicated with arrowheads. **G)** RFLP RT-PCR amplifying a NheI RFLP present on the endogenous129 *Rnf12* allele, and the *Rnf12* transgene. Relative expression analysis was performed with RNA isolated from undifferentiated and day 3 differentiated ES cell lines. **H)** RT-PCR amplifying a length polymorphism distinguishing *Xist* emanating from the mutated 129 allele and the wild type Cas allele, with RNA isolated from undifferentiated and day 3 differentiated ES cell lines. **I)** *Xist* expression in undifferentiated *Rnf12* transgenic *Xist* $^{\text{intron 1}+/-}$ ES cells, and an *Xist* $^{\text{intron 1}+/-}$ control cell line was quantified qPCR. **J)** Table summarizing the results obtained with female wild type, *Rnf12* transgenic, *Xist* $^{\text{intron 1}+/-}$ and *Xist* $^{\text{intron 1}+/-}$ *Rnf12* transgenic ES cell lines.

We conclude that the *Xist* intron 1 region is not essential for suppression of XCI in undifferentiated ES cells, but may play a role later during differentiation. Furthermore, RNF12-mediated activation of XCI is independent from the *Xist* intron 1 region.

RNF12 regulates Xist

RNF12 could regulate XCI through activation of *Xist* or suppression of *Tsix*, or both. Previously, we analyzed *Xist* transgenic male ES cell lines with a BAC RP24-180B23 integration covering *Xist* only [174], or a BAC RP23-338B22 sequence containing both *Xist* and *Tsix* (**Figure 4A**). These male transgenic ES cell lines also contained 16 copies of an ms2 bacteriophage repeat sequence located in exon 7 of the endogenous *Xist* gene, allowing separate detection by RNA-FISH of autosomal versus endogenous *Xist* spreading [92]. Differentiation of transgenic male ES lines containing the *Xist-Tsix* transgene resulted in expression of *Xist* from the autosomal integration site in cell lines containing multicopy integrations. Autosomal spreading of *Xist* in these cell lines is most likely due to accumulation of enough *Xist* RNA to silence at least one copy of *Tsix*, allowing spreading of *Xist* in *cis*. Integration of truncated transgenes that lack *Tsix* would facilitate this process [174]. This also explained autosomal *Xist* spreading in BAC RP-24-180B23 single copy male transgenic ES cell lines upon differentiation, because *Tsix* is not covered by this BAC [174]. We used two of these, *Xist* only, BAC RP-24-180B23 ES cell lines to introduce 129 BAC RP24-240J16 transgenes covering *Rnf12*, and found *Xist* spreading on the single endogenous X (**Figure 4B** and **C**), confirming previous results. We also found a significant increase in the number of cells with autosomal *Xist* spreading, indicating that RNF12 activates XCI through *Xist*. Next, we introduced an *Rnf12* transgene (BAC RP24-240J16) in a single copy *Tsix* male transgenic ES cell line that lacks transgenic *Xist* (BAC RP23-447O10). These double transgenic ES cell lines contain a Cas X chromosome which allowed RFLP mediated discrimination of endogenous (Cas) and transgenic (129) *Tsix*. Analysis of these cell lines indicated that transgenic over-expression of RNF12 does not lead to down-regulation of *Tsix*, as measured by qPCR and by RNA-FISH examining the relative number of *Tsix* pinpoint signals (**Figure 4D**, **E** and **G**). Interestingly, allele specific RT-PCR indicated that endogenous *Tsix* (Cas) is even down-regulated in samples with higher *Xist* expression, indicating *Xist*-mediated silencing of *Tsix* in *cis* (**Figure 4F**). Taken together, these results indicate that *Xist* and not *Tsix* is the functionally most important downstream target of RNF12.

RNF12 is required for XCI

We previously found that the rate of initiation of XCI is reduced in differentiating female $Rnf12^{+/-}$ ES cells, compared to wild type ES cells [174]. The RNF12 protein level in these $Rnf12^{+/-}$ female cells is equal to that in male cells [174], but XCI is still occurring at a higher rate than in male cells. This indicated the presence of additional X-encoded XCI activators, but did not exclude the possibility that RNF12 is essential for XCI. To address this point, we generated $Rnf12^{-/-}$ female ES cells by targeting the wild type Cas *Rnf12* allele in $Rnf12^{+/-}$ ES cells (**Figure 5A**). Correct targeting was confirmed by RT-PCR, showing loss of a targeted RFLP located in exon 5 of *Rnf12* (**Figure 5B**). The presence of two X chromosomes in these $Rnf12^{-/-}$ female ES cells was ascertained by X chromosome DNA-FISH analysis and amplification of an RFLP in the *Xist* gene (**Figure 5C**, and data not

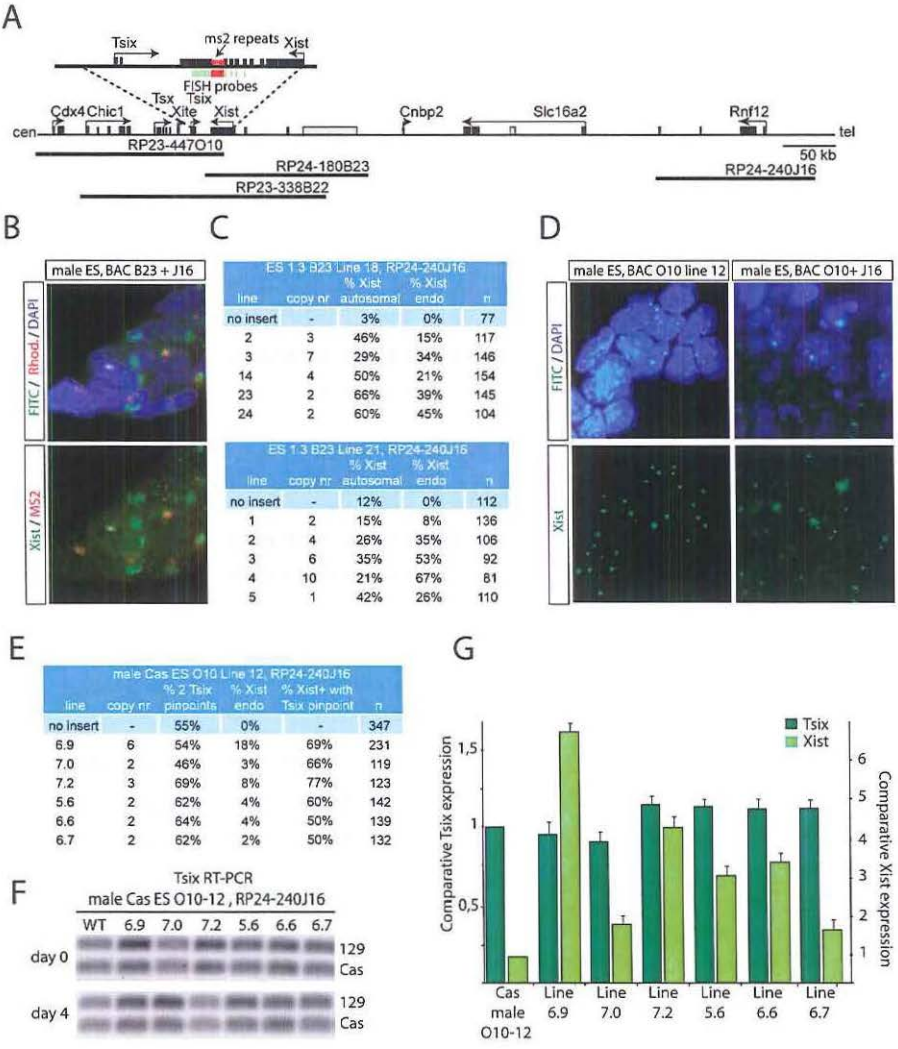

Figure 4: RNF12 activates *Xist* directly, but does not inhibit *Tsix*
A) Map showing part of the mouse X chromosome, the location of the BAC sequences used, and the position of ms2 repeats within *Xist*. RNA-FISH probes are indicated in green and red, and non-annotated genes in grey. **B)** RNA-FISH analysis detecting endogenous *Xist* (ms2, rhodamine and FITC positive) and exogenous *Xist* (FITC) from the autosomally integrated *Xist*-only BAC RP24-180B23 in day 3 differentiated male ES cells transgenic for *Rnf12* (BAC RP24-240J16). **C)** Table summarizing RNA-FISH results from B). Copy number of the *Rnf12* transgene was determined by gDNA qPCR. Shown are the percentage of autosomal and endogenous *Xist* clouds; N, number of cells analyzed. **D)** RNA-FISH analysis detecting endogenous and transgenic *Tsix* (FITC, pinpoint signals) and endogenous *Xist* (FITC, clouds) in day 3 differentiated *Tsix* transgenic male cells (left panels) and day 4 differentiated *Tsix* transgenic male cells with additional copies of an *Rnf12* transgene (right panels).**E)** Table summarizing results obtained with single copy *Tsix* transgenic male ES cell lines with a *Rnf12*

shown). Western blotting analysis confirmed the absence of RNF12 protein in the knockout cells (**Figure 5D**). RT-PCR and qRT-PCR of pluripotency associated genes and differentiation markers gave information that differentiation of the *Rnf12*$^{-/-}$ ES cells was not different from that of wild type ES cells (**Figure 5E, 5F** and **Figure S5**). However, *Xist* RNA-FISH analysis showed that differentiating *Rnf12*$^{-/-}$ ES cells only sporadically initiate XCI (**Figure 5G, H** and **I**). qPCR analysis confirmed that *Xist* is not detectably up-regulated when measured for a population of *Rnf12-/-* cells upon differentiation. Moreover, DNA-FISH detecting a whole chromosome X paint probe at day 7 and 10 of differentiation excluded X chromosome loss (**Figure S5**). The few *Rnf12*$^{-/-}$ cells that initiated XCI appeared in clusters, suggesting clonal expansion of a few cells that initiated XCI (**Figure S5**). We therefore conclude that RNF12 is an essential factor in XCI.

RNF12 activates the Xist promoter

Evidently, the *Rnf12*$^{-/-}$ knockout cells present the possibility to study control of gene expression by RNF12. Therefore, we next performed micro-array expression analysis comparing day 3 differentiated *Rnf12*$^{-/-}$ and wild type cells. We found that *Xist* was the only gene that was subject to differential regulation, showing pronounced down-regulation (**Figure 5J**). Interestingly, none of the known downstream targets of RNF12 appeared affected in our analysis. This may be due to our ES cell differentiation system resulting in a mixed population of cells at different stages of differentiation. In addition, the 3-day-time span allowed in our studies for cell differentiation may have prevented detection of effects on downstream targets which are expressed at later stages of differentiation. Nevertheless, our results indicate that the main function of RNF12 at this early stage of differentiation concerns the regulation of XCI. The observed dependency of *Xist* transcription on RNF12 might be effectuated by RNF12 acting through the *Xist* promoter. To test this, we expressed *Xist* promoter luciferase reporter constructs, both transiently and stably, in wild type female and *Rnf12*$^{-/-}$ ES cell lines and differentiated these cells for 3 days. The results revealed an unequivocal correlation between RNF12 expression and luciferase expression (**Figure 5K**). Our results therefore demonstrate that RNF12 activates the *Xist* promoter, although this does not exclude a role for other *cis* regulatory sequences, further away from the *Xist* promoter, in RNF12-mediated activation of XCI.

Figure 4: continued
transgene, 4 days after differentiation. Shown are copy number of the *Rnf12* transgene, percentage of cells with two *Tsix* signals, cells with an *Xist* cloud, and the percentage of cells with an *Xist* cloud and *Tsix* pinpoint signal (n is number of cells analyzed). **F)** Allele specific RT-PCR detecting transgenic (129) and endogenous (Cas) *Tsix* in undifferentiated and day 4 differentiated *Tsix /Rnf12* double transgenic ES cells. **G)** qPCR analysis to quantify *Xist* and *Tsix* expression in day 4 differentiated *Tsix /Rnf12* double transgenic ES cells, and a control cell line without an *Rnf12* transgene.

Discussion

In ES cells, RNF12 exerts its main function in XCI

Here, we present evidence that RNF12 is an essential activator of random XCI. RNF12 acts in *trans* on the *Xist* promoter, in differentiating mouse ES cells, to activate *Xist* transcription, leading to *Xist* RNA cloud formation and spreading of the silencing complex over the future inactive X chromosome in *cis*. Although our results show that RNF12 acts in *trans*, it is to be expected that the close proximity of the *Rnf12* gene to the *Xist* locus, taken together with the dose-dependent action of RNF12, is quite crucial for well-tuned regulation of XCI. Such proximity most likely facilitates rapid down-regulation of *Rnf12* in *cis* upon initiation of XCI, leading to a lower nuclear RNF12 content, thereby preventing inactivation of the second X chromosome.

Whole genome expression analysis suggests that the major function of RNF12 in ES cells is its regulation of *Xist* RNA expression, hence XCI. This is a very surprising finding, as RNF12 has been implicated in many other biological pathways. Apparently, in the present cell differentiation system, loss of expression of RNF12 does not cause a deviation from the wild type differentiation process to such an extent that it affects gene expression other than that of *Xist*. However, also based on our studies we do not exclude a function for RNF12 at later stages of cell differentiation, or in mouse development. In addition, redundant pathways or proteins such as RNF6, a close homologue of RNF12, may prevent full phenotypic expression of loss of RNF12. However, RNF12 exerts a predominant role in targeting *Xist*, as evidenced by our observation that *Xist* is largely silenced in the RNF12 deficient cells.

While our manuscript was under review, Shin et al. (2010) published a paper suggesting that RNF12 might be required in particular for imprinted XCI in mice [981]. Remarkably, that study included the observation that RNF12 depletion did not prevent initiation of random XCI in a significant percentage of *Rnf12-/-* ES cells derived from mouse blastocysts. This discrepancy with our findings might be explained by experimental differences, such as differences concerning the design of the knockout, the genetic background of the ES cells, or the cell derivation and culture procedures. Differences in cell differentiation protocols have been shown to have a pronounced impact on the XCI process [982]. Also, ES cells derived from embryos with a different genetic background could express XCI activators and XCI inhibitors at different levels, allowing XCI in either a lower or a higher percentage of *Rnf12-/-* cells. Future studies comparing the two independently generated *Rnf12-/-* ES cell lines will yield useful information about these points.

Other XCI activators

Although our observations provide evidence that RNF12 is an essential factor for the XCI process to occur in differentiating ES cells, we anticipate that other XCI activators act in parallel, and might independently regulate *Xist* or *Tsix*, or both. Dosage compensation mechanisms in species such as *D. melanogaster* and *C. elegans* also involve multiple factors and pathways, possibly leading to increased fidelity of these mechanisms [899]. In such a mechanism involving multiple factors, RNF12 would be the dose-dependent factor that is required to exceed the cumulative threshold limit to proceed towards initiation of XCI. It is feasible that female *Rnf12*$^{-/-}$ cells sometimes do initiate XCI (**Figure 6A**), as a consequence of the stochasticity of the process. This would be compatible with a

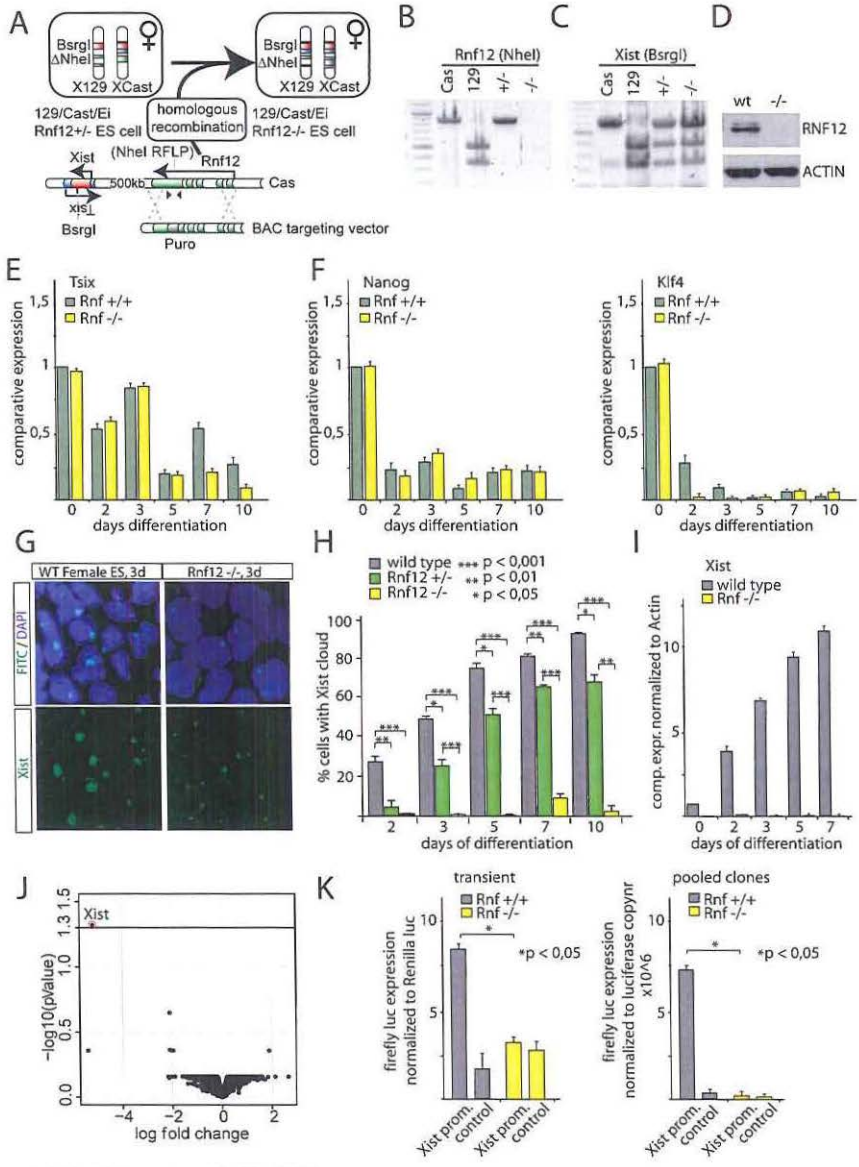

Figure 5: RNF12 is essential for XCI

A) Targeting strategy to generate *Rnf12*$^{-/-}$ ES cells. The Cas *Rnf12* allele of the previously generated heterozygous *Rnf12*$^{+/-}$ ES cells (Cas/129) was targeted with a BAC construct containing a puromycin selection cassette disrupting the open reading frame of *Rnf12*. **B)** PCR RFLP analysis with primers spanning a NheI RFLP descriminating the Cas (no NheI site) and the 129 (NheI site present) alleles, which was used to insert the targeting cassette. **C)** PCR RFLP analysis confirming the presence of two X chromosomes in *Rnf12*$^{-/-}$ ES cells. PCR primers span a BsrgI RFLP located in *Xist*. **D)** Western

mechanism, in which the combined total activity of all putative XCI activators exclusive of RNF12 is just below or around the threshold to initiate XCI. Interestingly, *Xist* cloud formation is also sporadically found in male cells, but in contrast to female *Rnf12*$^{-/-}$ cells, this represents a lethal condition and will be selected against.

Our studies indicate that RNF12 participates in *Xist* promoter activation, through an action which requires the presence of the minimal promoter. Although the direct protein target(s) of RNF12 remain elusive, its reported E3 ubiquitin ligase activity [893] would be compatible with RNF12 targeting an inhibitor of *Xist* transcription through proteasome-mediated degradation. This does not exclude that RNF12 might be involved, in addition or alternatively, in activation of a transcription factor driving *Xist* expression through positive regulation of transcription. Furthermore, RNF12 could be involved in regulation of *cis*-regulatory sequences other than the *Xist* promoter, yet to be identified and further away from the *Xist* locus.

A function for RNF12 in maintaining Xist expression

Selection against cells inactivating the X chromosome containing the wild type allele of *Rnf12* in the heterozygous *Rnf12*+/- ES cells could point to a continued requirement for *Rnf12* in maintaining *Xist* expression, following the early stages of differentiation. From the fact that male *Rnf12*-/*Y* knockout male mice are viable [981], it can be concluded that RNF12 deficiency is compatible with survival of differentiated cells in which XCI does not play any role. Hence, it would be difficult to explain the observed selection against cells inactivating the wild type X chromosome in the heterozygous *Rnf12*+/- ES cells by loss of any possible function of RNF12 independent of XCI. If RNF12 would be required for maintaining *Xist* expression and XCI, the cells inactivating the wild type allele and becoming deficient in RNF12 can be expected to lose *Xist* expression and to reactivate the Xi. In contrast, cells inactivating the X chromosome containing the mutated allele, keeping one functional allele of *Rnf12*, will be able to maintain *Xist* expression and XCI. In a population of cells this will lead in skewed XCI of the mutated allele. In fact, such a mechanism might also be relevant to explain the reported defect in imprinted XCI resulting from an *Rnf12* mutation [981].

Figure 5: continued
analysis of RNF12 protein and ACTIN in wild type and *Rnf12*$^{-/-}$ ES cells. **E)** qRT-PCR analysis detecting *Tsix* expression in female wild type and *Rnf12*$^{-/-}$ ES cells differentiated for up to 10 days. Results were normalized to Actin. **F)** qRT-PCR analysis as in (H), but now detecting Nanog (left graph) and Klf4 (right graph) expression. **G)** RNA-FISH analysis detecting *Xist* (FITC) in day 3 differentiated female wild type and *Rnf12*$^{-/-}$ ES cells. **H)** Bar graph showing the percentage of female wild type, *Rnf12*$^{+/-}$ and *Rnf12*$^{-/-}$ ES cells that initiated XCI, as determined by *Xist* RNA-FISH, at different time points of differentiation. *** $p<0.001$; ** $p<0.01$; * $p<0.05$, Student's T-test. **I)** qRT-PCR detecting *Xist* in female wild type and *Rnf12*$^{-/-}$ ES cells differentiated for up to 7 days. Results were normalized to *Actin*. **J)** Genome wide expression analysis comparing day 3 differentiated *Rnf12*$^{-/-}$ and wild type ES cells. Shown are the Log fold expression change and the adjusted P value. **K)** Luciferase assay detecting expression of an *Xist*-promoter-luciferase construct in female wild type and *Rnf12*$^{-/-}$ ES cells differentiated for 3 days. For transient experiments, cells were co-transfected at day 0 with the *Xist*-promoter-luciferase or control vector (empty luciferase vector) and a Renilla plasmid. Results were normalized to Renilla expression. For stable pooled clones, the promoter constructs were transfected, clones were pooled after selection and differentiated 3 days prior to analysis.

Imprinted XCI involves activation of *Xist* on the Xp, and the observed phenotype concerns lack of this imprinted XCI of the Xp when the mutant *Rnf12* allele is inherited from the mother. It was observed that no female embryos were born, inheriting a mutated *Rnf12* allele from either a $Rnf12^{-/-}$ or a $Rnf12^{+/-}$ mother in crosses with wild type males. In contrast, the mutated allele was transmitted to male offspring. Maternal storage of RNF12 in the oocyte was proposed to play a crucial role in imprinted silencing of the Xp in the early embryo [981]. *Rnf12* is at a 46cM distance of the centromere, so that it can be expected that many haploid oocytes generated by the first meiotic division (the reduction division) of $Rnf12^{+/-}$ oocytes, which occurs at the time of ovulation, will contain both wild type and *Rnf12* mutated alleles, as a consequence of meiotic recombination. Hence, we anticipate that there will be ongoing expression of *Rnf12* in a high percentage of oocytes transmitting the mutated *Rnf12* allele, until fertilization triggers meiotic division II. The recombined wild type and mutant alleles which are present within one haploid oocyte, will be exposed to the same maternal storage of RNF12. Taken together with the observation that $Rnf12^{+/-}$ oocytes did not give rise to female offspring carrying the mutant allele, whereas female offspring carrying the wild type allele were obtained at the expected mendelian ratio from these oocytes [981], this argues against a predominant role for maternal storage in imprinted XCI. Rather, we favor the hypothesis that continued transcription of *Rnf12* throughout ovulation and after fertilization is required for sustained expression of RNF12, activation of *Xist* from the Xp, and maintenance of the inactive Xp. Future research will be required to address this hypothesis.

The link to pluripotency

Our results indicate a negative correlation between NANOG and RNF12 expression. NANOG and the other pluripotency factors OCT4 and SOX2 have been shown to be recruited to the *Xist* intron 1 region in undifferentiated ES cells, and were proposed to play a role in *Tsix* independent suppression of *Xist* [191]. In this regulatory mechanism, ablation of *Tsix* did not result in up-regulation of *Xist* in undifferentiated ES cells, and *Tsix* was not required for repression of *Xist* located on the inactivated paternal X chromosome in the inner cell mass. This pointed to an important role for recruitment of NANOG, OCT4 and SOX2 to *Xist* intron 1 in suppression of *Xist* in ES and ICM cells [191]. However, the present findings show that the intron 1 region is dispensable, in silencing the XCI process in undifferentiated ES cells. Deletion of *Xist* intron 1 caused an effect, but only in the form of skewing of XCI, which was notable at later stages of differentiation. Interestingly, a previous study analyzing an *Xist* mutant allele that lacks the intron 1 region but leaves the *Xist* promoter intact, also did not show up-regulation of the mutated allele in undifferentiated ES cells [94]. Although these latter results support our findings, they should be interpreted with caution because the selection cassette was still present in the cells analyzed by Marahrens et al. [94].

Like for the role of RNF12, this points to the presence of additional mechanisms, involved in suppression of XCI. *Tsix* and *Xite* are the most likely candidate genes taking part, and the combined action of these repressive mechanisms may be sufficient to suppress *Xist*. However, even with all the repressive elements in place RNF12 can induce *Xist* expression and XCI in undifferentiated ES cells [174]. This points towards another

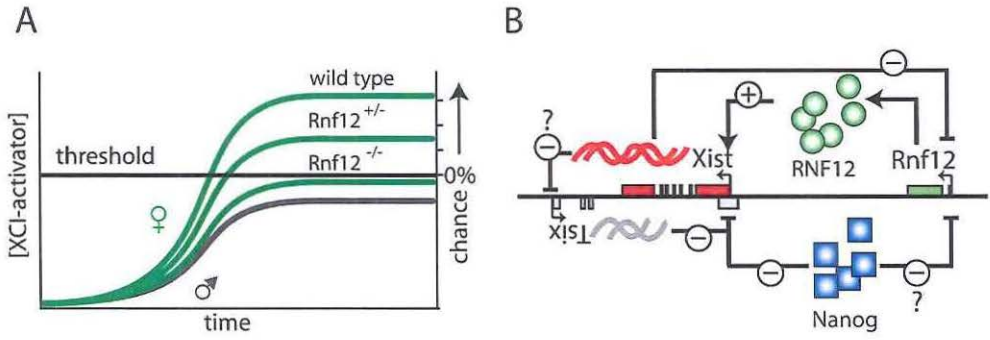

Figure 6: RNF12 and its role in the XCI regulatory network
A) In wild type and *Rnf12*$^{+/-}$ cells the XCI activator concentration is above the threshold required to generate a probability to initiate XCI. In contrast, in most *Rnf12*$^{-/-}$ cells the XCI activator concentration is not sufficient to reach the threshold required to initiate XCI. **B)** The regulatory network of XCI. *Xist* is repressed in *Tsix* dependent and independent pathways (NANOG binding in intron 1). Activation of XCI is accomplished by RNF12 through activation of the *Xist* promoter, and possibly *Xist* mediated silencing of *Tsix*. Finally, *Rnf12* is repressed by *Xist* and possibly NANOG.

mechanism involved in *Xist* suppression, in which the nuclear concentration of the XCI activator may be too low in undifferentiated ES cells and ICM cells to allow *Xist* expression and initiation of XCI, even in the absence of repressive elements such as the intron 1 region. Future research should clarify whether these mechanisms indeed act synergistically in silencing the XCI process.

The negative correlation of RNF12 and NANOG expression that we report could reflect the differentiation state of the ES cells, and does not necessarily entail a cross-regulatory role for these proteins. Nevertheless, NANOG and other pluripotency factors are also recruited to the *Rnf12* promoter in ES cells, where it might be involved in down-regulation of *Rnf12* (**Figure 6B**) [983], which opens the intriguing possibility that NANOG might also be implicated in regulation of the initiation of XCI through suppression of *Rnf12*. This highlights the complexity of the overall mechanism and the interconnection of the different players involved in XCI, but also reinforces the predominant role of RNF12 in this process.

Methods

ES cell culture

ES cells were grown in standard ES medium containing DMEM, 15% foetal calf serum, 100 U ml^{-1} penicillin, 100 mg ml^{-1} streptomycin, non-essential amino acids, 0.1mM ß-mercaptoethanol, and 1000 U ml^{-1} LIF. To induce differentiation, ES cells were split, and pre-plated on non-gelatinised cell culture dishes for 60 minutes. ES cells were then seeded in non-gelatinised bacterial culture dishes containing differentiation medium to induce embryoid body (EB) formation. EB-medium consisted of IMDM-glutamax, 15% foetal calf serum, 100 U ml^{-1} penicillin, 100 mg ml^{-1} streptomycin, non-essential amino acids, 37.8 µl l^{-1} monothioglycerol and 50 µg/ml ascorbic acid. EBs were plated on coverslips 1 day prior to harvesting, and allowed to grow out.

Transgenesis and generation of Knockout ES cell lines

For the *Rnf12* rescue experiments, an ampicillin-puromycin resistance cassette was inserted in the backbone of BAC RP24-240J16 by homologous recombination in bacteria. The modified BAC was electroporated in to female heterozygous *Rnf12+/-* cells [174], and colonies were picked after 8-10 days of puromycin selection, expanded and differentiated. BAC copynumber was determined by qPCR, and transgene specific expression was determined by allele specific RT-PCR, as described previously [174].

To generate the female homozygous *Rnf12 -/-* ES cell line, the previously generated *Rnf12+/-* ES cell line was targeted with an *Rnf12* BAC targeting construct containing an ampicillin-puromycin cassette disrupting the open reading frame of *Rnf12*. To generate this targeting construct, targeting arms were PCR amplified using primers GCCTTCGAACATCTCTGAGC, GAGCCGGACTAATCCAAACA, cloned into pCR-BluntII-TOPO (Invitrogen), and linearized with NheI to introduce an ampicillin-puromycin cassette from pBluescript. The targeting cassette was inserted in a Cast/Ei *Rnf12* BAC RP26-81P4 by homologous recombination in bacteria, and the resulting construct was used to target specifically the Cast/Ei X chromosome of the *Rnf12 +/-* ES cell line. Colonies were selected under neomycin and puromycin selection, and the absence of *Rnf12* expression was confirmed by Western analysis.

To generate the *Xist* intron 1 deletion, a BAC targeting construct was generated by homologous recombination, replacing intron 1 by a floxed neomycin cassette. Targetting arms were PCR amplified using primers 5'Forw: CATCAGGCTTGGCAGCAAGT, 5'R: CCTTGTTGGTCCAGACGACTATT and 3'Forw: CCAGACCAGGTCTTTGTATGCA, 3'Rev: GTGCTCCTGCCTCAAGAAGAA. Correctly targeted clones were identified by allele specific RFLP analysis using primers CAGTGGTAGCTCGAGCCTTT and CCAGAAGAGGGAGTCAGACG, followed by BsrGI digestion. The neomycin cassette was removed by transient transfection with a CrePAC vector and selection with puromycin. The final cell lines were verified by Southern blotting.

Rnf12 and Xist reporter constructs

To generate the *Rnf12* promoter cherry reporter cell lines, the *Rnf12* promoter was PCR amplified using previous described primers [984], and cloned into pCR-BluntII-TOPO and sequence verified. The *Rnf12* promoter was then released from pCR-BluntII-TOPO by digestion with SacI and KpnI, and blunt cloned into an AseI-BamHI fragment from pmCherry-N1 (Clonetech), thereby replacing the pCMV promoter of pmCherry-N1 with the *Rnf12* promoter. The resulting construct was used to electroporate in Oct-GFP and Nanog-GFP ES cell lines. Both pooled cell lines and single colonies were expanded, and cherry expression was analysed by FACS analysis using a BD FACSAria apparatus.

The *Xist* promoter was amplified using primers: TCCCAAGGTATGGAGTCACC, and GGAGAGAAACCACGGAAGAA, and cloned into pGL3-basic vector. As a control, the promoter less pGL3-basic vector was transfected.

Stable pooled cell lines of wild type or *Rnf12* -/- ES cells were generated by co-transfection with a puromycin or hygromycin selection vector. Expression of Luciferase was determined using the Bright-Glo luciferase assay system (Promega) and measured using a Promega luminometer. Results were normalized to the amount of protein present in the cell lysate measured by nanodrop, and copynumber of *Xist* promoter integration determined by qPCR. qRT-PCR using primers detecting luciferase (TCTAAGGAAGTCGGGGAAGC and CCCTCGGGTGTAATCAGAAT) confirmed the results obtained. For transient luciferase experiments, cells were co-transfected using the *Xist* reporter constructs and a control Renilla construct, using Lipofectamine 2000. Luciferase activity was measured using the Dual Glo luciferase system (Promega)

Xist RNA-FISH, immunofluorescence and Western analysis

Xist RNA-FISH was performed as described [174, 179]. Immunofluorescence was performed using standard procedures. RNF12 and NANOG were detected using a mouse anti- RNF12 antibody (1:250, Abnova), and a rabbit anti-NANOG antibody (1:100, SC1000, Calbiochem). ImageJ software was used to measure staining intensities; at least 100 cells were measured for each indicated time point, and background correction was performed. Western blotting was performed as previously described [174].

Expression analysis

RNA was isolated using Trizol reagent (Invitrogen) using manufacturer's instructions. DNAse treatment was performed, and cDNA was prepared using SuperScriptII (Invitrogen), using random hexamers. qRT-PCR was performed using a Biorad thermocycler, using primers described in **Table S1**. Results were normalized to *Actin*, using the ΔCT method.

Whole genome wide expression analysis of female wild type and *Rnf12*-/- ES cells differentiated for 3 days was performed with Affymetrix Mouse Genome 430 2.0 Arrays. Differentially expressed genes were identified using Limma (Bioconductor package) in R software.

Acknowledgements

We would like to thank Cathérine Dupont for helpful comments and help with experiments. Rudolf Jaenisch for supplying Nanog-GFP and Oct4-GFP ES cell lines. Elvira Myronova, Selma van Staveren and Reinier van der Linden are acknowledged for their help with experiments. We also thank all department members for helpful discussions.

Supplemental Data

Supplemental Data contains five figures and one table.

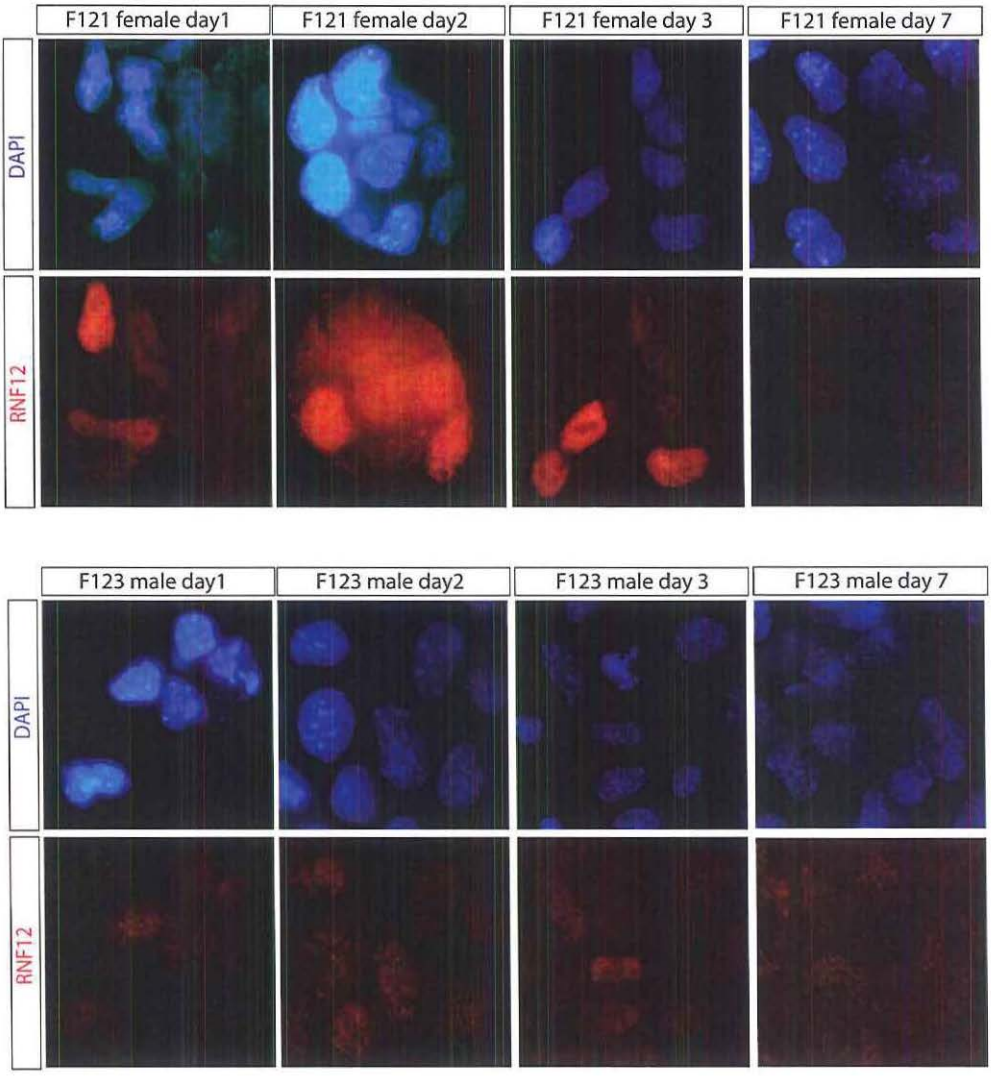

Figure S1
Immunocytochemistry detecting *RNF12* (rhodamine) at different stages of differentiation of female and male ES cells.

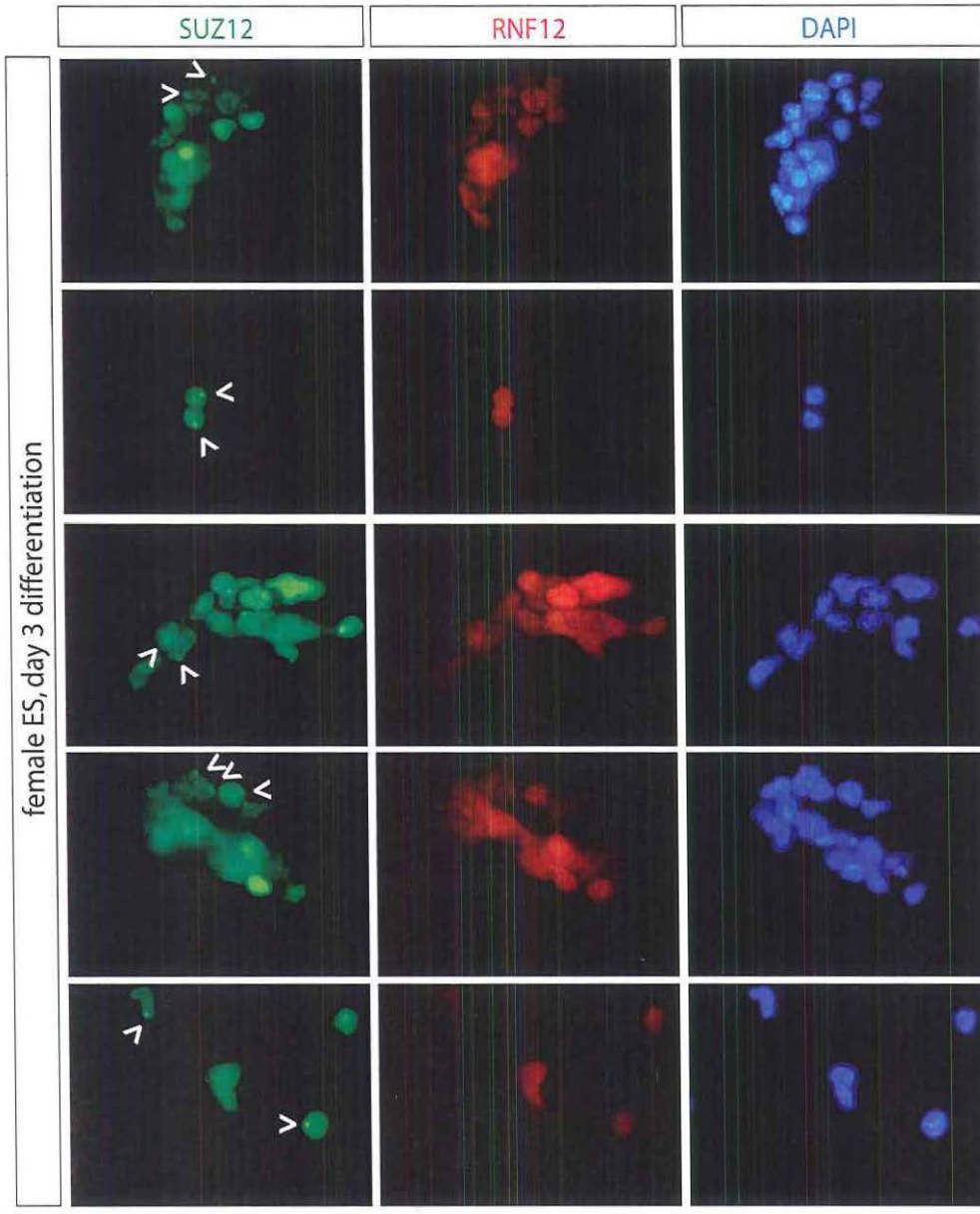

Figure S2
Immunocytochemistry detecting *RNF12* (rhodamine) and *SUZ12* (FITC) in day 3 differentiated female ES cells. *SUZ12* accumulations on the Xi are indicated with arrowheads.

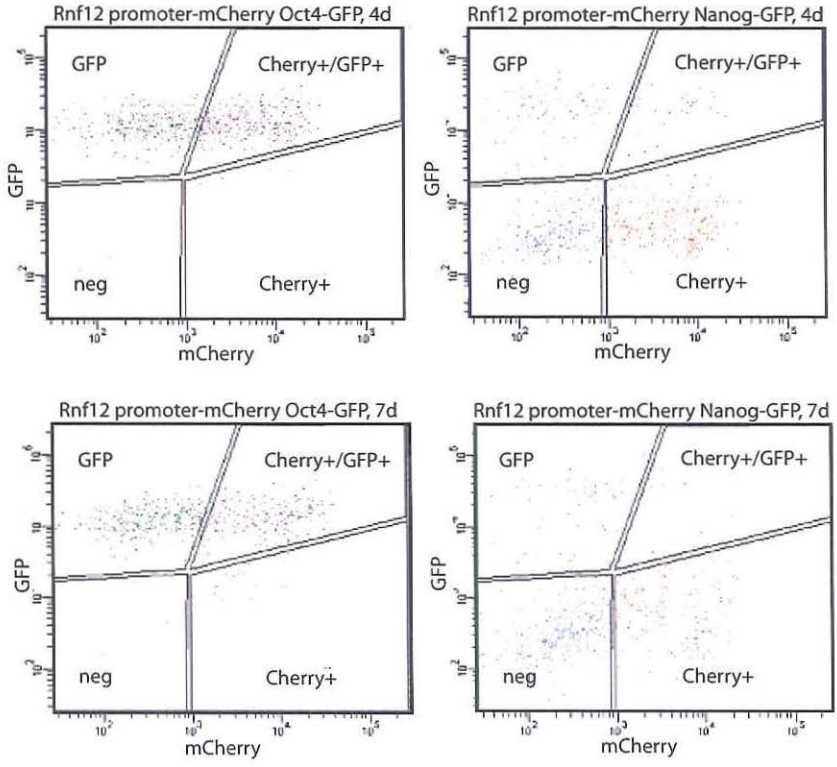

Figure S3
FACS analysis of NANOG-GFP (right panel) and OCT4-GFP (left panel) ES cells transgenic for an *Rnf12*-mCherry promoter construct. FACS plots show results of day 4 (upper panel) and day 7 (lower panel). Cells are gated for GFP+, Cherry+, GFP+Cherry+ or negative. 10.000 cells analyzed per time point.

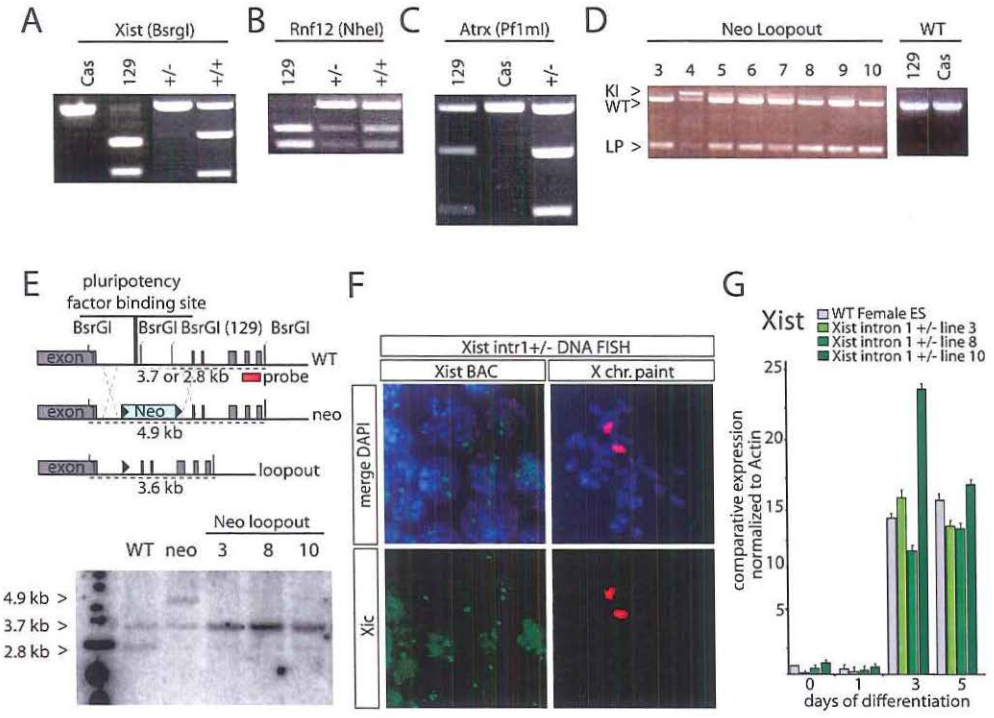

Figure S4

A) RFLP-PCR amplifying a BsrgI RFLP located in *Xist* intron 1. The BsrgI site is present on the targeted 129 allele, and is disrupted by the targeting event. **B,C)** Analysis of RFLPs in *Rnf12* (B) and *Atrx* (C) confirmed the presence of 2 X chromosomes in *Xist* intron 1 targeted ES cells. **D)** Confirmation of loop out of the neomycin resistance cassette. Primers amplify a region across the neomycin cassette. **E)** Map and targeting strategy for the intron 1 deletion. The map shows expected allele specific fragment sizes prior to, and after targeting and Cre mediated loopout. Bottom panel shows Southern analysis of female wild type, *Xist* $^{intron\ 1+/-}$ neo clone (neo) and neo loop out clones 3, 8 and 10. **F)** DNA-FISH detecting the *Xist* locus in *Xist* $^{intron\ 1+/-}$ cells (left panels), and X-paint DNA-FISH analysis (Rhodamine red, right panels). **G)** qRT-PCR analyzing *Xist* expression in female wild type and *Xist* $^{intron\ 1+/-}$ ES cells during a differentiation assay for up to 5 days. Results were normalized to *Actin*.

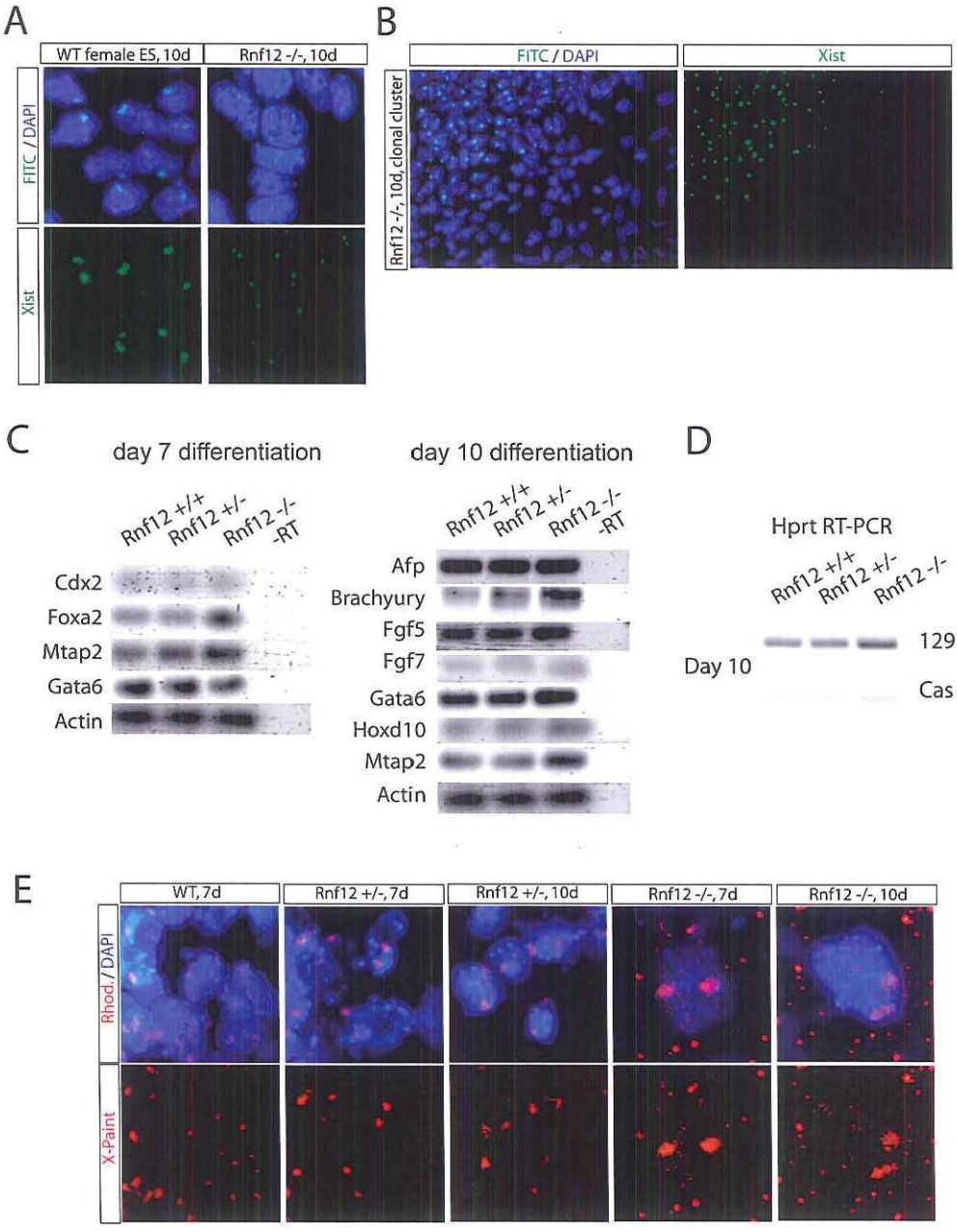

Figure S5
A) RNA-FISH analysis detecting *Xist* (FITC) in day 10 differentiated female wild type and *Rnf12*$^{-/-}$ ES cells. **B)** Example of clonal cluster of cells which have initiated XCI in *Rnf12*$^{-/-}$ ES cells differentiated for

Figure S5: continued
10 days as detected by *Xist* RNA-FISH. **C)** RT-PCR examining expression of several differentiation markers with RNA of day 7 (left panel) and day 10 (right panel) differentiated female wild type, *Rnf12*$^{+/-}$ and *Rnf12*$^{-/-}$ ES cells. **D)** Allele specific RT-PCR determining *Hprt* with a 129 and Cas origin, indicating the presence of both X chromosomes in all cell lines tested. **E)** DNA-FISH detecting a whole chromosome X paint probe in wild type, *Rnf12*$^{+/-}$ and *Rnf12*$^{-/-}$ ES cells differentiated for 7 or 10 days. Slides were first used for RNA-FISH, and subsequently denatured and hybridized to the DNA probe. Virtually all cells in the *Rnf12*$^{-/-}$ ES cells which did not show *Xist* clouds stained positive for the presence of two X chromosomes.

Table S1: Primers used in this study:

Primer	Forward	Purpose	Digest	Ref
Kpn1-RLIM Prom	TTGGTACCCTAGTTAGAGCCTCGAGG AGGCCTT	*Rnf12* promoter		984
PlusProm-Sac1	CCTAGGAGCTCGCCAGCTCGGAGAC GTAGCTCA	*Rnf12* promoter		984
mXistI 1-3L	CAGTGGTAGCTCGAGCCTTT	*Xist* RFLP	BsrgI	
mXistI 1-3R	CCAGAAGAGGGAGTCAGACG	*Xist* RFLP	BsrgI	
Atrx RFLP FW	TCCCCAATTA AAGGTGTTGA	*Atrx* RFLP	PflmI	
Atrx RFLP RV	AATTCACGTTCTCCTCTTTCACT	*Atrx* RFLP	PflmI	
Nhe GenA F	GCCTTCGAACATCTCTGAGC	*Rnf12* RFLP	NheI	174
Nhe GenA R	GAGCCGGACTAATCCAAACA	*Rnf12* RFLP	NheI	174
Rnf12 arm F	GCCTTCGAACATCTCTGAGC	Targeting arms		174
Rnf12 arm R	GAGCCGGACTAATCCAAACA	Targeting arms		174
Luc qPCR 1 F	TCTAAGGAAGTCGGGGAAGC	Luciferase qPCR		
Luc qPCR 1 R	CCCTCGGGTGTAATCAGAAT	Luciferase qPCR		
b-actin for	ACTATTGGCAACGAGCGGTTC	qPCR		174
b-actin rev	AGAGGTCTTTACGGATGTCAACG	qPCR		174
Nanog for	AGGATGAAGTGCAAGCGGTG	qPCR		191
Nanog Rev	TGCTGAGCCCTTCTGAATCAG	qPCR		191
Oct3/4 for	CCCCAATGCCGTGAAGTTG	qPCR		191
Oct3/4 rev	TCAGCAGCTTGGCAAACTGTT	qPCR		191
Sox2 for	CACAGATGCAACCGATGCA	qPCR		191
Sox2 rev	GGTGCCCTGCTGCGAGTA	qPCR		191
Klf4 for	GTGCCCCGACTAACCGTTG	qPCR		134
Klf4 rev	GTCGTTGAACTCCTCGGTCT	qPCR		134
Xist for	GCCTCAAGAAGAAGGATTGC	qPCR		174
Xist rev	GGGATTGTTTGTCCCTTTGG	qPCR		174
Rnf12 ex4-5 for	GGTCCACCACCACAGAGC	qPCR		
Rnf12 ex4-5 rev	TGACCACTTCTTGTTGTATTTCC	qPCR		
AFP for	CCTATGCCCCTCCCCCATTC	qPCR		
AFP rev	CTCACACCAAAGCGTCAACACATT	qPCR		
T-S764	ATGCCAAAGAAAGAAACGAC	qPCR		61
T-AS1579	AGAGGCTGTAGAACATGATT	qPCR		61
Gata6-S917	ACCTTATGGCGTAGAAATGCTGAGG GTG	qPCR		61
Gata6-AS1250	CTGAATACTTGAGGTCACTGTTCTCG GG	qPCR		61
Mtap2-S629	CATCGCCAGCCTCGGAACAAACAG	qPCR		61
Mtap2-AS867	TGCGCAAATGGAACTGGAGGCAAC	qPCR		61
Cdx2-2 for	TCCAGGCTGAGCCATGA	qPCR		61
Cdx2-2 rev	CGTGGGTAGGAGGAGAGGAAT	qPCR		61
Hoxd10 for	CTGAGGTTTCCGTGTCCAGT	qPCR		67
Hoxd10 rev	TTCTGCCACTCTTTGCAGTG	qPCR		67
Fgf7 for	CCATGAACAAGGAAGGGAAA	qPCR		67
Fgf7 rev	TCCGCTGTGTGTCCATTTAG	qPCR		67
Foxa2 for	ACACGCCAAACCTCCCTACT	qPCR		
Foxa2 rev	GGCACCTTGAGAAAGCAGTC	qPCR		
Fgf5 for	GCTGTGTCTCAGGGGATTGT	qPCR		
Fgf5 rev	TCTTGGCTTTCCCTCTCTTG	qPCR		
Gapdh ex-intr3 for	CCTGGGGCTCACTACAGACC	qPCR		
Gapdh ex-intr 3 rev	AATCTCCACTTTGCCACTGC	qPCR		

Tsix X9 for	TGACCAGTACCTCGCAAGTTC	qPCR		191
Tsix X9 rev	CTAAGAGCACCTGGCTCCAC	qPCR		191
NS18	GGTAACAATTTTCCCGCCATGTG	*Tsix* RFLP	MnlI	137
NS19	GGAAATAAACGGAACGCAGTACC	*Tsix* RFLP	MnlI	137
Tsix1 for	ACCATGACCAAAGCAACTCC	Copy-number		174
Tsix1 rev	CTCCTCCAGTACCATGTCTGC	Copy-number		174
Rnf4-5 for	AGCCCCGATGAAAATAGAGG	Copy-number		174
Rnf4-5 rev	GGCATTTCTGGATAATCTTTGG	Copy-number		174
Zfp42 for	GCACCCATATCCGCATCCAC	Copy-number		174
Zfp42 rev	GCATTTCTTCCCGGCCTTTG	Copy-number		174
Xist LP 1445	ACTGGGTCTTCAGCGTGA	RT-PCR LP		
Xist LP 1446	GCAACAACGAATTAGACAACAC	RT-PCR LP		
Xist LP2 1447	GGGAATAGGTAAGACACACTG	RT-PCR LP		
Rnf12 cDNA for	TAAAGAGGGTCCACCACCAC	RT-PCR RFLP	NheI	174
Rnf12 cDNA rev	GGCAGAGAGCCACTTTCATC	RT-PCR RFLP	NheI	174
Hprt SfaNI cas for	ATGCCCAGCGTCGTGATTAG	RT-PCR RFLP	SfaNI	
Hprt SfaNI cas REV	TGGCAACATCAACAGGACTC	RT-PCR RFLP	SfaNI	

Addendum: Mice deleted for Xist intron 1 do not show an X chromosome inactivation phenotype

Tahsin Stefan Barakat, Nilhan Gunhanlar and Joost Gribnau
(work in progress)

Abstract

Inactivation of one of the two X chromosomes in placental mammals is essential for survival of females, and is initiated during embryonic development. This X chromosome inactivation (XCI) process is coupled to mouse development, and is suppressed or reversed in undifferentiated pluripotent cells, including female mouse embryonic stem (ES) cells, cells in the inner cell mass (ICM) of the female embryo, and female primordial germ cells (PGCs). The molecular coupling between the pluripotent state and lack of XCI has been proposed to involve direct suppression of *Xist*, the master *cis* regulator of the inactivation process, by recruitment of the pluripotency factors OCT4, SOX2, and NANOG to a region in *Xist* intron 1. Here, we have generated a mouse model with a genetic ablation of all pluripotency factor binding sites in *Xist* intron 1. The female $Xist^{\Delta intron1/+}$ and $Xist^{\Delta intron1/\Delta intron1}$ mice were found to be healthy and gave birth to offspring with a Mendelian distribution of the mutation. This indicates the absence of a role for the deleted region in imprinted XCI. In addition, from analysis of adult tissues, we conclude that random XCI was not affected. We conclude that the *Xist* intron 1 pluripotency factor recruitment site is not essential for *Xist* repression *in vivo*.

Introduction

Eutherian females inactivate one of their two X chromosomes in a process called X chromosome inactivation (XCI), to achieve a balanced dosage of X-linked and autosomal genes, compared to males [30]. In the female mouse embryo, XCI is initiated at the 2-4 cell stage, and is imprinted resulting in the exclusive inactivation of the paternal X chromosome [53, 985-986]. This form of imprinted XCI is maintained in the extra-embryonic tissues, but is reversed in the cells of the inner cell mass (ICM) of the blastocyst, where during a short window in development two active X chromosomes are tolerated [54]. Upon further differentiation, random XCI is initiated in the post-implantation epiblast, which will give rise to all embryonic cell lineages. Female embryonic stem (ES) cells, derived from the ICM harbor two active X chromosomes, and undergo random XCI upon *in vitro* differentiation, whereas female epiblast stem cells (EpiSCs), derived from the post-implantation embryo, represent a post-XCI state, in which one of the X chromosomes is transcriptionally silenced (for review, see [987]).

The non-coding RNA *Xist* is essential for XCI to occur. Expression of this X-transcribed RNA is up-regulated, and subsequent spreading of *Xist* in *cis* results in heterochromatinization and transcriptional shut-down of the X chromosome [74, 84-85, 93]. Recent years have highlighted progression in the understanding of *Xist* regulation in ES cells, their differentiated progeny and embryos. We have shown that an increased concentration of the X-encoded XCI-activator RNF12 upon differentiation results in XCI initiation [174], and *Xist* up-regulation does not occur in the absence of this crucial activator [911]. Suppression of *Xist* in undifferentiated cells might be a result of absence of *Xist* activation, as over-expression of *Rnf12* can result in *Xist* upregulation in undifferentiated ES cells [174]. *Xist* is also negatively regulated by its antisense partner gene *Tsix*, which is highly expressed in undifferentiated ES cells [118-119, 180, 988]. As *Xist* up-regulation is coupled to differentiation [190], and *Xist* is suppressed in undifferentiated cells, the pluripotency factor network has been implicated in direct and indirect suppression of *Xist* [192]. Indirect mechanisms might include activation of *Tsix* in undifferentiated cells by pluripotency factors [186, 989], and suppression of XCI activators [990]. A direct interaction between *Xist* suppression and the pluripotency factor network has been proposed to involve a region within *Xist* intron 1 [191].

Chromatin immunoprecipitation experiments have shown that the key pluripotency factors NANOG, OCT4 and SOX2 bind *Xist* intron 1 in both male and female undifferentiated ES cells, but not in differentiated cells, mouse embryonic fibroblast [191] and EpiSCs [991]. Genetic ablation of *Nanog* in male ES cells, which does not result in a loss of recruitment of OCT4 and SOX2 to the *Xist* intron 1 region, resulted in a modest up-regulation of *Xist* expression, whereas forced down-regulation of *Oct4* resulted in loss of binding of all pluripotency factors to the intron 1 region and a drastic increase of *Xist* expression suggested to be independent of *Tsix* regulation [191]. These correlative data have been proposed to support the hypothesis that the key pluripotency factors NANOG, OCT4 and SOX2 are crucial for a *Tsix*-independent repression *Xist* in undifferentiated ES and ICM cells. In support of this, it has been found that only NANOG expressing ICM cells undergo reactivation of the paternal inactivated X chromosome [367], which further supports a crucial role for NANOG in *Xist* repression. Furthermore, the intron 1 region contains a developmentally regulated DNAse hypersensitivity site [992], and recruitment of two other transcription factors *Prdm14* and *Tcf3* to *Xist* intron 1 [194-195], support a role for this region in *Xist* suppression.

We recently addressed the question whether the *Xist* intron 1 region is required for *Xist* suppression in undifferentiated ES cells, by generating a targeted deletion of all reported pluripotency factor binding sites in a female ES cell line [911]. Surprisingly, deleting *Xist* intron 1 did not affect XCI initiation, as $Xist^{\Delta intron1/+}$ ES cell lines initiated random XCI with normal kinetics without preferential inactivation of the Δintron1 allele, and undifferentiated $Xist^{\Delta intron1/+}$ ES cells did not show aberrant *Xist* expression. We reported only mild skewing towards inactivation of the mutant allele during later stages of differentiation, which argues against an important role for the *Xist* intron 1 region in the regulation of XCI. Here we study the role of the *Xist* intron 1 region in XCI *in vivo*. *Xist* intron 1 knockout mice appear to be fertile, give birth to normal offspring, and show random XCI in all tissues analyzed. We conclude that the *Xist* intron 1 region is not required for XCI regulation *in vivo*.

Results

To generate a mouse model in which all reported pluripotency factor binding sites in *Xist* intron 1 were deleted, a polymorphic 129/Sv-Cast/Ei *Xist* $^{intron\ 1(2lox)/+}$ ES cell line 29 [911], in which a 1,2 kb region of *Xist* intron 1 is replaced by a floxed neomycin cassette, was used to generate chimaeric mice. Germ line transmission was verified by genotyping for the presence of the neomycin cassette integrated in *Xist* (data not shown). *Xist* $^{intron\ 1(2lox)/+}$ females were bred to males expressing pCAGGS-Cre, to loop out the selection cassette. Loopout of the selection cassette was verified by PCR on genomic tail-tip derived DNA. The resulting *Xist* $^{\Delta intron\ 1/+}$ mice were bred to wild type mice, and showed transmission of the deletion to both male and female offspring, in a Mendelian distribution (**Figure 1** and **Table 1A**). Crosses of *Xist* $^{\Delta intron\ 1/Y}$ males with heterozygous *Xist* $^{\Delta intron\ 1/+}$ females resulted in homozygous offspring (**Figure 1**), which were successfully used to breed with *Xist* $^{\Delta intron\ 1/Y}$ males. The *Xist* $^{\Delta intron\ 1/Y}$ male and *Xist* $^{\Delta intron\ 1/\Delta intron\ 1}$ female offspring followed a Mendelian distribution and resulted in a normal litter size.

To analyze the level of skewing in adult mice, female heterozygous *Xist* $^{\Delta intron\ 1/+}$ mice were bred to Cast/Ei males. The resulting F1 hybrid female mice, carrying a Cast/Ei derived X chromosome with the wild type *Xist* intron 1 region, and one *Xist* intron 1 deleted allele on a mixed C57Bl/6 and 129/Sv X chromosome was used to assess skewing of random XCI. Randomness was determined by amplification of a length polymorphism in *Xist* used to determine allele specific expression analysis with cDNA obtained from different organs of wild type and *Xist* $^{\Delta intron\ 1/-}$ littermates. In the wild type mice we found the expected 60:40 ratio favoring *Xist* expression from the C57Bl/6 (**Figure 2**), indicating skewed XCI in favour of the C57Bl/6 X chromosome due to differences in XCE strength between the C57Bl/6 and Cast/Ei X chromosomes [445]. Subsequent analysis X-linked gene expression examing *Mecp2*, *G6pdx* and *Atp7a* using RFLPs and length polymorphisms that distinguish between C57Bl/6 and Cast/Ei expression showed a reciprocal expression of these genes favoring Cast/Ei expression. In *Xist* $^{\Delta intron\ 1/+}$ female mice (N=2) allele specific *Xist* and X-linked gene expression was indifferent from to wild type litter mates, which indicates that *Xist* intron 1 heterozygous females undergo normal random XCI (**Figure 2**). Random XCI was also found in informative female offspring obtained from matings between *Xist* intron 1 mutant males with wild type F1 hybrid females carrying a C57Bl/6 and a Cast/Ei X chromosome (N=2, data not shown).

Discussion

Here we have generated a mouse model in which the pluripotency factor binding site in *Xist* intron 1 region, proposed to be important for *Xist* suppression in undifferentiated cells, is deleted. Surprisingly, *Xist* intron 1 deleted mice are healthy, fertile and undergo random X chromosome inactivation. These results indicate that the *Xist* intron 1 region is not essential for *Xist* suppression *in vivo*.

It was previously suggested that recruitment of pluripotency factors to the *Xist* intron 1 region is required for *Xist* repression in undifferentiated cells [191]. However, we found that genetic ablation of this region did not result in aberrant *Xist* expression in ES

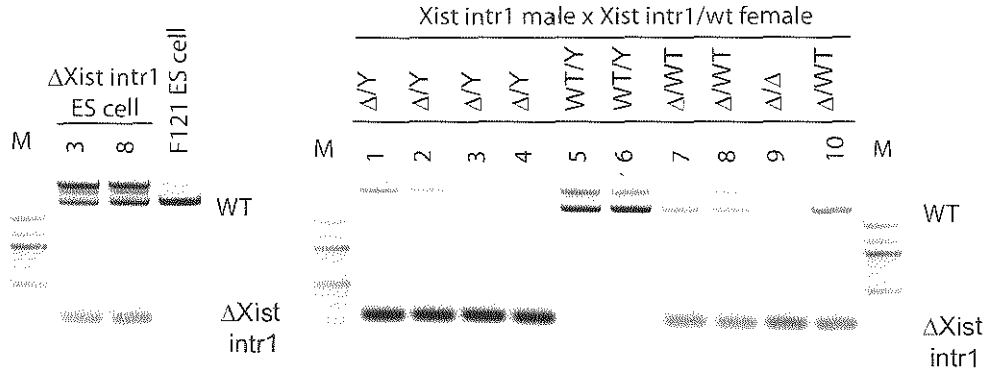

Figure 1: **Genotyping of *Xist* intron 1 mutant mice**
Left panel: genotyping of wild type and *Xist*$^{intron\ 1\ +/-}$ ES cells.
Right panel: example of a litter of mice obtained after mating of an *Xist* intron 1 mutant male with a heterozygous *Xist* intron 1 deleted female, genotyped by PCR on genomic DNA. Animal 1 till 6 are males (data not shown), of which 4 show the presence of a band diagnostic for the *Xist* intron 1 deletion (*ΔXist* intron 1). Animal 7 till 10 are females, with animal 9 showing loss of the wild type allele, diagnostic of a homozygous deleted female.

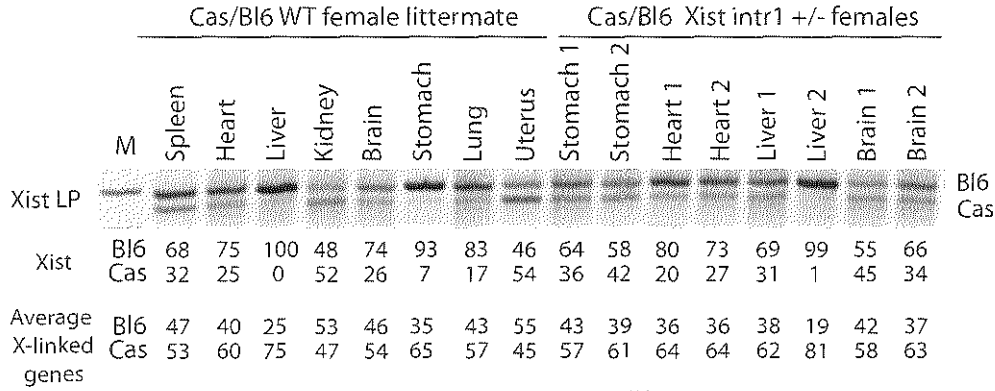

	Average all tissues	Cas/Bl6 WT female	Cas/Bl6 Xist intr1 +/- females 1	2
Xist	Bl6	73	67	74
	Cas	27	33	36
Average X-linked genes	Bl6	43	40	33
	Cas	57	60	67

Figure 2: ***Xist* intron 1 deleted females show random X chromosome inactivation in adult tissues**
Upper panel shows RT-PCR for a length polymorphism differentiating between *Xist* expression from Cast/Ei and C57Bl/6 in a wild type hybrid mice, and two hybrid *Xist* intron 1 mutant females. Allele specific ratios are plotted under the gel. Average X-linked gene expression, as determined for *Mecp2*, *G6pdx* and *Atp7a* is plotted as well.

cells, but this does not exclude a role for this region *in vivo* [12]. Two of the pluripotency factors recruited to this region, OCT4 and SOX2, are already expressed from the morula stage onwards in pre-implantation embryos were imprinted XCI occurs. However, the inactivated paternal X chromosome of imprinted XCI only becomes reactivated at a later stage in epiblast cells that express *Nanog* [367]. It was therefore hypothesized that NANOG binding to the *Xist* intron 1 region is required for proper reactivation of the inactive X chromosome [993]. The same reactivation function of NANOG might be required in PGCs and in mouse iPS cells, which both show reactivation of the inactive X chromosome [68-69]. Alternatively, it was hypothesized that the paternal *Xist* intron 1 region might carry an imprint, which would prevent specific recruitment of OCT4 and SOX2 to the paternal X chromosome, thereby preventing suppression of *Xist* in *cis* [993]. Binding of NANOG to both alleles during later stages of development would then allow erasure of the imprint, and repression of both *Xist* alleles in cells of the ICM, followed by random XCI in the post-implantation epiblast. The present data argue against both models. In the heterozygous mice analyzed, random XCI was observed, both when the *Xist* intron 1 deletion was transmitted through the mother or the father, indicating proper reactivation of the X chromosome. Although imprinted XCI was not investigated directly, the normal Mendelian distribution of offspring obtained in all crosses with *Xist* intron 1 mutant mice argues against a failure of imprinted XCI, as such a failure would result in female embryonic lethality during post-implantation stages [93-94].

In previous *in vitro* studies [911], we did not find compelling evidence for an important role of the *Xist* intron 1 region in *Xist* suppression, as *Xist* $^{\Delta intron\ 1/+}$ ES cells underwent XCI with normal kinetics, and no aberrant *Xist* activation was detected in undifferentiated cells. Although these results indicate that pluripotency factor binding to the *Xist* intron 1 region might not be crucial for *Xist* suppression *in vitro*, it cannot be ruled out that redundant mechanisms work together to prevent up-regulation of *Xist* in undifferentiated cells. Indeed, as antisense *Tsix* transcription is important for *Xist* suppression, it might be that a more subtle effect of the *Xist* intron 1 region can only be revealed when *Tsix* is inhibited in *cis*. In agreement with this, a recent study has reported that the combined removal of the *Xist* intron 1 region and the *Tsix* transcriptional start site results in loss of repression of *Xist* from autosomally integrated transgenes [994]. However, in that study, only transgenes were investigated, and therefore the results might have been affected by differences in transgene copy number and position effect variegation. A definitive answer can only be obtained when both the *Xist* intron 1 region and *Tsix* are removed in *cis* from the endogenous loci.

An alternative mechanism explaining the coupling of differentiation to *Xist* up-regulation might involve the developmentally regulated activity of *Xist* activators. Under such a scenario, pluripotency factor mediated *Tsix* activation [186, 989] and lack of *Xist* activation will result in the absence of *Xist* accumulation in undifferentiated cells. In agreement with this, *Rnf12*, the only identified XCI-activator to date, becomes up-regulated upon differentiation of female ES cells [174]. A negative correlation between RNF12 and NANOG expression has been observed in differentiating ES cells [911], and *Rnf12* expression seems to be negatively regulated by pluripotency factors [911, 983, 990]. Similar mechanisms might apply *in vivo*, where up-regulation of RNF12 might result in *Xist* activation in imprinted and random XCI, and reactivation of the imprinted paternal X

Xist intr1-/Y x WT female	4	26	11 (42%)	15 (58%)	0 (0%)	15 (100%)		
WT male x Xist intr1+/- female	3	20	8 (40%)	12 (60%)	6 (75%)	9 (75%)		
Xist intr1-/Y Xist intr1+/- female	4	32	14 (44%)	18 (56%)	4 (29%)	10 (71%)	7 (39%)	11 (61%)
Xist intr1-/Y x Xist intr1-/- female	3	15	9 (60%)	6 (40%)	0 (0%)	9 (100%)	0 (0%)	6 (100%)

Table 1: *Xist* intron 1 mice give birth to viable offspring in Mendelian distribution
The different types of crossings, number of pups obtained and their genotype is indicated.

chromosome in the ICM might occur by down-regulation of *Rnf12* expression and other XCI-activators by pluripotency factors. Therefore, an important area of future research involves the unravelling of the molecular interplay between pluripotency factors and XCI activators both *in vitro* and *in vivo*.

Methods

All animal experiments were in accordance with the legislation of the Erasmus MC Animal Experimental Commission. Generation of *Xist* $^{\Delta intron\ 1/+}$ ES cells has been described [911]. Tail-tip derived DNA was isolated according to standard procedures, and genotyping of the *Xist* intron 1 deletion was performed by PCR using primers 9,999 XIn1b (ccttgttggtccagacgactatt)
and 11,82 XIn1e (cactggactgggagagaggg). To assess XCI skewing, hybrid female mice were sacrificed by cervical dislocation, parts of organs were collected, snap-frozen and triturated using micro-pestils in 1 ml of Trizol reagent (Invitrogen). After an additional centrifugation to clear debris, 700 µl was added to 300 µl fresh Trizol, and RNA was purified following manufacturer's instructions. RNA was reverse-transcribed with SuperScript II (Invitrogen), using random hexamers. Allele specific *Xist* expression was analyzed by RT-PCR amplifying a length polymorphism using primers *Xist* LP 1445 (actgggtcttcagcgtga) and *Xist* LP 1446 (gcaacaacgaattagacaacac). To determine allele specific X-linked gene expression of *Atp7a*, *Mecp2* and *G6pdx*, primers 335 moF3930 (agggcaaacgtgtagcaatggtag) and 336 moF4812 (agagcttgttctaactcactgttct) were used for *Atp7a* amplifying a length polymorphism, [995], primers (catggtagctgggatgttagg) and (gcaatcaattctactttagagcg), for *Mecp2* amplifying a DdeI RFLP in *MeCP2*, and primers (ggagtgatgaactcagggaagc) and (atgtagctgggtttactggtgg) to amplify a ScrFI RFLP in *G6PD*. PCR products were gel purified and digested with the indicated restriction enzymes and analyzed on a 2% agarose gel stained with ethidium bromide. Allele specific expression was determined by measuring relative band intensities using a Typhone image scanner and ImageQuant software.

Chapter 6

RNF12 initiates X chromosome inactivation by targeting REX1 for degradation

This chapter has been published in

Cristina Gontan, Eskeatnaf Mulugeta Achame, Jeroen Demmers, Tahsin Stefan Barakat, Eveline Rentmeester, Wilfred van IJcken, J. Anton Grootegoed and Joost Gribnau (2012)
"RNF12 initiates X chromosome inactivation by targeting REX1 for degradation"
Nature 485: 386-390

RNF12 initiates X chromosome inactivation by targeting REX1 for degradation

Cristina Gontan[1], Eskeatnaf Mulugeta Achame[1], Jeroen Demmers[2], Tahsin Stefan Barakat[1], Eveline Rentmeester[1], Wilfred van IJcken[3], J. Anton Grootegoed[1] and Joost Gribnau[1,4]

[1]Department of Reproduction and Development, [2]Proteomics Center, and [3]Biomics Department, Erasmus MC, University Medical Center, Rotterdam, The Netherlands
[4]corresponding author

Contact details:
Joost Gribnau
Department of Reproduction and Development
Erasmus MC
Room Ee 09-71
PO Box 2040
3000 CA Rotterdam
The Netherlands
Phone +31-10-7043069
Fax +31-10-7044736
Email: j.gribnau@erasmusmc.nl

Evolution of the mammalian sex chromosomes has resulted in a heterologous X and Y pair, where the Y chromosome has lost most of its genes. Hence, there is a need for X-linked gene dosage compensation between XY males and XX females. In placental mammals, this is achieved by random inactivation of one X chromosome (XCI) in all female somatic cells [30]. Up-regulation of *Xist* transcription on the future inactive X chromosome (Xi) acts against *Tsix* antisense transcription, and spreading of *Xist* RNA in *cis* triggers epigenetic changes leading to XCI. Previously, we have shown that the X-encoded E3 ubiquitin ligase RNF12 is up-regulated in differentiating mouse embryonic stem cells (ESCs) and activates *Xist* transcription and XCI [174]. Here, we have identified the pluripotency factor REX1 as a key target of RNF12 in the XCI mechanism. RNF12 causes ubiquitination and proteasomal degradation of REX1, and *Rnf12* knockout mouse ESCs show an increased level of REX1. Using ChIP-seq, REX1 binding sites were detected in *Xist* and *Tsix* regulatory regions. Over-expression of REX1 in female ESCs was found to inhibit *Xist* transcription and XCI, whereas male *Rex1*+/- ESCs showed ectopic XCI. From this, we propose that RNF12 causes REX1 breakdown through dose-dependent catalysis, thereby representing an important pathway to initiate XCI. *Rex1* and *Xist* are present only in placental mammals, which points to co-evolution of these two genes and XCI.

The initiation of XCI in female cells implies a need for X-linked XCI activators which act in a dose-dependent manner to sense the number of X chromosomes present per diploid genome [179, 189]. We recently identified X-encoded RNF12 as a dose-dependent activator of XCI in mouse ESCs [174]. Additional transgenic copies of *Rnf12* resulted in initiation of XCI in male cells, and on both X chromosomes in a high percentage of female cells [174]. Random XCI was found to be markedly reduced in differentiating *Rnf12*+/- and *Rnf12*-/- female ESCs, which indicated an important role for RNF12 in the regulation of XCI, although the mechanism by which this E3 ubiquitin ligase initiates XCI remained elusive[911, 981].

To address this question, we generated FLAG-*Rnf12* transgenic female *Rnf12*+/- ESCs to identify interaction partners of RNF12 by FLAG-affinity purification. RNF12 is very unstable and the addition of the proteasome inhibitor MG132 facilitates its detection (**Figure 1a**). FLAG-RNF12 was purified from nuclear extracts of two FLAG-RNF12 ESC lines (**Supplementary Figure 1A**). Purified RNF12 samples and control samples were separated on SDS polyacrylamide gels (**Supplementary Figure 1B**) and analyzed by mass spectrometry (**Supplementary Table 1**). The only transcription factor consistently co-purifying with RNF12 was REX1 (**Figure 1B** and **Supplementary Table 1**). Previous studies have demonstrated that *Rex1* expression strictly correlates with the pluripotent state of ESCs [996], and REX1 has been implicated in suppression of genes involved in ESC differentiation [997]. We performed the reverse experiment, using two transgenic female ESC lines expressing a FLAG-V5-tagged REX1 fusion protein (**Supplementary Figure 1C**). In both REX1 purifications (**Supplementary Figure 1D, E**), performed with nuclear extracts of undifferentiated transgenic ESCs, RNF12 was present as a prominent interacting partner (**Figure 1B**). Co-purified RNF12 was non-ubiquitinated, but mass spectometry analysis and phosphatase treatment indicated that a significant fraction of RNF12 is phosphorylated (**Supplementary Figure 1F**). We confirmed the REX1-RNF12 interaction by co-immunoprecipitation of endogenous RNF12 and REX1 from undifferentiated female

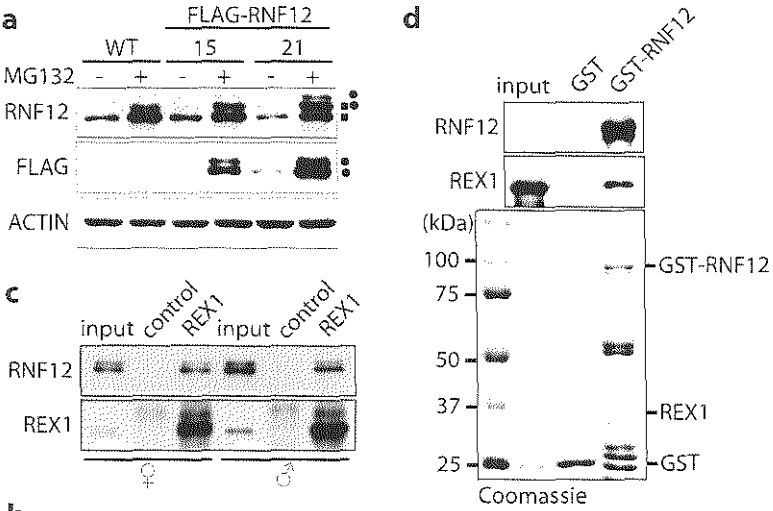

b

FLAG purifications

Protein	Mascot	Peptides	Mascot	Peptides	Mascot	Peptides	Mascot	Peptides
RNF12	1308	21(40)	1490	23(48)	1214	18(95)	1535	22(132)
REX1	124	2(5)	61	1(4)	558	11(71)	603	11(89)

Figure 1: RNF12 interacts with REX1 in mouse ESCs
A) Nuclear extracts of wild-type (WT) and transgenic FLAG-RNF12 ESC clones 15 and 21 were immunoblotted with RNF12 and FLAG antibodies (running positions of WT RNF12 and FLAG-RNF12 is indicated with ▪ and •). Where indicated, cells were treated with proteasome inhibitor (MG132). ACTIN was used as a loading control. **B)** Mass spectrometry analysis of FLAG-affinity purifications from FLAG-RNF12-expressing ESC clones 15 and 21, and FLAG-REX1-expressing clones 3 and 11. Mascot score, number of unique peptides and total number of peptides identified (between brackets) are shown for RNF12 and REX1 proteins in each of the purifications. **C)** REX1-RNF12 co-immunoprecipitation from nuclear extracts of female (left) and male (right) ESCs. Immunoprecipitations with REX1 antibody or control rabbit IgG were immunoblotted with RNF12 and REX1 antibodies. **D)** Direct binding of recombinant GST-RNF12 to recombinant REX1. RNF12 and REX1 are detected by immunoblotting (upper panels) and by Coomassie staining of a SDS-PAGE gel (lower panel). GST alone was used a negative control.

and male ESCs nuclear extracts (**Figure 1C**), and co-immunoprecipitation of recombinant GST-RNF12 and REX1 (**Figure 1D**). Mapping of the RNF12 region(s) involved in the interaction with REX1 indicated that both the N-terminal and C-terminal halfs of RNF12 contribute to the interaction (**Supplementary Figure 2A, B**).

We generated two catalytically inactive RNF12 mutants (**Figure 2A**). Transient expression in ESCs showed a increased stability of the RNF12 mutants (**Supplementary Figure 2C**), indicating that auto-ubiquitination contributes to the high turn-over of RNF12. To test whether REX1 is a bona fide substrate of RNF12, we transfected combinations of expression vectors encoding wild-type or mutant RNF12-GFP, with REX1-Cherry fusion proteins into HEK293 cells (**Figure 2B** and **Supplementary Figure 3A, B**). FACS analysis of REX1-Cherry transfected HEK 293 cells showed a more than ten-fold decrease in

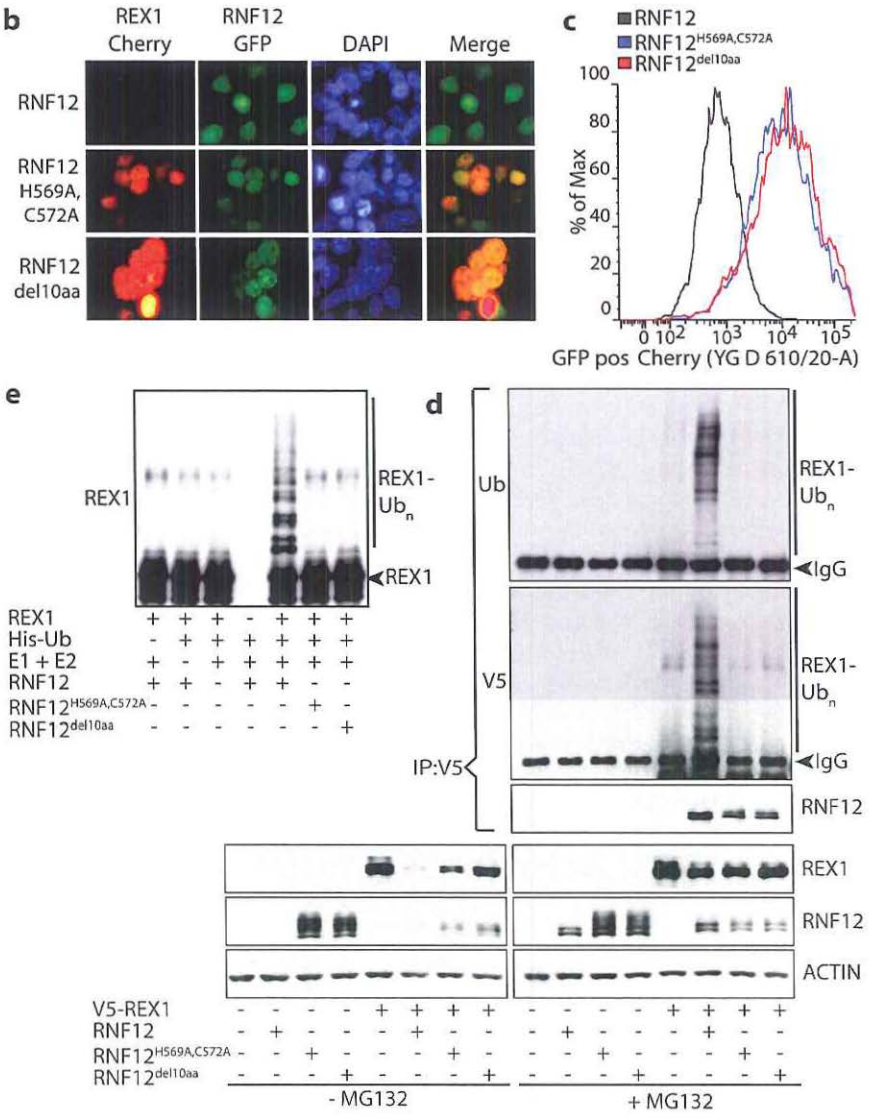

Figure 2: RNF12 polyubiquitinates and targets REX1 for proteasomal degradation
A) Sequence alignment of the RING finger domain corresponding to the WT and two catalytically inactive RNF12 mutants (two arginine substitutions are shown in red). **B)** Analysis of the fluorescence in HEK293 cells, 24 h after transfection with REX1-Cherry fusion expression vector alone or in combination with wild-type or catalytically inactive RNF12-GFP expression constructs. **C)** Quantification

Cherry intensity when cells were cotransfected with wild-type RNF12 compared to co-transfection with the RNF12 mutants (**Figure 2C** and **Supplementary Figure 3C, D**). This result suggests a strict correlation between RNF12 expression and REX1 degradation.

To provide evidence that REX1 is indeed ubiquitinated by RNF12, HEK293 cells were transfected with V5-REX1, and either RNF12 wild-type or the two inactive RNF12 mutants. REX1 was degraded in the presence of wild-type RNF12 but not in the presence of the RNF12 mutants (**Figure 2D**), and degradation was blocked by the proteasome inhibitors MG132 or epoxomicin (**Figure 2D** and **Supplementary Figure 4**). We subjected the nuclear extracts to immunoprecipitation with anti-V5 agarose beads, and probed with V5 and ubiquitin antibodies to visualize poly-ubiquitinated REX1 (**Figure 2D**, and **Supplementary Figure 4**). Mass spectrometric analysis detected five putative lysine acceptor sites for ubiquitin linkage (**Supplementary Figure 5**). In addition, an ubiquitination assay performed with recombinant proteins revealed poly-ubiquitination of REX1 only in the presence of wild-type RNF12, but not in the presence of either of the two RNF12 mutants (**Figure 2E**). These results indicate a direct role for RNF12 in targeting REX1 for degradation by the proteasome in an ubiquitin-dependent manner.

Our results predict that RNF12 and REX1 protein levels show a reciprocal correlation. Indeed, we found a pronounced increase of the REX1 protein level in *Rnf12-/-* ESCs (**Figure 3A**). Western blot analysis of RNF12 and REX1 protein levels in female wild-type ESCs indicated that REX1 is quickly down-regulated upon differentiation, coinciding with an initial increase in RNF12 (**Figure 3B**). In *Rnf12-/-* ESCs, the REX1 protein level is also down-regulated but the starting level is much higher. Comparison of the REX1 protein level in wild-type, *Rnf12+/-* and *Rnf12-/-* female ESCs, and in wild-type male cells, by immunoblotting, indicates that the REX1 level is very low in wild-type female ESCs (**Supplementary Figure 6B**), in agreement with a high ubiquitination-dependent turnover of REX1. Female *Rnf12+/-* cells and wild-type male cells display a lower RNF12 expression level and an increased REX1 protein level, although this relationship was not strictly two-fold which may be related to the pluripotent state of the ESC lines and enzyme kinetics (**Supplementary Figure 6A** and **Figure 3C**). *Rnf12* gene dosage did not affect other known factors involved in XCI, including YY1, NANOG and SUZ12 (**Figure 3B** and **Supplementary Figure 6A**). *Rex1* gene transcription, analyzed by qPCR, was not affected in *Rnf12-/-* cells (**Supplementary Figure 6B**), indicating that the down-regulation of REX1 by RNF12 is post-transcriptional.

Figure 2: continued
of **B** by FACS analysis. **D)** Left bottom panels show nuclear protein extracts of HEK293 cells co-transfected with the indicated expression constructs for V5-REX1, WT RNF12, or the catalytically inactive RNF12 mutants. Immunoblots were probed with the indicated antibodies. Right bottom panels show the same transfections, but in the presence of MG132. Upper panels: V5-tagged REX1 was immunoprecipitated with anti-V5 agarose beads and analysed by immunoblotting to detect the poly-ubiquitinated REX1 (REX1-Ub_n) with V5 and ubiquitin (Ub) antibodies. RNF12 co-immunoprecipitated with REX1 was detected with RNF12 antibody. **E)** REX1 ubiquitination assay with recombinant proteins. Recombinant REX1, His-ubiquitin, UBE1 (E1), UbcH5a (E2), recombinant RNF12 and RNF12 mutants were added in the indicated combinations. Ubiquitinated forms of REX1 were detected by immunoblotting with REX1 antibody.

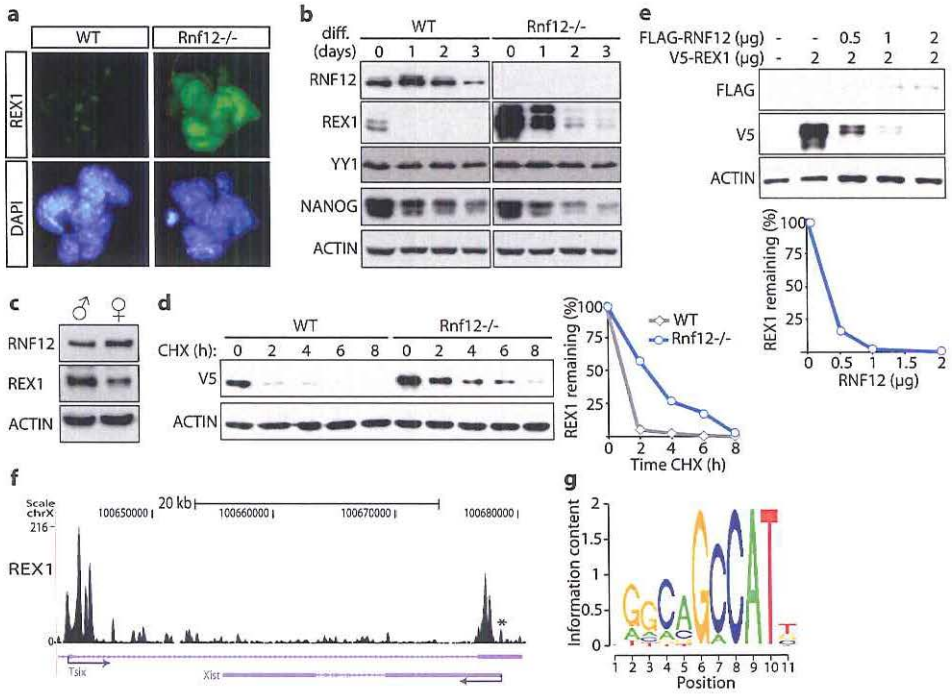

Figure 3: RNF12 is a dose-dependent regulator of REX1 expression
A) REX1 immunostaining (green) on WT and *Rnf12-/-* ESCs. **B)** Immunoblots of WT and *Rnf12-/-* ESCs at day 0, 1, 2 and 3 of differentiation, probed with antibodies against RNF12, REX1, YY1 and NANOG. **C)** RNF12 and REX1 protein levels were detected in female and male ESC nuclear extracts by immunoblotting. **D)** REX1 half-life measurements in WT and *Rnf12-/-* ESCs. ESCs were transiently transfected with V5-REX1 and treated 24 h post-transfection with 100 µg/ml cycloheximide (CHX) for the indicated times. Left panel: nuclear protein extracts were immunoblotted for V5-REX1 with V5 antibody. Right panel: quantitation of the REX1 level, using ImageJ software, at different time points compared to t=0 h (100%) in WT or *Rnf12-/-* ESCs. **E)** REX1 degradation by RNF12 is dose-dependent. FLAG-RNF12 or V5-REX1 constructs were co-transfected into HEK293 cells. Upper panel: levels of V5-REX1 and FLAG-RNF12 visualized by immunoblotting with V5 or FLAG antibodies. Bottom panel: quantification of the V5-REX1 level in cells co-transfected with RNF12, compared to the 100% level in cells transfected only with V5-REX1 plasmid. ACTIN was used as a loading control in **B-E.** **F)** REX1 binding pattern in the *Xist/Tsix* genomic region in female ESCs, as determined by V5-REX1 ChIP-sequencing. Identified sequence reads were plotted relative to genomic location and visualized using UCSC Genome Browser. Location and transcription start sites (arrows) of the *Tsix* and *Xist* loci are indicated. The asterisk marks a REX1 binding site in the *Xist* promoter. **G)** The REX1 consensus motif highly enriched in the genome-wide REX1 ChIP-seq peaks.

The marked increase of REX1 protein level in *Rnf12-/-* cells, points to an increase in REX1 protein stability in the absence of RNF12. Indeed, half life experiments, after cycloheximide treatment of V5-Rex1 transfected wild type and *Rnf12-/-* ESCs, indicate a strong increase in the half life (t½) of REX1 in *Rnf12-/-* ESCs (t½ >2hrs) compared to wild-type cells (t½ < 0.5hrs) (**Figure 3D**). Also, the REX1 protein level is down-regulated more effectively with an increasing dose of RNF12, as detected in HEK293 cells co-transfected

with a fixed concentration of V5-*Rex1* and an increasing concentration of FLAG-*Rnf12* expression vectors (**Figure 3E**). We previously found that male (as well as female) ESC lines stably over-expressing *Rnf12* show ectopic XCI [174]. To determine if over-expression of *Rnf12* would also affect the REX1 level, we stably introduced a BAC covering *Rnf12* into male ESCs, resulting in ectopic XCI at day 3 of differentiation (**Supplementary Figure 6C**). When undifferentiated, these clones show a lower level of REX1, which confirms that over-expression of RNF12 in male cells lowers REX1 stability (**Supplementary Figure 6C**). qPCR analysis showed that *Xist* is up-regulated in ESCs transiently over-expressing wild type RNF12, which is not observed using mutant RNF12, demonstrating that an intact RING-finger is required for initiation of XCI (**Supplementary Figure 6D**).

For RNF12 to function as an XCI-activator through degradation of REX1, REX1 could either repress *Xist* or activate *Tsix*. Indeed, a recent ChIP-qPCR study identified REX1 recruitment to the *Tsix* regulatory element *DXPas34*, which was found to be important for effective elongation of RNA polymerase II [989]. To identify all binding sites of REX1 in the region encompassing *Xist* and *Tsix*, we performed ChIP-seq analysis on undifferentiated FLAG-V5-*Rex1* female ESCs. This analysis confirmed enrichment for previously published REX1 binding sequences in *Tsix* [989], and showed specific REX1 binding sites in the *Xist* promoter and promoter distal region (**Figure 3F**), although REX1 recruitment to the *Xist* promoter was detected only in the presence of MG132. The observed genome-wide REX1 peaks revealed a highly enriched consensus binding motif (**Figure 3G**). Recruitment of REX1 to *Xist* and *Tsix* was also detectable, but less prominent in the absence of MG132 (**Supplementary Figure 7**). This result may explain why REX1 recruitment to *Xist* was not detected in a previous study [989] which did not include the use of proteasome inhibitors. Our results indicate that REX1 may perform a dual function, in the repression of *Xist* and the activation of *Tsix*.

To elucidate the role of REX1 in XCI, we analyzed XCI in day-3-differentiated *Rex1+/-* male ESCs [998] and control male ESCs. As expected, we found a small percentage of male control cells that contained *Xist* clouds (1%), detected with *Xist* RNA-FISH. In contrast, as many as 7.5% of the *Rex1+/-* male cells showed *Xist* clouds, hence initiation of XCI, supporting a dose-dependent role for REX1 in repression of XCI (**Figure 4A, B**). We next analyzed the female ESC lines over-expressing FLAG-V5-tagged REX1 and determined the percentage of cells that initiated XCI after 3 days of differentiation, by *Xist* RNA-FISH. For both REX1 over-expressing lines (Rex1_3 and Rex1_11) we detected a severely reduced number of cells with an *Xist* coated Xi, compared to wild-type female cells (**Figure 4C, D**), indicating a strong inhibition of XCI. *Rnf12-/-* cells showed no *Xist* clouds, consistent with our previous studies [911]. To test whether the XCI phenotype in *Rnf12-/-* ESCs was directly related to the resulting increased REX1 level we performed *Rex1* knock-down experiments in *Rnf12-/-* ESCs. A reduction in *Rex1* expression by more than 50%, 3 days after transient transfection of a *Rex1* shRNA vector, resulted in a more than 5-fold induction of *Xist*, in agreement with a mechanism in which REX1 acts downstream of RNF12 to activate XCI (**Figure 4E**). Next we analyzed the RNA expression level of *Rex1*, *Xist* and *Tsix* by qPCR in undifferentiated and day-3-differentiated wild-type and *Rex1* over-expressing ESC lines. In the latter cells, *Rex1* mRNA expression was 2.8-4.5-fold up-regulated before differentiation, followed by partial down-regulation at day 3 of

Figure 4: REX1 dependent regulation of XCI

differentiation due to silencing of endogenous *Rex1* and reduced expression of the transgene (**Figure 4F**). qPCR analysis of differentiation and pluripotency markers provided evidence that the *Rex1* over-expressing ESC lines undergo proper differentiation, which implies that the XCI phenotype is not a consequence of a differentiation defect (**Supplementary Figure 8**). Our analysis also indicated that *Tsix* expression was slightly up-regulated in undifferentiated REX1 over-expressing compared to wild type cells. Expression of *Tsix* was down-regulated at day 3 of differentiation, but was still higher than in wild type cells, consistent with our combined *Xist/Tsix* RNA-FISH analysis and supporting a role for REX1 in activation of *Tsix* (**Figure 4F** and **Supplementary Figure 9**). In contrast, up-regulation of *Xist* expression during differentiation was markedly reduced in the cells over-expressing REX1 (**Figure 4F** and **Supplementary Figure 9**). Our ChIP-seq data showing REX1 binding in the *Xist* regulatory regions, and genetic studies also indicated that *Xist* is under direct control of RNF12 [911]. To test a direct action on *Xist* independent of *Tsix* in more detail, we transiently transfected male ESCs harboring a non-functional *Tsix* stop allele with a *Rex1* expression vector. This *Rex1* over-expression resulted in suppression of *Xist*, providing further evidence for a *Tsix* independent pathway in the repression of *Xist* by REX1 (**Figure 4G**). We next performed luciferase assays with a luciferase reporter gene linked to the *Xist* promoter alone (*Xist*-luc), or including the distal region covering the REX1 recruitment sites in *Xist* exon1 (*Xist*-2p-luc). The constructs were transiently transfected into female wild-type cells, two *Rex1* over-expression ESC lines, and *Rnf12-/-* ESCs, and luciferase activity was measured at day 3 of differentiation. We found that both reporter constructs were down-regulated in the female *Rnf12-/-* and *Rex1* over-expression cell lines compared to a wild-type control female cell line (**Figure 4H**).

Figure 4: continued
A) *Xist* RNA-FISH (FITC) on day-3-differentiated WT and *Rex1+/-* male ESCs. **B)** Quantification of *Xist* clouds in **A** (n>100, error bars represent 95% Wilson confidence interval). **C)** *Xist* RNA-FISH (FITC) on day-3-differentiated female WT, *Rex1* over-expressing clones 1_3 and 1_11, and *Rnf12-/-* ESCs. **D)** Top panel: nuclear extracts of WT, transgenic FLAG-V5-REX1 lines 3 and 11 and *Rnf12-/-* ESCs were immunoblotted with REX1 antibody (open triangle: endogenous REX1, closed triangle: FLAG-V5-REX1). ACTIN was used as a loading control. Bottom panel: quantification of *Xist* clouds in **C** (n>200). Average percentage of cells with *Xist* clouds is shown. **E)** *Xist* and *Rex1* qPCR analysis of *Rnf12-/-* ESCs 72h after transfection with a *Rex1* shRNA construct or a control vector. **F)** qPCR analysis of *Rex1*, *Xist* and *Tsix* expression in undifferentiated and day-3-differentiated WT and the Rex1_3 and Rex1_11 clones. **G)** qPCR analysis of *Rex1* and *Xist* expression in day-3-differentiated male *Tsix*-stop ESCs, after transient transfection with a *Rex1* or control (mock) expression vector. **H)** Upper panel, schematic representation of constructs used in the luciferase reporter assay: empty vector, *Xist* promoter (*Xist*-luc) and *Xist* promoter + proximal part of exon 1 (*Xist*-2p-luc) constructs. Lower panel: luciferase activity of the different constructs in WT, Rex1_3 and Rex1_11 clones, and *Rnf12-/-* female ESCs, tranfected with the corresponding reporter constructs and differentiated for 3 days. All data in (**D**,**E**,**F**,**G** and **H**) represent the average ± s.d (n = 3). **I)** The XCI regulatory network. Prior to differentiation of ESCs *Xist* is repressed by *Tsix* dependent and independent mechanisms, regulated by different factors. The RNF12 protein level is low leading to repression of *Xist* and activation of *Tsix*, respectively. Upon differentiation, the RNF12 nuclear protein concentration increases, resulting in an enhanced rate of degradation of REX1 and subsequent activation of *Xist*. **J)** Phylogenetic tree, showing the presence or absence of XCI, *Xist*, *Rnf12*, *Yy1* and *Rex1* in different species (n.d., not determined, n.a. not applicable).

Down-regulation was more prominent for the *Xist*-2p-luc construct in all cell lines, suggesting that REX1 represses *Xist* through the *Xist* promoter and its downstream region. Taken together with the previous findings [989], we suggest that REX1 inhibits XCI by repression of *Xist*, and by activation of *Tsix*. This leads to a model in which, upon ESC differentiation or during development, an increased RNF12 concentration results in a decrease in the nuclear REX1 concentration. Because RNF12 is X-encoded, this effect will be more pronounced in differentiating female cells compared to male cells, allowing de-repression of *Xist* in female cells only (**Figure 4I**).

Recently, *Rex1* homozygous knockout ESCs and mice have been generated [997, 999]. Although no effect on XCI has been reported, *Rex1-/-* embryos were born at a sub-Mendelian ratio [999]. From the present study, we would expect that the threshold for initiation of XCI might be lower, in both male and female *Rex1-/-* embryos compared to wild-type embryos, resulting in aberrant initiation of XCI. The fact that some live *Rex1-/-* offspring was generated, indicates that additional factors, possibly acting downstream or independent of RNF12, exert control over the XCI process. Interestingly, *Rex1* is present only in placental mammals, representing a retro-transposed copy of *Yy1*, a gene also implicated in the regulation of XCI [1000] (**Figure 4J**). *Rex1* is not present in marsupials, which also lack *Xist* mediated XCI. This suggests co-evolution of *Xist* and *Rex1* in conjunction with the appearance of an XCI mechanism which requires *Xist*. In contrast to REX1, we found that YY1 expression is not up-regulated in *Rnf12-/-* cells (**Figure 3B**). Co-immunoprecipitation experiments using HEK293 cells indicate that YY1 and RNF12 interact (**Supplementary Figure 10**), but YY1 is not ubiquitinated by RNF12. Although our findings do not preclude a role for RNF12 mediated control of YY1 they clearly emphasize that the RNF12-mediated control of REX1 concerns a specific interplay, which does not occur between RNF12 and YY1, which evolved after a retro-transposition event generated the *Rex1* retrogene. We propose that the origin of *Rex1* has played a key role in the evolution of random XCI in placental mammals.

Methods Summary

REX1 was identified as an RNF12 interaction partner by mass spectrometry analysis on FLAG affinity purified FLAG-RNF12, isolated from nuclear extracts of day 3 differentiated FLAG-*Rnf12* transgenic ESC lines treated with the proteasome inhibitor (MG132). Protein purification and mass spectrometry analysis were done as described in [1001]. For the ubiquitination assay in HEK293 cells, the cells were transiently transfected with polyethylenimine (PEI) (Polysciences Inc.) with the indicated expression vectors. The REX1 ChIP and ChIP-sequencing (ChIP-seq) experiments were performed as described in [1002] with minor modifications. RNA-FISH was performed as described in [179]. For the luciferase reporter assay, ESCs were transfected with the indicated vectors, using lipofectamine 2000 (Invitrogen). Firefly and Renilla luciferase activity were measured using a Dual-Luciferase reporter assay system (Promega). A full description of the methods can be found in the Supplementary Information.

Acknowledgements

We would like to thank Reinier Van der Linden and Cheryl Maduro for their help with some of the experiments, Akiko Inagaki, Charlotte Andrieu-Soler, Daniel Warmerdam, Long Zhang and Adone Mohd-Sarip for experimental advice, and Claire Rougeulle and Rudolf Jaenisch for providing the *Tsix*-stop cells. This work was supported by grants from the Netherlands Organisation for Scientific Research (NWO-TOP and NWO-VICI) and the ERC to J.G.

Author Contributions

C.G. and J.G. designed the experiments. C.G. performed most experiments assisted by E.R.. T.S.B., C.G. and J.G. generated the *Rnf12*-/- ES cells. C.G., J.D., W.IJ. and E.M.A. performed the mass spectrometry and sequencing analysis. J.G., J.A.G. and C.G. wrote the manuscript.

Supplementary Information

Methods

Plasmids and antibodies

The coding sequences of *Rnf12*, *Rex1* and *Yy1* were amplified from mouse ESC cDNA and cloned into a TOPO blunt vector (Invitrogen). RNF12^{H569A,C572A} and RNF12^{del10aa} amino acid mutants were generated by PCR site-directed mutagenesis. For mammalian expression, the wild-type and two mutant *Rnf12* coding sequences were subcloned into pCAG-FLAG, a CAG-driven expression vector containing a FLAG-tag (a kind gift from D. van den Berg) and pEGFP-N3 (Clontech) vectors; *Rex1* and *Yy1* were subcloned into pCAG-FLAG-V5 and *Rex1* also into a modified pCherry-C1 vector (kind gifts from H. Lans). *Rex1* cDNA and *Rnf12* cDNA and truncated forms were subcloned into pGEX-6P-1 (GE Healthcare) vector for expression in bacteria. For the *Rex1* knock down experiments, a mouse Rex1 shRNA sequence ACGGAGAGCTCGAAACTAA [989] was cloned into pSuper-GFP-Neo (Oligoengine) and a pSuper-GFP-Neo-control-shRNA was used as a control.
For the luciferase reporter constructs, DNA fragments containing the REX1 binding sites within the *Xist* promoter alone (*Xist*-luc, nt -548 to +47) or including the *Xist* promoter distal region (*Xist*-luc-2p, nt -548 to +2161) were amplified by PCR and cloned into the promoterless pGL4.10 [luc2] vector (Promega). All constructs were checked by DNA sequencing. Antibodies used were against V5 (Invitrogen), Flag-M2 (Sigma), NANOG (Calbiochem), OCT4 (Santa Cruz), SOX2 (R&D systems), REX1 (Abcam and Santa Cruz), SUZ12 (Upstate), RNF12 (Abnova), YY1 (Santa Cruz), Ubiquitin (Enzo) and β-ACTIN (Sigma).

Cell culture and DNA transfection

Mouse ESCs were grown and differentiated as previously described [179]. FLAG-*Rnf12* and FLAG-V5-*Rex1* transgenic ESC lines were generated by electroporation of *Rnf12*+/- [174] and wild-type female ESC lines F1 2-1 (129/Sv-Cast/Ei), with pCAG-FLAG-*Rnf12* or pCAG-FLAG-V5 vectors followed by puromycin selection. F1 2-1, F1 2-3 (129/Sv-Cast/Ei), 1.3 (16xms2), *Rnf12*+/-, and *Rnf12*-/- ESC lines have been described [174, 911]. Male 1.3 *Rnf12* over-expressing ESC lines were generated as described in Jonkers et al. [174]. The E14tg2a control and *Rex1*+/- male ESC line with a gene trap insertion in intron 3 of *Rex1* has been previously characterized [998], and was obtained from BayGenomics (gene trap clone no. XB238). ESCs were transfected using lipofectamine 2000 (Invitrogen), according to the manufacturer's instructions. For the *Rex1* knock-down experiments, *Rnf12*-/- ESCs were transfected with pSuper-GFP-Neo Rex1 shRNA or control vectors and after 24 h GFP positive cells were sorted by FACS and 48 h later cells were harvested for RNA isolation. HEK293 cells were cultured under standard conditions in DMEM (Dulbecco's modified Eagle's medium) supplemented with 10% (v/v) FCS (fetal calf serum) and penicillin-streptomycin, and transfected with polyethylenimine (PEI) (Polysciences Inc.).

Nuclear extract preparation

Unless otherwise indicated, cells were treated with proteasome inhibitor (15 μm MG132, Sigma) for 3 h before harvesting. We also tested the effect of the proteasome inhibitor epoxomicin (1 μM). ESCs and HEK293 cells were scraped from the culture dishes in ice cold PBS plus protease inhibitor (Roche). Embryoid bodies (EBs) grown in suspension, were collected by centrifugation, and washed twice in ice-cold PBS plus protease inhibitor. Nuclear extracts were prepared as described in [1003] but instead of dialysed, were diluted 1:1 with buffer 0 (20 mM Hepes pH 7.6, 20% glycerol, 1.5 mM MgCl2, 0.2 mM EDTA, 0.5 mM DTT, 15 μM MG132 and protease inhibitors). To confirm phosphorylation of RNF12, female ESCs nuclear extracts were incubated for 30 min at 30°C in the presence or absence of lambda protein phosphatase (New England Biolabs).

Protein purification and mass spectrometry

Protein purification and mass spectrometry analysis were done essentially as described in [1001]. Briefly, nuclear extract from Flag-*Rnf12* ESCs at day 3 of differentiation or FLAG-V5-*Rex1* undifferentiated ESCs were incubated with Flag M2 antibody-agarose beads (Sigma) for 3 hours at 4°C, in the presence of Benzonase (Novagen). Bound proteins were eluted with Flag-tripeptide (Sigma). Elutions were pooled by TCA precipitation, proteins were separated by SDS-PAGE and the gel was stained with the colloidal blue staining kit (Invitrogen). Mass spectrometry analysis was performed on a capillary liquid chromatography system (Nanoflow LC-MS/MS 1100 series; Agilent Technologies) coupled to a mass spectrometer (LTQ-Orbitrap; Thermo Fisher Scientific).

GST pull-down assays

Recombinant GST-*Rex1*, GST-*Rnf12* full-length cDNA and the truncated forms were expressed at 20°C overnight in *E. coli* BL21 (Invitrogen). Cells were harvested and flash-frozen. 50 mL lysis buffer (25 mM Hepes pH 7.6, 10% glycerol, 0.5 M NaCl, 0.01% NP-40mM, 4 mM DTT, 2.5 mM MgCl2, 50 μM ZnCl2, 0.15 mg/ml lysozyme and protease inhibitors) was added per litre of culture. After sonication, soluble GST fusion proteins were bound to glutathione-sepharose beads (GE Healthcare) and analyzed by Coomassie staining. For *in vitro* binding assays, the GST tag was removed from the GST-REX1 fusion protein though enzymatic digestion with PreScission Protease (GE Healthcare).
RNF12-bound beads were equilibrated in buffer 100 (20 mM Hepes pH 7.6, 10% glycerol, 100 mM KCl, 1.5 mM MgCl2, 0.2 mM EDTA, 0.02% NP40, 0.5 mM DTT, protease inhibitors) and incubated for 2 hours at 4°C in the presence of Benzonase (Novagene) with nuclear extracts of HEK293 cells transiently expressing V5-tagged Rex1 protein, or with 0.5 ug recombinant REX1 protein. Nuclease Benzonase was added to the extract to show DNA-independence of the REX1-RNF12 interaction. Bound proteins were eluted with sample buffer and analyzed by immunoblotting.

Immunoprecipitation

Undifferentiated female and male ESC nuclear extracts were incubated for 2 h with REX1 antibody or control rabbit IgG (Santa Cruz), followed by addition of protein A Sepharose (Amersham) for 1 h. After washing, bound proteins were eluted with SDS sample buffer and analysed by immunoblotting with RNF12 and REX1 antibodies.

Ubiquitination assays

For the ubiquitination assay in HEK293 cells, the cells grown in 10-cm dishes were transiently transfected for 48 h with 2 μg wild-type or mutant *Rnf12* expression vectors, in the absence or presence of 2 μg V5-tagged *Rex1 or Yy1* expression vectors. Where indicated, cells were treated with proteasome inhibitor MG132 (15 μM for 3 h, Sigma) or epoxomicin (1 μM for 6h, Sigma) before harvesting. Cells were collected by scraping in ice cold PBS and nuclear extracts were prepared as described above. To detect protein expression, 10% of the nuclear extracts were used for immunoblotting with antibodies against REX1, YY1 or RNF12, and ACTIN was used as a loading control. To recover V5-tagged REX1 and YY1, 15 μl of V5 antibody-agarose beads (Sigma) were added to the nuclear extracts and the mixture was rotated for 1.5 h at 4 °C. The beads were washed with buffer 150 (20 mM Hepes pH 7.6, 10% glycerol, 150 mM KCl, 1.5 mM MgCl2, 0.2 mM EDTA, 0.02% NP40, 0.5 mM DTT, protease inhibitors). Bound proteins were eluted with sample buffer and visualized by immunoblotting. Co-immunoprecipitated RNF12 was detected with RNF12 antibody and poly-ubiquitinated REX1 with V5 and Ub antibodies.
The *in vitro* ubiquitination assay was carried out by adding recombinant REX1 (1 μg), GST-*Rnf12* wild-type or mutant (0.5 μg), E1 (55 ng UBE1, Boston Biochem), E2 (300 ng UbcH5a, Boston Biochem) and His-Ub (2 ug, Sigma) to ubiquitination buffer (50 mM Tris pH 7.5, 150 mM NaCl, 5 mM $MgCl_2$, 2 mM ATP, 1 mM DTT and protease inhibitors) to a final volume of 30 μl. The reactions were incubated at 30 °C for 1 h, terminated by boiling for 5 min with sample buffer, and resolved by SDS-PAGE gel followed by immunobloting with anti-Rex1 antibody.

Quantitative real-time PCR

Total RNA was extracted by using Trizol (Invitrogen) and then reverse transcribed by with Superscript II reverse transcriptase (Invitrogen) according to the manufacturer's instructions. Real-time PCR was performed using SYBR Green (Sigma) in a CFX384 real-time PCR machine (Bio-Rad). Actin was used as a normalization control. All qPCR data represents the mean ± s.d. of triplicate samples performed on cDNA isolated from three independent experiments. The primer sequences used for qPCR are listed in the **Supplementary Table 3**, and **Supplementary Table 2** list the primers used for ChIP-qPCR.

Immunofluorescence staining

ESCs were grown on coverslips without feeders and fixed with 4% paraformaldehyde for 10 min at room temperature. Subsequently, cells were permeabilized with 0.4% Triton X-100 in PBS for 10 min at RT and blocked with 10% goat serum in PBST (PBS with 0.05% Tween 20) for 30 min at RT. The coverslips were incubated with REX1 antibody overnight at 4°C. After washing with PBST, cells were incubated with the secondary antibody, Alexa Fluor 488 goat anti-rabbit IgG (Molecular Probes) for 1 hour at RT. After a final wash with PBS, coverslips were mounted with Vectashield Plus DAPI (Vector Laboratories). Images were acquired using a fluorescence microscope (Axioplan2; Carl Zeiss).

RNA-FISH

RNA-FISH was performed as described in [179] with minor modifications. Pre-plated female ESCs were seeded on gelatin-coated coverslips without feeders in EB differentiation media (IMDM + Glutamax (GIBCO), 15% FCS, 50 μg/μl ascorbic acid, NEAA, penicillin-streptomycin, 37.8 μl/l monothioglycerol (97%)). At day three of differentiation, cells were fixed and subjected to RNA-FISH. *Xist* clouds were counted for three different coverslips per cell line analyzed. The *Xist* probe was a 5.5kb BglII cDNA fragment covering *Xist* exon 3-7. The *Tsix* probe was a 5.1 kb SalI-SacII fragment of *Tsix* intron 3.

ChIP and ChIP-sequencing

The ChIP and ChIP-sequencing (ChIP-seq) experiments were performed as described [1002] with minor modifications. Briefly, female ESCs expressing V5-tagged REX1 and control wild-type ESCs were grown without feeders to 80% confluence ($3 \cdot 10^7$ cells per ChIP or $1 \cdot 10^8$ cells per ChIP-seq). For ChIP-seq and ChIP (where indicated), the cells were treated for 3 h with proteasome inhibitor (15 μm MG132, Sigma) before chromatin was cross-linked for 10 min at RT with 1% formaldehyde. The cross-linking reaction was stopped by addition of 0.125 M glycine. Sonicated chromatin was immunoprecipitated with 60 μl of pre-blocked V5 antibody-agarose beads (Sigma) for each ChIP-seq. Purified ChIP-DNA was prepared for sequencing on a HiSeq 2000 sequencer (Illumina).
The data was analyzed using a combination of bioconductor packages (Shortread, ChIP-Seq, and MACS). Illumina reads (36bp) were aligned against the mouse genome (*M. musculus* NCBI build 37) using Solexa Genome Analyzer ELAND Software. Aligned reads were imported, filtered, normalized and coverage was calculated using Shortread and ChIP-Seq packages. The resulting coverage graph was visualized using the USCS Genome Browser. The significance of peaks was calculated using MACS package. Peaks with a fold change of >=4 and fdr<=0.001 were taken as significant.

Luciferase reporter assay

ESCs were seeded into 24-well plates in differentiation medium and after 24 h transfected with 0.8 μg of the indicated vectors, using lipofectamine 2000 (Invitrogen). To normalize for transfection efficiency, a GL4.74 (hluc/TK) vector (Promega) expressing *Renilla* luciferase was co-transfected. Firefly and *Renilla* luciferase activity were measured 48 h post-transfection using a Dual-Luciferase reporter assay system (Promega) according to manufacturer's instructions. Three independent experiments were performed in triplicate, and the data are shown as the mean ± s.d.

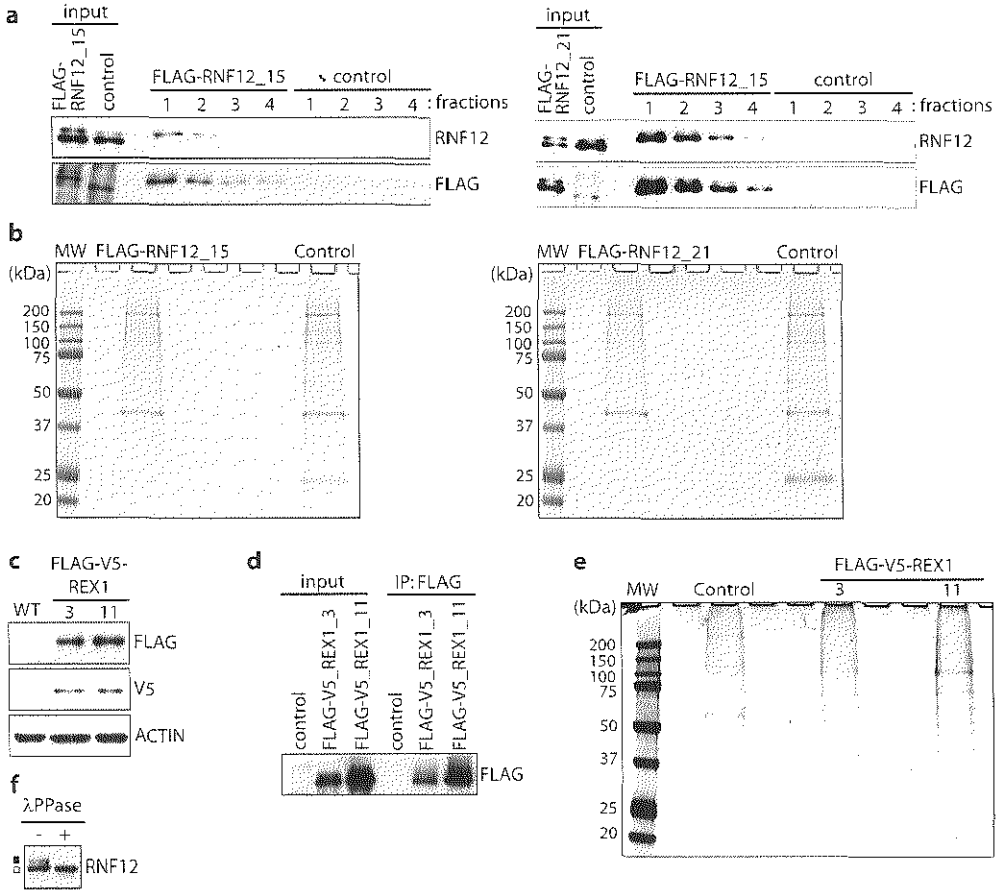

Supplementary Figure 1: Purification of FLAG-tagged proteins
A) Purification of FLAG-RNF12 by FLAG-affinity from nuclear extracts of wild-type (WT) and two FLAG-RNF12 transgenic ESC lines were immunoblotted with RNF12 and FLAG antibodies. Inputs and elution fractions from the FLAG-RNF12 and control cell lines are shown. **B)** Proteins from **A** were resolved by SDS-PAGE and stained with Coomassie. **C)** Nuclear extracts of WT and two FLAG-V5-REX1 transgenic ESC lines were immunoblotted with FLAG and V5 antibodies. ACTIN was used as a loading control. **D)** Purification of FLAG-V5-Rex1 by FLAG-affinity from nuclear extracts of WT and two FLAG-V5-REX1 transgenic ESC lines were immunoblotted with FLAG antibody. Inputs and elution fractions from the FLAG-V5-REX1 and control cell lines are shown. **E)** Proteins from **D** were resolved by SDS-PAGE and stained with Coomassie. **F)** Nuclear extracts of undifferentiated WT ESC were incubated in the presence (+) or absence (-) of λPPase and immunoblotted with RNF12 antibody (running positions of the unphosphorylated and phosphorylated forms of WT RNF12 are indicated with □ and ■).

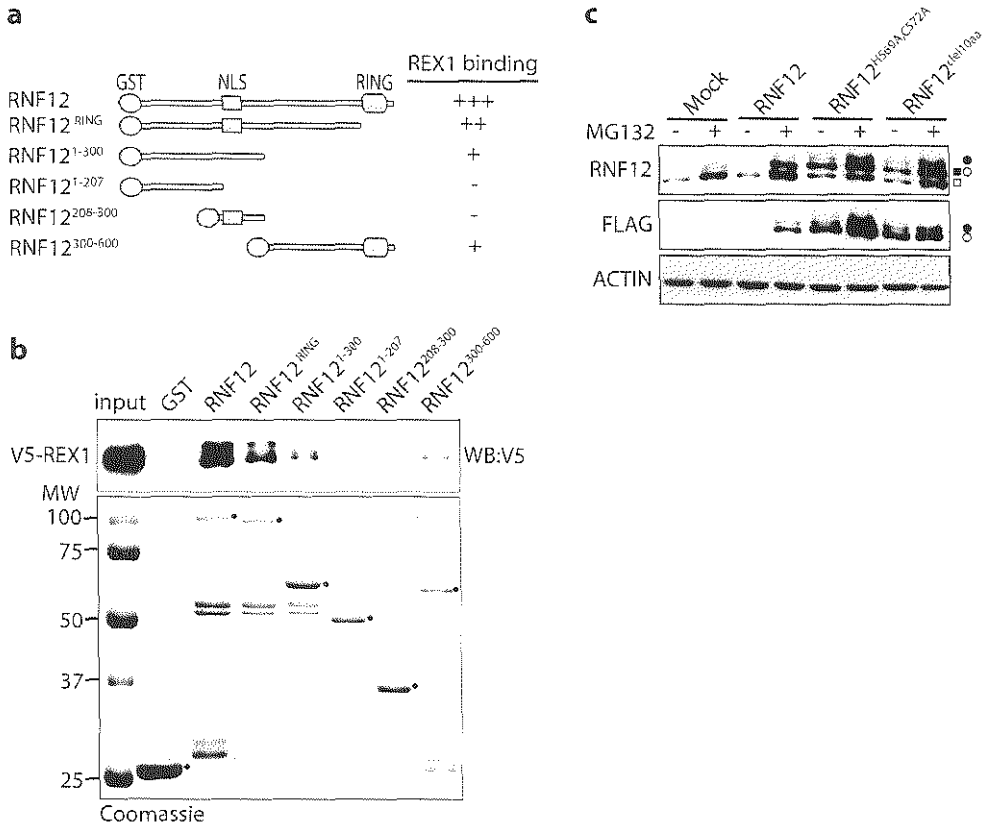

Supplementary Figure 2: Mapping of RNF12-interacting domains with REX1
A) Schematic representation of GST-RNF12 recombinant protein and the different truncation mutants used in **B**. NLS: nuclear localization signal; RING: RING finger domain. Relative level of binding of the different GST-RNF12 mutants to REX1, from the experiment in **B**, is indicated. **B)** GST pull-down with immobilized WT GST-RNF12 or the indicated truncated recombinant GST-RNF12 proteins from nuclear extract of HEK293 cells transfected with a V5-Rex1 expression construct. Upper panel: input and bound fractions were analysed by immunoblotting with V5 antibody to detect REX1 binding to recombinant RNF12. Bottom panel: eluted control GST and the different GST-RNF12 truncated recombinant proteins were detected by SDS-PAGE and Coomassie staining. The black dots point to GST and the various GST-RNF12 proteins. **C)** ESCs were transiently transfected with WT RNF12 and the two catalytically inactive RNF12 mutants in the presence or absence of the proteasome inhibitor (MG132). "Mock" refers to the empty plasmid. Nuclear extracts were prepared and analysed by immunoblotting with RNF12 and FLAG antibodies (running position of WT RNF12 and FLAG-RNF12 is indicated with □,○, the phosphorylated forms with ■,●). ACTIN was used as a loading control.

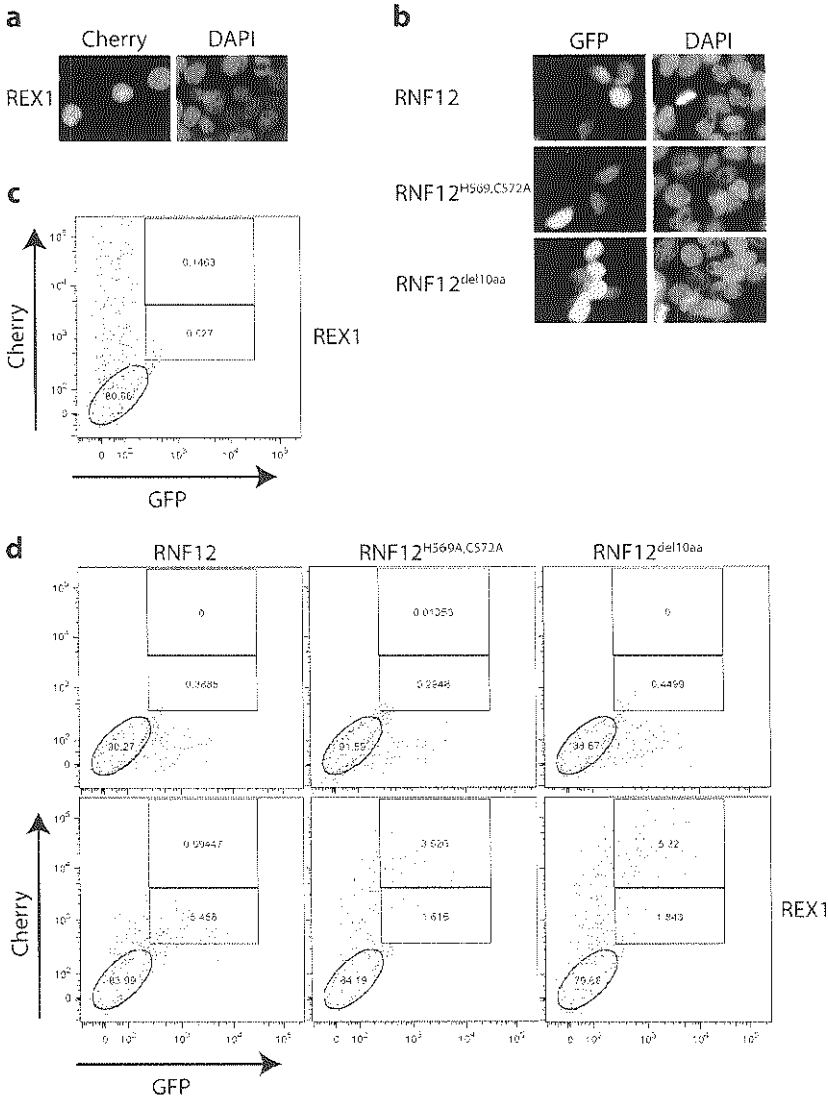

Supplementary Figure 3: Expression analysis of RNF12-GFP and REX1-Cherry in transgenic HEK293 cells

A), B), HEK293 cells seeded in a 12 well plate were transfected to test the expression constructs, with 0.6 µg of REX1-Cherry fusion expression vector **A** or 1.8 µg of WT or catalytically inactive mutant RNF12-GFP expression vectors, **B. C)** FACS analysis of HEK293 cells transfected with REX1-Cherry only. **D)** Upper panels show FACS analysis of HEK293 cells transfected with a RNF12-GFP vector, or two mutant RNF12-GFP fusion constructs. Bottom panels show the FACS profile of HEK293 cells co-transfected with REX1-Cherry in combination with either WT RNF12-GFP, or two different mutants RNF12-GFP. Shown in **C** and **D** is Cherry expression on the Y-axis, and GFP expression on the X-axis. The gated fractions represent the GFP positive, Cherry-high and Cherry-low cell populations.

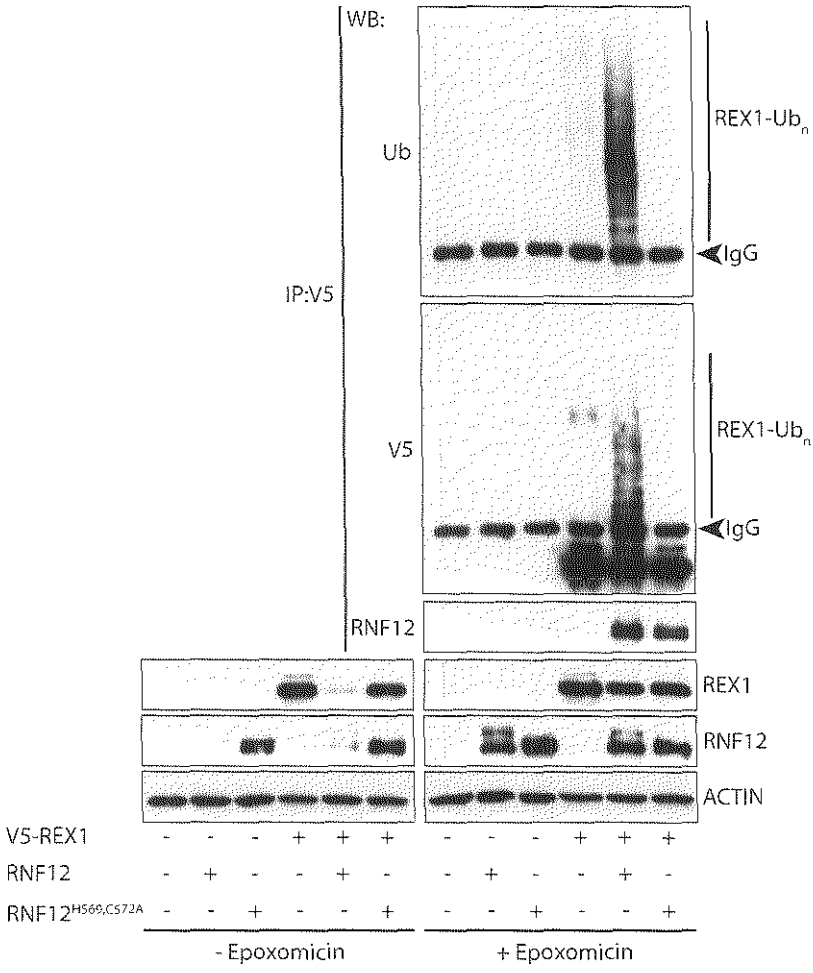

Supplementary Figure 4: REX1 ubiquitination assay in HEK293 cells
Left bottom panels show nuclear protein extracts of HEK293 cells co-transfected with the indicated expression constructs for V5-REX1, WT RNF12, or the catalytically inactive RNF12^{H569A,C572A} mutant. Immunoblots were probed with the indicated antibodies. Right bottom panels show the same transfections, but cells were treated with 1 μM epoxomicin for 6 hours before protein harvest. Upper panels, V5-tagged REX1 was immunoprecipitated with anti-V5 agarose beads and analysed by immunoblotting to detect the poly-ubiquitinated REX1 with V5 and ubiquitin antibodies. RNF12 co-immunoprecipitated with REX1 was detected with RNF12 antibody.

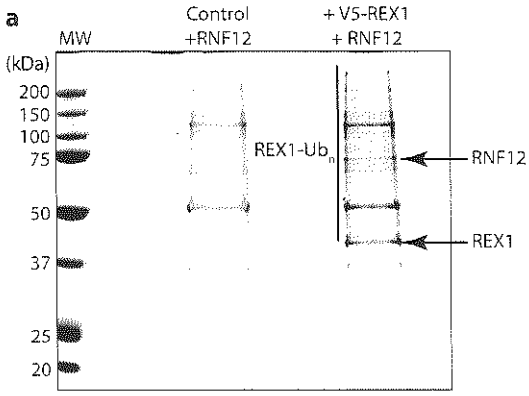

b

REX1
Peptides
LTLKQDEARPVQNTR
GTKQEKTEVTQETPPLR
QEKTEVTQETPPLR
AFTESSKLK
AFTESSKLKR

c

REX1
[1-288] mass = 32397.9
Cleavege at KR
Zinc finger domains

MNEQK...K...TSGQK...ALDR...QDEARPVQNTR...VTYTIR...
...GEFSEPILEEDFLFK...QVLEASSLLESSLEYMTK...QE...VGASS
LLAGGPAEKPEGGVYCGVLSMLECPQAGCK...K...DK...K...R...AFTESS...R...
...R...THIR...R...SFIQSNNQK...AGK...C

d

Ubiquitin sequence
MQIFV...TLTG...TITLEVEPSDTIENV...AK...IQD...EGIPPDQQRLIFAG...QKEDGRTLSDYNIQ...ESTKHLVLRLRGG

Ubiquitin linkages			
Lys	Peptides	Counts	Functions
K11	TLTGKTITLEVEPSDTIENVK	multiple	proteasomal degradation, misfolded proteins, ERAD
K48	LIFAGKQIEDGR	multiple	proteasomal degradation
K63	TLSDYNIQKESTIHLVLR	weak hit with low score	signalling, trafficking, DNA damage response

Supplementary Figure 5: REX1 is polyubiquitinated by RNF12
A) V5-affinity purification from nuclear extracts of HEK293 cells co-transfected with *Rnf12* and V5-*Rex1* expression constructs or *Rnf12* only in the control. 48 hours after transfection, cells were treated with MG132 for 3 hours before protein harvest. Purified proteins were resolved on a SDS-PAGE gel and stained with Coomassie. Putative bands representing RNF12, REX1 and poly-ubiquitinated REX1 are indicated. **B)** Sequences of the REX1-ubiquitinated peptides, identified by mass spectrometry, with the diglycine-modified lysine highlighted in red. Mass spectrometry analysis was done as described in the Methods section, with the modification that D2-iodoacetamide was used as alkylating agent to block cysteine residues. **C)** Amino acid sequence of mouse REX1. Highlighted in alternating black and grey are the peptides theoretically obtainable after trypsin digestion. Underlined are the peptides actually detected by mass spectrometry. Putative target lysines for ubiquitination are indicated in red. Green-shaded regions mark the four zinc finger domains and (*) marks the residues known to bind DNA. **D)** Table shows the ubiquitin sequence with the seven lysine residues highlighted in red and the polyubiquitin linkages that were present in the V5-REX1-RNF12 sample.

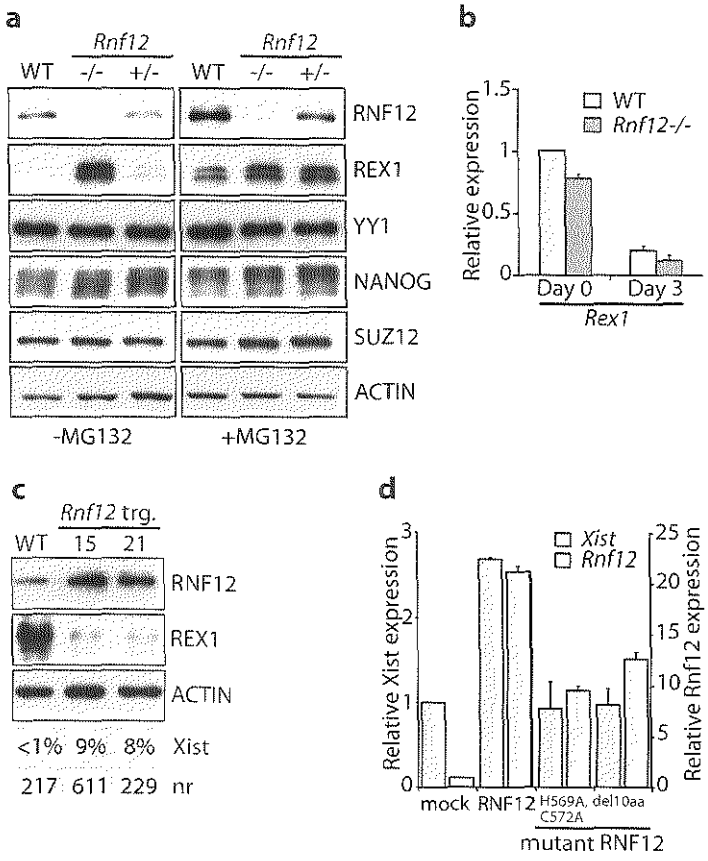

Supplementary Figure 6: RNF12 and REX1 protein levels show a reciprocal correlation
A) RNF12, REX1, YY1, NANOG and SUZ12 protein levels were compared by immunoblotting of nuclear extracts from undifferentiated WT, *Rnf12-/-* and *Rnf12+/-* female ESCs in the absence or presence of MG132. ACTIN was used as a loading control. **B)** WT and *Rnf12-/-* female ESCs have a similar *Rex1* mRNA level. *Rex1* expression was analysed by qPCR in WT and *Rnf12-/-* undifferentiated ESCs and at day 3 of differentiation. **C)** Nuclear extracts of wild-type and *Rnf12* transgenic male ESC lines 15 and 21 were immunoblotted with REX1 and RNF12 antibodies. ACTIN served as a loading control. Bottom panels show the percentage of cells with *Xist* clouds at day 3 of differentiation, and the total number of cells counted for each cell line. **D)** Male ESCs transiently transfected with an empty vector, or vectors expressing WT or two mutant forms of RNF12 were differentiated for 3 days. *Xist* RNA and *Rnf12* expression was determined by qPCR. All data represent the average expression ± s.d. ($n = 3$)

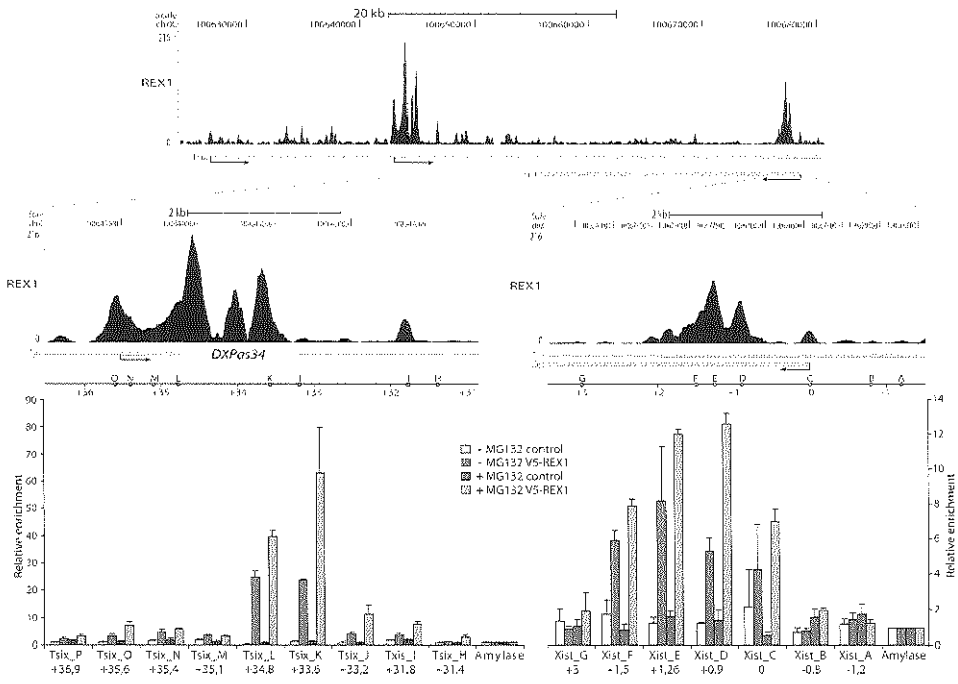

Supplementary Figure 7: Detailed view and confirmation of REX1 binding sites in the *Xist-Tsix* region

Upper panel: REX1 binding pattern in the *Xist/Tsix* genomic region in female ESCs, as determined by V5-REX1 ChIP-sequencing. Identified sequence reads were plotted relative to genomic location and visualized using UCSC Genome Browser. Location and transcription start sites (arrows) of the *Tsix* and *Xist* loci are indicated. **Middle panels**: higher magnification of the REX1 binding profile around the *DXPas34* region and the *Tsix* start site (left) or the *Xist* start site (right). Distance from the *Xist* transcriptional start site is indicated in kbs and genomic areas amplified in the V5-REX1 ChIP experiments (**lower panels**) are indicated by a red dot and the letters A to O. **Lower panels**: V5-REX1 ChIP using V5-REX1 expressing ESCs or control ESCs in the presence or absence of MG132. Relative enrichment over the *Amylase* negative control genomic region is indicated. Amplified regions are indicated in the **middle panels**, and the distance (in kbs) of the amplified regions from the *Xist* start site is indicated. All data represent the average expression ± s.d. (n = 3).

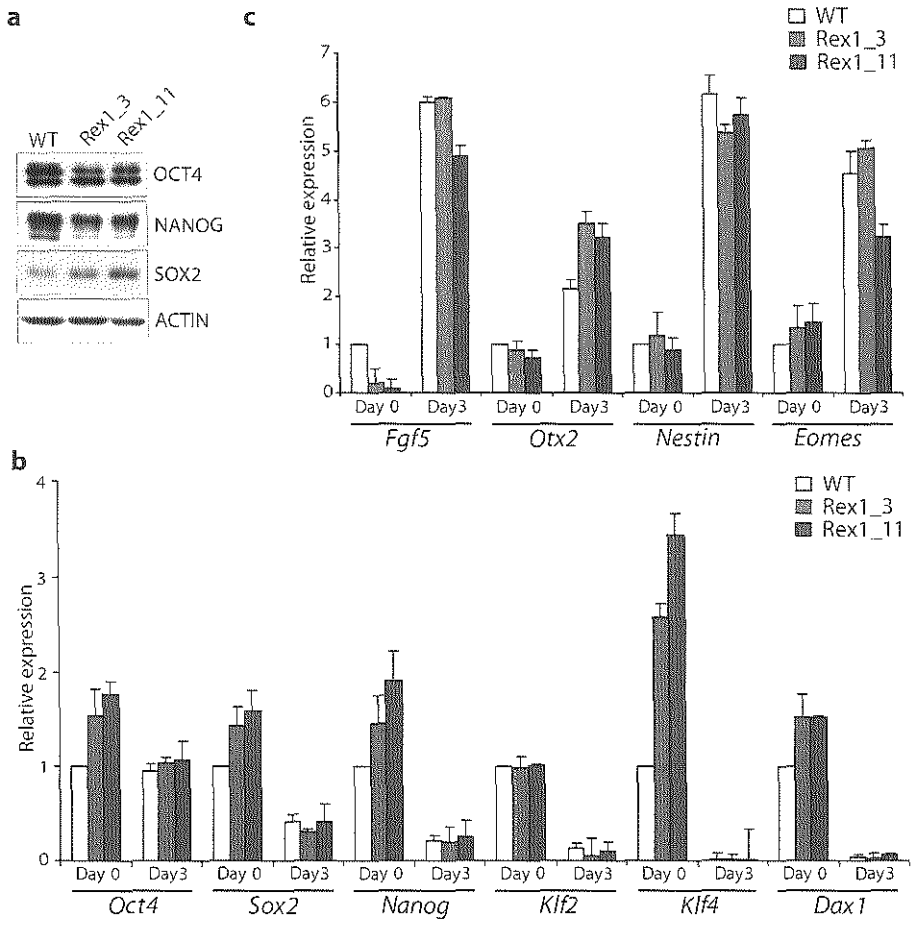

Supplementary Figure 8: Expression analysis of Rex1 over-expression ESC lines
A) Immunoblots with nuclear extracts of undifferentiated WT and Rex1 over-expression cell lines 3 and 11 detecting OCT4, NANOG, and SOX2. ACTIN was used as a loading control. **B), C)** Quantitative-PCR analysis of pluripotency markers *Oct4, Sox2, Nanog, Klf2, Klf4* and *Dax1*, and differentiation markers, *Fgf5, Otx2, Nestin* and *Eomes* in undifferentiated and day-3-differentiated WT and the Rex1_3 and Rex1_11 clones. Shown is the average expression ± s.d. (n = 3).

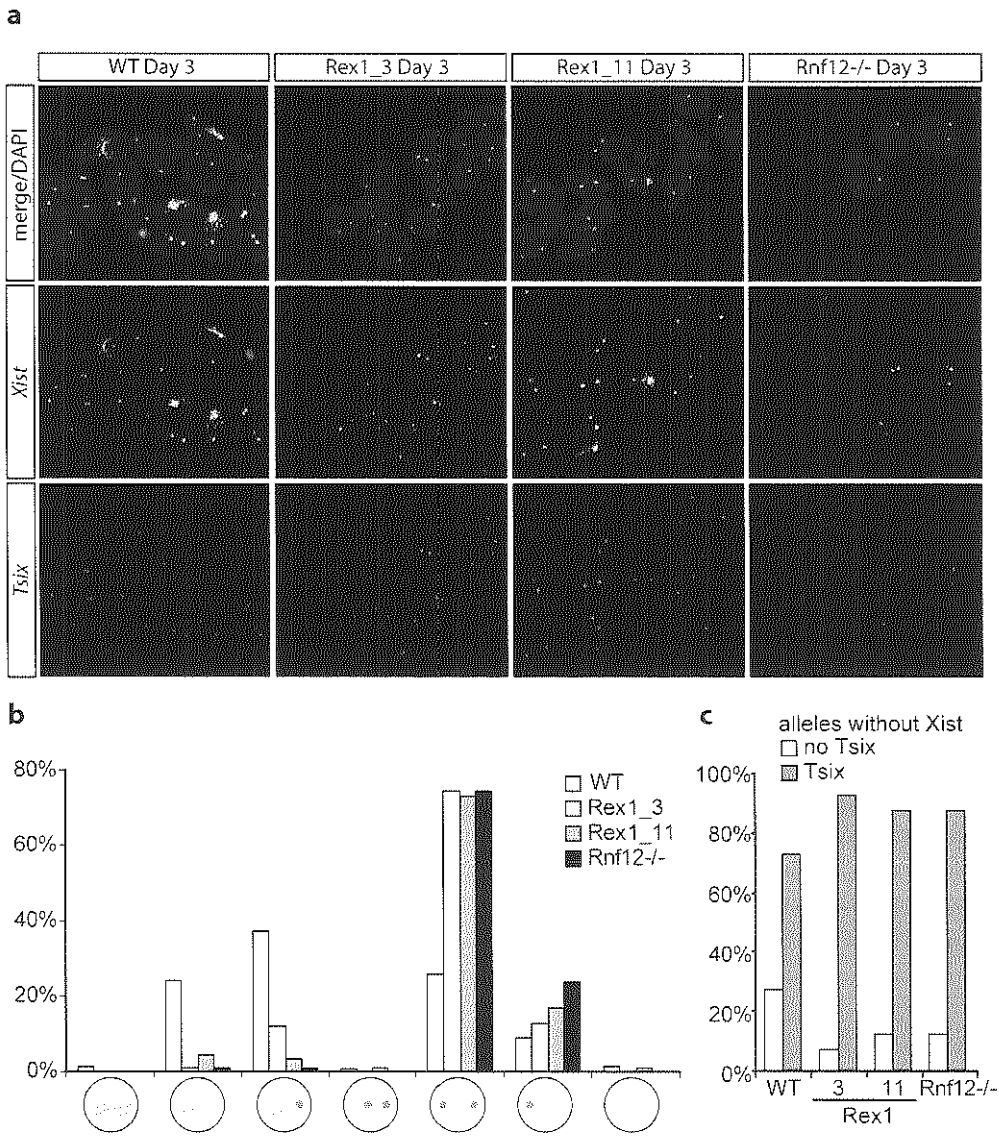

Supplementary Figure 9: *Xist* and *Tsix* expression in wild type and REX1-over-expression cell lines

A) *Xist* and *Tsix* RNA-FISH (bottom panel: *Tsix* in rhodamine; middle panel: *Xist* in FITC; top panel: merged *Xist-Tsix* signals and DNA stained with DAPI) on day-3-differentiated female WT, two *Rex1* over-expressing transgenic ESC lines and *Rnf12-/-* ESCs. **B)** Quantification of the *Xist* and *Tsix* RNA-FISH experiment described in **A**. **C)** The percentage of *Tsix* positive and negative alleles within the fraction of *Xist* negative alleles described in **A**. Shown is relative percentage of all observed combinations of *Xist* and *Tsix* expression ($n > 100$ per cell line).

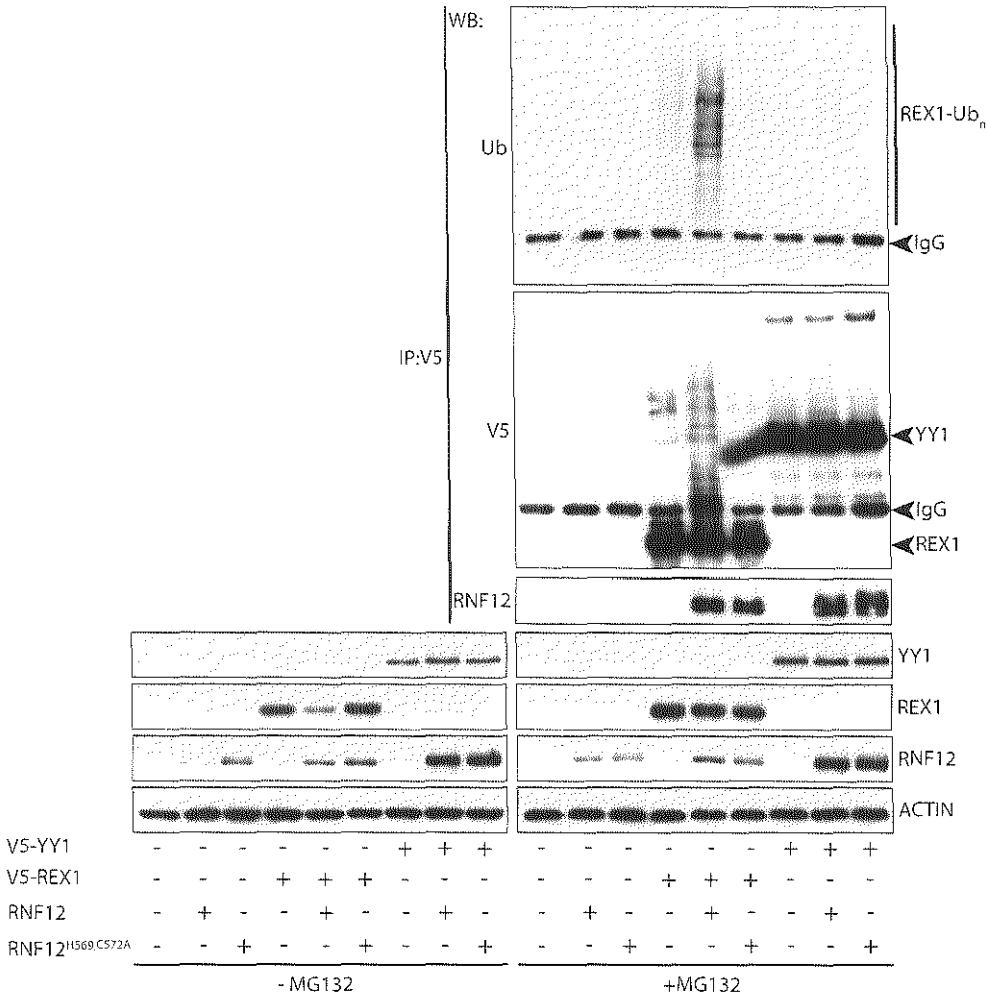

Supplementary Figure 10: RNF12 binds but does not ubiquitinate YY1
Ubiquitination assay in HEK293 cells, left bottom panels show nuclear protein extracts of HEK293 cells co-transfected with the indicated expression constructs encoding V5-YY1, V5-REX1, WT RNF12, or a catalytically inactive RNF12 mutant. Immunoblots were probed with the indicated antibodies. Right bottom panels show the same transfections, but in the presence of MG132. Upper panels, V5-tagged REX1 or V5-YY1 were immunoprecipitated with anti-V5 agarose beads and analysed by immunoblotting to detect the poly-ubiquitinated forms, if present, with V5 and ubiquitin antibodies. RNF12 co-immunoprecipitated with REX1 or YY1 was detected with RNF12 antibody.